

MODAL IDENTIFICATION OF NONLINEAR SUBSTRUCTURES AND
IMPLEMENTATION IN STRUCTURAL COUPLING ANALYSIS

A THESIS SUBMITTED TO
THE GRADUATE SCHOOL OF NATURAL AND APPLIED SCIENCES
OF
MIDDLE EAST TECHNICAL UNIVERSITY

BY

ÖZGE ARSLAN

IN PARTIAL FULFILLMENT OF THE REQUIREMENTS
FOR
THE DEGREE OF MASTER OF SCIENCE
IN
MECHANICAL ENGINEERING

AUGUST 2008

Approval of the thesis:

**MODAL IDENTIFICATION OF NONLINEAR SUBSTRUCTURES AND
IMPLEMENTATION IN STRUCTURAL COUPLING ANALYSIS**

submitted by **ÖZGE ARSLAN** in partial fulfillment of requirements for the degree
of **Master of Science in Mechanical Engineering Department, Middle East
Technical University** by,

Prof. Dr. Canan Özgen
Dean, Graduate School of **Natural and Applied Sciences**

Prof. Dr. S. Kemal İder
Head of Department, **Mechanical Engineering**

Prof. Dr. H. Nevzat Özgüven
Supervisor, **Mechanical Engineering Dept., METU**

Examining Committee Members

Prof. Dr. Mehmet Çalışkan
Mechanical Engineering Dept., METU

Prof. Dr. H. Nevzat Özgüven
Mechanical Engineering Dept., METU

Prof. Dr. Ozan Tekinalp
Aerospace Engineering Dept., METU

Assist. Prof. Dr. Yiğit Yazıcıoğlu
Mechanical Engineering Dept., METU

Dr. Ender Cigeroğlu
Mechanical Engineering Dept., METU

Date:

I hereby declare that all information in this document has been obtained and presented in accordance with academic rules and ethical conduct. I also declare that, as required by these rules and conduct, I have fully cited and referenced all material and results that are not original to this work.

Name, Last Name : Özge Arslan

Signature :

ABSTRACT

MODAL IDENTIFICATION OF NONLINEAR SUBSTRUCTURES AND IMPLEMENTATION IN STRUCTURAL COUPLING ANALYSIS

Arslan, Özge

M.S., Department of Mechanical Engineering

Supervisor: Prof. Dr. H. Nevzat Özgüven

August 2008, 111 pages

In this work, a new method is suggested for the modal identification of nonlinear structures and for the use of the modal data in calculating response of the nonlinear system to harmonic excitation. Nonlinearity in mechanical structures is usually encountered in connection regions. In this study, the nonlinear part of such a structure is modeled as a single nonlinear element and modal parameters of the structure are obtained as a function of displacement amplitude. Identification and modeling of nonlinear elements can be done through modal tests conducted at different response levels. Response level dependent modal parameters are used in calculating the response of the system to harmonic excitation at any forcing level. Furthermore, the modal model of a nonlinear substructure can be used in structural coupling of the nonlinear system with a linear one, and in structural modification problems where a nonlinear structure is modified with linear elements. Validation of the modal model proposed, and the use of this model in harmonic response computation, structural coupling and structural modification problems are demonstrated with several case studies.

Keywords: Structural Nonlinearity, Nonlinear Modal Parameters, Coupling Analysis

ÖZ

DOĞRUSAL OLMAYAN YAPILARIN TİTREŞİM BİÇİM TANILAMASI VE YAPISAL BİRLEŞİM ANALİZİNDE KULLANIMI

Arslan, Özge

Yüksek Lisans, Makina Mühendisliği Bölümü

Tez Yönetici: Prof. Dr. H. Nevzat Özgüven

Ağustos 2008, 111 sayfa

Bu çalışmada, doğrusal olmayan özellik gösteren yapıların titreşim biçim tanılanması ve elde edilen sonuçların yapının harmonik tahrik tepkilerinin çözümlenmesinde kullanılması için yeni bir yaklaşım sunulmuştur. Mekanik yapılarda doğrusal olmayan özellikler genellikle bağlantı noktalarında görülmektedir. Böyle bir yapının, doğrusal olmayan kısmı tek bir eleman olarak modellenmiş ve yapının biçim parametreleri yer değiştirme genliğine bağlı olarak bulunmuştur. Önerilen yöntemle farklı yer değiştirme genliklerinde yapılacak ölçümlerle doğrusal olmayan elemanların tanılanması ve modellenmesi sağlanabilir. Elde edilen, yer değiştirme genliğine bağlı biçim parametreleri, doğrusal olmayan sistemin herhangi bir harmonik tahrik kuvveti altındaki tepkisinin çözümlemesi için kullanılabilir. Ayrıca, doğrusal olmayan yapı için oluşturulan model doğrusal yapılarla birleşim analizinde ve doğrusal olmayan yapılarda yapısal değişiklik analizinde kullanılabilir. Sunulan modelin ve bu modelin harmonik tepki hesaplanmasında, yapısal birleşim ve yapısal değişiklik problemlerinde kullanımının doğrulanması örnek çalışmalarla gösterilmiştir.

Anahtar kelimeler: Yapısal Doğrusalsızlık, Doğrusal Olmayan Biçim Parametreleri, Birleşim Analizi

To My Great Parents, Güldane and Rasim Arslan

ACKNOWLEDGEMENTS

I wish to express to my deepest gratitude to my advisor, Prof. Dr. H. Nevzat ÖZGÜVEN for his guidance, interest, criticism and understanding throughout this study.

I would like to thank Murat AYKAN for his technical assistance, suggestions and friendship during the preparation of this thesis.

My special thanks go to my colleagues and friends for their neverending support and encouragement, especially my officemates Gözde and Hatice, and my dear friends Emre, Pınar, Banu and Mine. Their comfort and friendship during difficult times were irreplaceable.

I am sincerely thankful and indebted to each member UYAR family who always embraced me as their own child. Without their heartfelt support, this study would not be complete.

I am grateful to my dear mom and dad who always believed in me and provided every means of support they could have. Words to describe my admiration and love for them are inexistent.

My exceptional thanks go to Kıvanç UYANIK for his patience, presence and company throughout the preparation of this study.

Domestic Master of Science Scholarship provided by the Scientific and Technological Research Council of Turkey (TÜBİTAK) is thankfully acknowledged.

TABLE OF CONTENTS

ABSTRACT	iv
ÖZ.....	v
ACKNOWLEDGEMENTS	vii
TABLE OF CONTENTS	viii
LIST OF TABLES	x
LIST OF FIGURES.....	xi
LIST OF SYMBOLS AND ABBREVIATIONS.....	xvi
CHAPTERS	
1. INTRODUCTION.....	1
1.1 Structural Nonlinearity	1
1.1.1 Detection of Nonlinearity	1
1.1.2 Types of Nonlinearity.....	5
1.1.2.1 Cubic Stiffness	6
1.1.2.2 Piecewise Linear Stiffness.....	6
1.1.2.3 Coulomb Friction	7
1.2 Literature Survey	8
1.3 Objective of the Study.....	12
1.4 Scope of the Thesis.....	12
2. MODAL IDENTIFICATION OF NONLINEAR STRUCTURES	14
2.1 Introduction	14
2.2 Forced Harmonic Response Characteristics of Nonlinear Structures	14
2.2.1 Representation of Nonlinear Forces by the Nonlinearity Matrix	15
2.2.2 Describing Function Approach in the Computation of Nonlinearity Matrix	16
2.3 Measurement of FRFs in Nonlinear Structures.....	18
2.3.1 Force Amplitude Controlled FRFs	18
2.3.2 Displacement Amplitude Controlled FRFs	20
2.4 Extraction of Modal Parameters – The Modal Model.....	22

3. HARMONIC RESPONSE ANALYSIS USING THE MODAL MODEL.....	25
3.1 Forced Harmonic Response Prediction Using the Modal Model.....	25
3.1.1 Grounded Nonlinear Element.....	26
3.1.2 Interconnected Nonlinear Element.....	28
3.2 Structural Coupling Analysis Using the Modal Model.....	30
3.3 Structural Modification Analysis Using the Modal Model.....	36
3.4 Numerical Solution Technique.....	38
4. CASE STUDIES	41
4.1 Forced Harmonic Response Prediction	41
4.1.1 Case Study 1	41
4.1.2 Case Study 2	53
4.1.3 Case Study 3	57
4.1.4 Case Study 4	62
4.1.5 Case Study 5	66
4.2 Coupling of Nonlinear Systems by Using Modal Model	72
4.2.1 Case Study 6	72
4.2.2 Case Study 7	76
4.3 Structural Modification in a Nonlinear System by Using Modal Model	81
4.3.1 Case Study 8	82
4.3.2 Case Study 9	83
4.4 Experimental Case Study	84
5. CONCLUSIONS	91
REFERENCES.....	94
APPENDICES	
A. HARMONIC INPUT DESCRIBING FUNCTIONS	98
B. CONFERENCE PAPER.....	99

LIST OF TABLES

TABLES

Table 1. Modal parameters obtained by identification of constant displacement point FRFs (α_{11}).....	44
Table 2. Modal parameters obtained by identification of constant displacement transfer FRFs (α_{15}).....	44
Table 3. Modal parameters obtained by identification of constant displacement FRFs	87

LIST OF FIGURES

FIGURES

Figure 1. SDOF system Nyquist and FRF (Bode) plot distortions for five types of nonlinear element excited with constant amplitude sinusoidal force; — low level, - - - high level. [2]	3
Figure 2. Idealized forms of common structural nonlinearities [2].....	5
Figure 3. Bode plot representation of FRFs of a nonlinear structure at different forcing levels. [28]	19
Figure 4. Nyquist plot representation of FRFs of a nonlinear structure at different forcing levels. [28]	20
Figure 5. Bode plot representation of FRFs of a nonlinear structure at different response levels. [28].....	21
Figure 6. Nyquist plot representation of FRFs of a nonlinear structure at different response levels. [28].....	21
Figure 7. Natural frequencies of a nonlinear system identified at different forcing levels.....	23
Figure 8. Damping ratios of a nonlinear system identified at different forcing levels.....	24
Figure 9. Discrete MDOF system possessing a grounded nonlinear element connected at the i^{th} coordinate. ($k_r^* = k_r + i h_r$).	26
Figure 10. Discrete MDOF system possessing a nonlinear element between the coordinates q and r . ($k_r^* = k_r + i h_r$).	29
Figure 11. A nonlinear MDOF system coupled with an MDOF linear system (both systems are structurally damped).	31
Figure 12. A discrete MDOF linear system subject to modification.....	36
Figure 13. Five DOF system with grounded cubic stiffness.	41
Figure 14. Point FRFs generated at constant displacement amplitudes	42
Figure 15. Transfer FRFs generated at constant displacement amplitudes	43

Figure 16. Variation of the modal parameters of the first mode with respect to response amplitude, X_1 . (* identified parameters, — fitted curve).....	45
Figure 17. Variation of the modal parameters of the second mode with respect to response amplitude, X_1 . (* identified parameters, — fitted curve).....	46
Figure 18. Variation of the modal parameters of the third mode with respect to response amplitude, X_1 . (* identified parameters, — fitted curve).....	47
Figure 19. Variation of the modal parameters of the fourth mode with respect to response amplitude, X_1 . (* identified parameters, — fitted curve).....	48
Figure 20. Variation of the modal parameters of the fifth mode with respect to response amplitude, X_1 . (* identified parameters, — fitted curve)	49
Figure 21. Frequency response of the system in Case Study 1 to a force level of $F_1 = 100$ N with increasing frequency sweep.....	50
Figure 22. Frequency response of the system in Case Study 1 to a force level of $F_1 = 100$ N with decreasing frequency sweep.....	50
Figure 23. Frequency response of the system in Case Study 1 to a force level of $F_1 = 100$ N with both increasing and decreasing frequency sweep.....	51
Figure 24. Frequency response of the system in Case Study 1 to a force level of $F_1 = 250$ N with both increasing and decreasing frequency sweep.....	51
Figure 25. Frequency response of the system in Case Study 1 to a force level of $F_5 = 100$ N with increasing frequency sweep.....	52
Figure 26. Frequency response of the system in Case Study 1 to a force level of $F_5 = 100$ N with decreasing frequency sweep.....	53
Figure 27. Polluted point FRF of the system in Case Study 1, obtained for $X_1 = 2.5$ cm.....	54
Figure 28. Variation of the modal parameters of the first mode with respect to response amplitude, X_1 . (* identified parameters, — fitted curve).....	55
Figure 29. Variation of the modal parameters of the second mode with respect to response amplitude, X_1 . (* identified parameters, — fitted curve).....	55
Figure 30. Variation of the modal parameters of the fifth mode with respect to response amplitude, X_1 . (* identified parameters, — fitted curve).....	56

Figure 31. Frequency response of the system in Case Study 2 to a force level of $F_1 = 100$ N with increasing frequency sweep.....	56
Figure 32. Frequency response of the system in Case Study 2 to a force level of $F_1 = 100$ N with decreasing frequency sweep.....	57
Figure 33. 5 - DOF viscously damped system with grounded velocity squared nonlinearity.....	58
Figure 34. FRFs generated at constant displacement amplitudes	58
Figure 35. Variation of the modal parameters of the first mode with respect to response amplitude, X_1 . (* identified parameters, — fitted curve)	59
Figure 36. Variation of the modal parameters of the third mode with respect to response amplitude, X_1 . (* identified parameters, — fitted curve)	60
Figure 37. Frequency response of the system in Case Study 3 to a force level of $F_1 = 100$ N	61
Figure 38. Frequency response of the system in Case Study 3 to a force level of $F_1 = 200$ N	61
Figure 39. Polluted point FRF of the system in Case Study 3, obtained for $X_1 = 0.07$ m.....	62
Figure 40. Variation of the modal parameters of the first mode with respect to response amplitude, X_1 . (* identified parameters, — fitted curve)	63
Figure 41. Variation of the modal parameters of the second mode with respect to response amplitude, X_1 . (* identified parameters, — fitted curve)	63
Figure 42. Variation of the modal parameters of the fifth mode with respect to response amplitude, X_1 . (* identified parameters, — fitted curve)	64
Figure 43. Pseudo receptance of the system in Case Study 4 to a forcing level $F_1 = 200$ N	65
Figure 44. Pseudo receptance of the system in Case Study 4 to a forcing level $F_1 = 500$ N	65
Figure 45. Point FRFs generated at constant displacement amplitudes	66
Figure 46. Transfer FRFs generated at constant displacement amplitudes	67
Figure 47. Variation of the modal parameters of the third mode with respect to relative response amplitude, Y_{12} . (* identified parameters, — fitted curve)	68

Figure 48. Variation of the modal parameters of the fourth mode with respect to relative response amplitude, Y_{12} . (* identified parameters, — fitted curve)	68
Figure 49. Variation of the modal parameters of the fifth mode with respect to relative response amplitude, Y_{12} . (* identified parameters, — fitted curve)	69
Figure 50. Variation of the modal parameters of the third mode with respect to relative response amplitude, Y_{12} . (* identified parameters, — fitted curve)	69
Figure 51. Variation of the modal parameters of the fourth mode with respect to relative response amplitude, Y_{12} . (* identified parameters, — fitted curve)	70
Figure 52. Variation of the modal parameters of the fifth mode with respect to relative response amplitude, Y_{12} . (* identified parameters, — fitted curve)	70
Figure 53. Pseudo receptance of the system in Case Study 5 to forcing level, $F_1 = 100$ N	71
Figure 54. Pseudo receptance of the system in Case Study 5 to forcing levels of $F_1 = 100$ N, 200 N, 500 N	71
Figure 55. Nonlinear system to be rigidly coupled with a linear system.	72
Figure 56. Transfer and point FRFs of the linear subsystem in Case Study 6.	73
Figure 57. Variation of the modal parameters of the first mode with respect to response amplitude, X_1 . (* identified parameters, — fitted curve)	74
Figure 58. Variation of the modal parameters of the second mode with respect to response amplitude, X_1 . (* identified parameters, — fitted curve)	74
Figure 59. Pseudo receptance of the coupled system in Case Study 6 for a forcing level, $F_1 = 2$ N.	75
Figure 60. Pseudo receptance of the coupled system in Case Study 6 for a forcing level, $F_1 = 2$ N.	76
Figure 61. A nonlinear system to be rigidly coupled with a linear system.	76
Figure 62. Point and transfer FRFs of the linear subsystem in Case Study 7.	77
Figure 63. Variation of the modal parameters of the first mode with respect to relative response amplitude, Y_{12} . (* identified parameters, — fitted curve)	78
Figure 64. Variation of the modal parameters of the second mode with respect to relative response amplitude, Y_{12} . (* identified parameters, — fitted curve)	78

Figure 65. Variation of the modal parameters of the third mode with respect to relative response amplitude, Y_{12} . (* identified parameters, — fitted curve)	79
Figure 66. Variation of the modal parameters of the first mode with respect to relative response amplitude, Y_{12} . (* identified parameters, — fitted curve)	79
Figure 67. Variation of the modal parameters of the second mode with respect to relative response amplitude, Y_{12} . (* identified parameters, — fitted curve)	80
Figure 68. Variation of the modal parameters of the third mode with respect to relative response amplitude, Y_{12} . (* identified parameters, — fitted curve)	80
Figure 69. Pseudo receptance of the system in Case Study 7 to different forcing levels.....	81
Figure 70. Pseudo receptance of the system in Case Study 8 to a forcing level $F_1 = 100\text{N}$	82
Figure 71. Response of the system in Case Study 9 to different forcing levels....	83
Figure 72. Experimental Setup.....	84
Figure 73. Stiffness characteristics of the experimental setup	85
Figure 74. FRFs obtained from force controlled tests.....	86
Figure 75. FRFs obtained from displacement controlled tests.....	86
Figure 76. Variation of the modal parameters with respect to response amplitude. (* identified parameters, — fitted curve)	88
Figure 77. Pseudo receptance of the system to $F = 0.1\text{ N}$	89
Figure 78. Pseudo receptance of the system to $F = 0.2\text{ N}$	89
Figure 79. Pseudo receptance of the system to $F = 0.5\text{ N}$	90
Figure 80. Pseudo receptance of the system to $F = 1\text{ N}$	90

LIST OF SYMBOLS AND ABBREVIATIONS

$[C]$: Linear viscous damping matrix
$[D]$: Dynamic structural modification matrix
$\{f\}$: Generalized external forcing vector
$\{F\}$: Amplitude vector of harmonic external forcing
i	: Unit imaginary number
$[H]$: Linear structural damping matrix
$[I]$: Identity matrix
$[K]$: Linear stiffness matrix
$[M]$: Linear mass matrix
$\{N\}$: Internal nonlinear forcing vector
n	: Number of degrees of freedom
v	: Describing function
$\{x\}$: Displacement vector
$\{X\}$: Complex amplitude vector of steady state harmonic displacements
$[\alpha]$: Receptance matrix
$[\Delta]$: Nonlinearity matrix
$[\Delta C]$: Viscous damping matrix of modifying system
$[\Delta K]$: Stiffness matrix of modifying system
$[\Delta M]$: Mass matrix of modifying system
$[\gamma]$: Receptance matrix of modified system
ω	: Excitation frequency

CHAPTER 1

INTRODUCTION

1.1 Structural Nonlinearity

In simplest words, nonlinearity is lack of linearity. However structural nonlinearity deserves a further description to be fully expressed. In engineering structures nonlinearity can arise from a number of reasons or their combination. These reasons can be listed as looseness, clearance or friction in structural joints, presence of components with input dependent dynamics and amplitude dependent materials. It is also possible for a structure to exhibit nonlinearity when large amplitudes are reached since most systems behave linearly in small amplitudes. Furthermore, each nonlinear system is specific within itself and requires a different approach. Therefore, once the nonlinearity of a structure is verified, type and quantity of the nonlinearity should be determined. In the following sections, symptoms and types of nonlinearity will be discussed.

1.1.1 Detection of Nonlinearity

Distortion of frequency response functions (FRFs) is undoubtedly the most common method for detection of nonlinearity in a system. If the FRFs a system for different levels do not overlap but separate, this indicates presence of nonlinearity. FRFs of linear systems do not change with different forcing levels. However, this is not the same for nonlinear systems. The type of nonlinearity in the system can be depicted by the form of distortion observed in the plot as long as the excitation type is known. In Figure 1, Nyquist and Bode plot representation of FRFs for different types of nonlinear elements that are harmonically excited are

shown. Distortions, especially around resonant regions, can be observed easily both in Nyquist and Bode plots.

It is also possible to observe the effects of nonlinearity in alternative FRF representations of nonlinear systems. So called carpet plots [1] also set a practical way of nonlinearity detection. Carpet plots, mainly used in damping prediction, are 3 dimensional plots in which one of the axes is the damping ratio and the others are the frequency range before and after the resonance frequency, respectively. In a linear system, the carpet plot is expected to be planar and parallel to the plane formed by both frequency axes. Any deviation from linearity results in variation of the damping ratio with respect to the frequency plane. In terms of clarity in visual intelligibility carpet plots establish a good option for detection of nonlinearity. On the other hand the method is quite restricted compared to use of other FRF representations such that it is sensitive to phase distortions, restricted to SDOF systems and requires prior information of the damping in the system.

In principle, any type of excitation reveals the nonlinearity in the system. In other words it is possible to detect nonlinearity by a simple visual assessment. However in order to state the exact type of the nonlinearity and quantify it, correct excitation method is to be selected since nonlinear systems respond in different ways to different types of excitation.

It is well-known that harmonic excitation generally produces the most apparent effects of nonlinearity. In this excitation type, all the input energy is concentrated at the frequency of excitation. Especially systems possessing polynomial stiffness nonlinearity exhibit strong nonlinear effects such as the jump phenomena under harmonic forcing. However, it has a main disadvantage in terms of the measurement time when compared to impact and/or random input excitation.

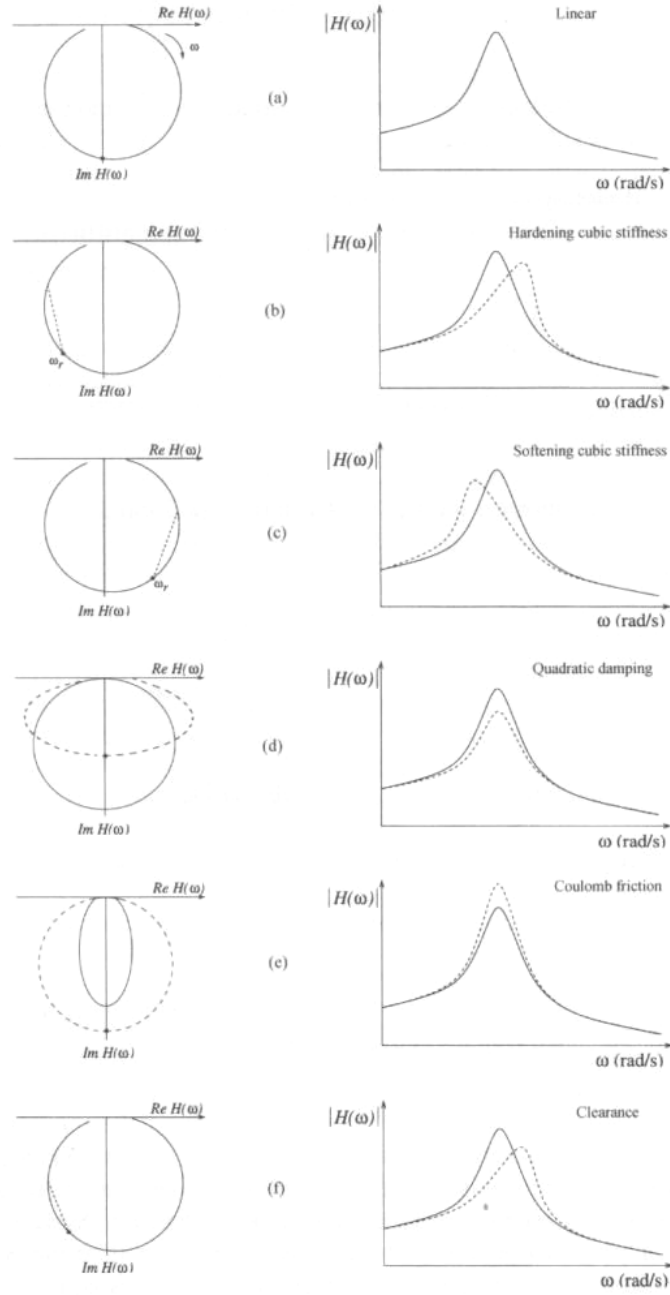


Figure 1. SDOF system Nyquist and FRF (Bode) plot distortions for five types of nonlinear element excited with constant amplitude sinusoidal force; — low level, - - - high level. [2]

Impact testing delivers responses with high crest factors which assist the excitement of nonlinearity. Usually the distortions produced this way are opposite to those obtained by harmonic excitation. Unlike harmonic excitation, energy associated with a single frequency is small which makes the evoking of nonlinearities more difficult [2].

The FRF of a nonlinear structure subjected to random excitation appears like that of a linear one. This is a consequence of the randomness of the amplitude and phase of the excitation. Due to this linearization effect, random excitation will be useful in detecting nonlinearity only when several tests are carried out with different rms levels of the excitation and the results are compared. Like in impact testing, excitation of nonlinearities is difficult as a result of the input spectrum spread over the frequency range. It should be noted that the linearized FRF obtained from this type of testing is not related to the linear counterpart of the nonlinear system but an averaged value between these two.

As mentioned before, structural nonlinearities respond in different forms according to the type of excitation employed. In consequence, identification and quantification methods for nonlinear systems are dependent on the type of input used and will provide reliable results only under correct excitation conditions.

Another distinguishing property between linear and nonlinear systems is reciprocity. Reciprocity holds if the FRF values at a single frequency stays constant when the input and output points are swapped [2]. Like distortion of FRFs, it allows a visual check to detect nonlinearity. He (Jimin He) [3] showed that reciprocal of FRF can be effectively used to detect nonlinearity in a structure. The method is based on the idea of separating the real and imaginary parts of the inverse receptance. In case of a nonlinear system, either real or imaginary part of the inverse receptance data reveals the nonlinearity in the system. The effect of stiffness nonlinearity shows up is the real part while damping nonlinearity is monitored in the imaginary part of the inverse FRF. However one should know

that reciprocity is a necessary but not sufficient condition for nonlinearity as structures with symmetrical nonlinearities also demonstrate reciprocity.

1.1.2 Types of Nonlinearity

In this section the most common nonlinearities encountered in structural dynamics will be listed. As expected, structural nonlinearities are usually displacement, velocity and/or frequency dependent. However, they are generally represented in idealized forms in order to provide the integration into analysis. Idealized forms of some of these nonlinearities are illustrated in Figure 2.

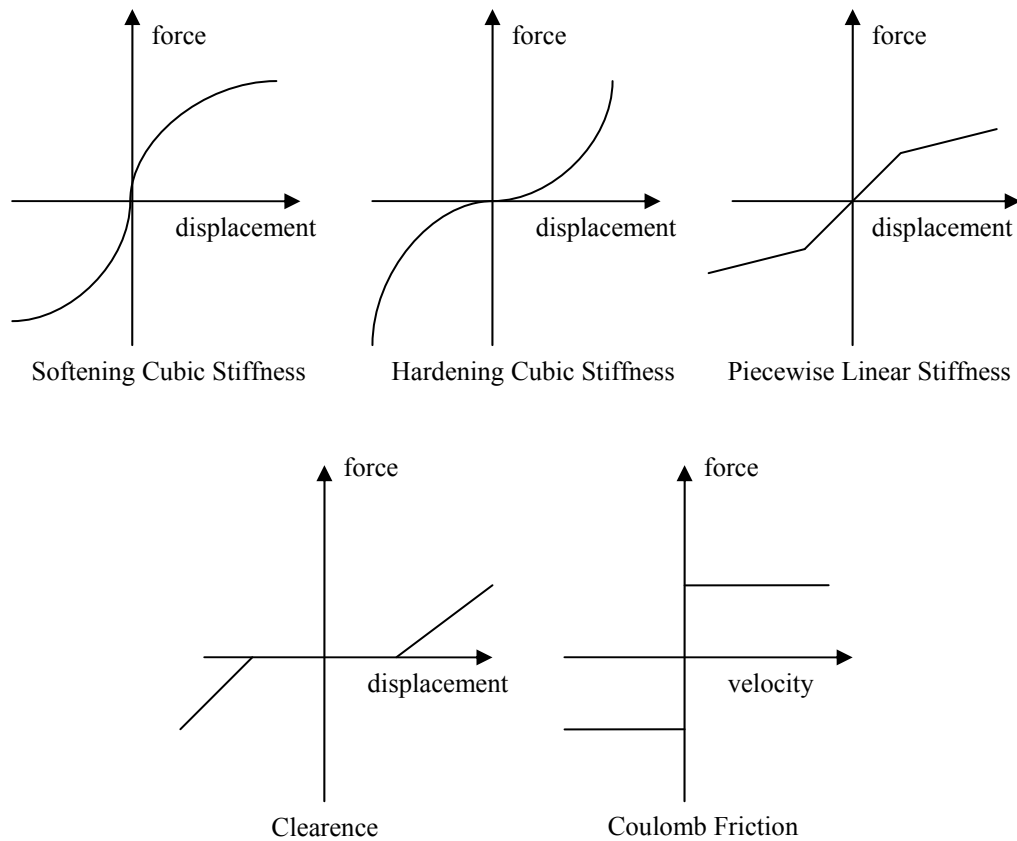


Figure 2. Idealized forms of common structural nonlinearities [2]

1.1.2.1 Cubic Stiffness

This type is the most frequently encountered type of polynomial stiffness. In this case force is directly proportional to the cube of displacement as in the following relation:

$$f_{nl}(x) = bx^3 \quad (1.1)$$

Here the proportionality constant, b , can be either positive or negative. Positive constant introduces greater restoring forces than the linear one at higher levels of excitation. Such systems are referred to have hardening characteristic. Similarly, systems representing decreasing stiffness behavior with increasing excitation levels are stated to have softening nonlinearity. Unlike hardening cubic systems, these systems always possess higher order polynomial terms that dominate stiffness. This is inevitable to provide stability since a softening cubic system is unphysical in the sense that the system tends to infinity after a certain distance from equilibrium.

FRF distortion characteristic of these systems can be observed in Figure 1 (b) and (c). The most important feature these figures present is the shift of resonance peak. FRFs of systems with cubic nonlinearity also introduce the jump phenomena. Because of the cubic term in the equation of motion there exist multiple solutions. In vibration testing, it is possible to obtain only one response depending on the frequency sweep direction. Overlay of both FRFs measured with increasing and decreasing frequency increments reveals this occurrence. With bending of FRFs around resonance frequency, a jump phenomenon is a strong indicative of nonlinearity in the system.

1.1.2.2 Piecewise Linear Stiffness

The form of stiffness function for this case is

$$f_s(x) = \begin{cases} k_2x + (k_1 - k_2)d, & x > d \\ k_1x, & |x| < d \\ k_2x - (k_1 - k_2)d, & x < -d \end{cases} \quad (1.2)$$

where k_1 and k_2 are the slopes of the first and second lines in force vs. displacement graph of piecewise stiffness in Figure 2, respectively, and d is the displacement value corresponding to the point where first slope ends and the second one begins.

This type of nonlinearity is encountered in many applications, for instance in ground vibration tests of aircrafts especially in pylon-store-wing assemblies or preloading bearing conditions. Typical results of such nonlinearity in a system can be seen in [4]. Clearance nonlinearity is a special case of piecewise linear stiffness where $k_1 = 0$.

1.1.2.3 Coulomb Friction

This type nonlinearity has the characteristic relation,

$$f_{nl}(x) = a \operatorname{sgn}(\dot{x}) \quad (1.3)$$

also as shown in Figure 2, where a is the magnitude of the nonlinear force resulting from this nonlinearity. Coulomb friction, also known as Coulomb damping, is common in interfacial motion. In such structures friction occurs along with clearance nonlinearities. Unlike other types of nonlinearities, it is most apparent at low levels of excitation. In extreme situations, stick-slip motion can occur. The characteristic FRF distortion is the reveal of higher damping with lower excitation levels.

1.2 Literature Survey

There exist a variety of studies in nonlinear structural dynamics area. Earlier studies mostly concentrate on detection, localization, and identification of nonlinearity. Mertens et al. [5] stated the importance of analyzing nonlinear systems separated from linear ones and validated their statement with experimental work. Use of modal analysis tool in the area of detection and identification of nonlinear structures were studied by a number of researchers. He and Ewins [6] presented one of the first studies in this field. They proposed a new approach for the interpretation of FRF data for the specific purpose of detecting and identifying nonlinearities. The method is used to locate the type of nonlinear element by separating the stiffness and damping effects (into the real and imaginary parts of the inverse FRF). They also introduced the concept of displacement amplitude dependent modal parameters which will be of use in this thesis. However, the method is restricted to SDOF models.

Lin and Ewins [7] investigated the possibility of locating structural nonlinearity by combining a finite element model containing modeling errors and the modal data measured at different response levels. The sensitivity of certain modes to localized nonlinearity has been defined in terms of modal parameters and it is suggested that relatively sensitive modes should be used in the location process in order to make nonlinearity location reliable in practice. First-order frequency response functions are calculated and analyzed to give an indication of which mode is the most sensitive one and should therefore be used in the location process. Lin [8] extended this concept further and employed in modeling and model updating of nonlinear structures. In his work he claimed the advantages of using FRF data over modal data to update an analytical model. On top of all, special attention is given to the application of the method to the case where both measured modes and coordinates are incomplete. The practical applicability of the method is assessed based on the GARTEUR (Group for Aeronautical Research and Technology in Europe) exercise which is intended to represent practical

problems in terms of the incompleteness of both measured modes and coordinates.

Vakakis and Ewins [9] examined the nonlinear distortions in the receptance plots of forced mechanical systems. The concept of FRF distortions in nonlinear systems is also mentioned in earlier sections this chapter. They observed the trend of natural frequencies of nonlinear structures and established a formulation of natural frequency both for damping and stiffness nonlinearity. In their work also a method for identifying and quantifying weak nonlinearities in the modal responses is suggested and tested with theoretical and experimental data.

Benhafsi et. al. [10] developed a parametric identification method based on the fact response of nonlinear systems can be associated with mode shapes that are constant over a certain dynamic range of the input. The method uses describing function theory to obtain the extended forms of backbone and limit curves. These are then used for the identification of both linear and nonlinear parameters of a multimode system. The feasibility of the method is demonstrated on simulated MDOF systems involving cubic nonlinearity. The method is restricted to systems whose mode shapes are insensitive to nonlinearities. Also proportional damping assumption is made. They also extended this study to localize the nonlinearity in a structure [11].

Özer and Özgüven [12] introduced a new method for localization of the physical coordinates to which nonlinear elements are connected in MDOF systems by using first order frequency response function data. They managed to determine the parametric values of nonlinearity provided that the nonlinearity is located at the ground connection of the structure. Case studies, in which theoretically calculated harmonic responses are used, are given to illustrate the application of the method. Theoretically calculated values are polluted in order to investigate robustness of the identification method under measurement errors. Later they extended this study to systems that possess nonlinear elements between any two coordinates [13]. The Sherman–Morrison matrix inversion method is used in this

study to put the response expression in a form where the nonlinearity term is isolated. Using measured responses, nonlinearity can be quantified thus identified. To demonstrate the applicability of the method case studies are given in this study as well.

Song and Wang [14] presented a method for identifying nonlinear element positions and their physical parameters in a multiple degree of system. In their study, first the local nonlinear restoring forces are modeled with polynomial series functions of the relative displacements and velocities, respectively. Then an iterative equation between excitation and response signals and the general frequency response function are derived. The nonlinear degree of freedom is extracted from the general system in the frequency domain based on this information. In short, when two different levels of excitation forces are imposed on a testing system, the frequency domain measurement data is used to detect the nonlinear element positions. In addition, an approach for nonlinear parameter identification is developed, which can be used to obtain the polynomial coefficients of the nonlinear stiffness and damping forces. The effectiveness of the method is demonstrated by numerical examples.

Studies on modeling and identification of nonlinearity have increased further in recent years. However, construction of reliable models for nonlinear structures is still uncertain. Former studies [15, 16] show that linear identification of nonlinear systems causes misleading results. In [15] Özgüven and İmregün applied linear modal analysis on classically damped nonlinear systems. The results showed highly complex modes that indicate nonlinear behavior since the initial damping was proportional. This indicated that linear identification methods can reveal nonlinearity in a structure but they fail to provide a reliable modal model. As linear modal analysis tools are not compatible with the nonlinear theory, majority of the studies in this field [15 - 17] focus on development of nonlinear modal analysis techniques. Setio et. al. [16] proposed a nonlinear modal analysis method to describe the dynamic behavior of nonlinear MDOF systems. The technique is based on nonlinear mode superposition approach. The calculation of nonlinear

natural frequencies and nonlinear normal modes were performed implicitly by the proposed approximation based upon the equivalent linearization approach. Some examples including experimental simulation were introduced to illustrate the efficiency, accuracy and advantages of the proposed methods.

Ferreira and Ewins [17] described a new Nonlinear Receptance Coupling Approach (NLRCA) for fundamental harmonic analysis based on describing functions. They proposed an analytical development of assembling many structures considering just the fundamental frequency. The approach is able to couple structures with local nonlinear elements, where the describing functions of all the nonlinear elements are known.

Richards and Singh [18] investigated reliability of approximating nonlinearities in discrete systems consisting of nonlinear elastic forces by polynomial models. Coherence functions are introduced which are based on a "reverse path" spectral approach, previously developed by the authors for MDOF systems. These coherence functions, as calculated from conditioned spectra, indicate the accuracy of the assumed mathematical models.

Chong and İmregün [19, 20] also suggested a nonlinear modal analysis for a multi-degree-of-freedom system that involves identifying modal parameters from measured response at first. For verification they used simulated nonlinear response data. They were able to predict the nonlinear response of the system for other excitation levels by using the modal parameter variations with respect to modal displacement. They also extended this idea for coupling of nonlinear systems with linear ones [21] and performed a numerical study on a system with friction damping nonlinearity [22]. The study presented in this thesis follows a similar approach with this study, in some respect.

Elizalde Siller [23] presented new nonlinear modal analysis methods to detect, localize, identify and quantify the nonlinearities in large systems, based on first order nonlinear FRFs as input data. The methods are first introduced in a direct-path, by analyzing a general theoretical system. Then, the concepts are extended

to undertake a nonlinear identification via the reverse-path of the same methodologies.

1.3 Objective of the Study

In this study it is aimed to establish an approach to predict forced harmonic response of nonlinear systems. The proposed approach bases on the fact that nonlinear structures exhibit linear behavior under certain conditions, which makes the use of linear modal identification methods possible. Modal parameters identified under these conditions are used to construct a modal model for the nonlinear system to be analyzed. In these terms, the study follows a similar approach with that of Chong and İmregün [19, 20]. However, in the present study physical displacements are used, unlike in references [19 – 22] in which modal displacements were employed. Furthermore, the present work uses a semi analytical approach for the modal model, and also extends the use of the modal model in structural modification problems in addition to response prediction and dynamic coupling analysis.

1.4 Scope of the Thesis

The outline of the thesis is as follows:

In Chapter 2, basic characteristics of forced harmonic response of nonlinear systems are reviewed. The theory of modal identification of nonlinear structures using quasi-linearization theory will be presented in this chapter. FRF measurements of nonlinear systems are also discussed. The methodology of modal identification and establishment of the modal model is presented.

In Chapter 3, implementation of the modal model of a nonlinear system in structural dynamic analysis is explained in detail. Computation of the forced harmonic response of a nonlinear system, once its modal model is obtained, to an arbitrary force level is given in the first section. Response prediction of a

nonlinear system coupled with a linear one using the modal model of the original nonlinear system, and the use of the modal model in structural modification analysis of a nonlinear system is presented. The numerical solution method employed in these harmonic response analyses is also given.

In Chapter 4, case studies to study the validity and efficiency of the presented methods are given. Case studies are selected such that all methods presented will be covered for different types of nonlinearities. In case studies theoretically generated FRFs are used as if they were results of harmonic vibration tests. In order to simulate and observe the effects of conditions in real measurements, selected case studies are solved by using polluted data. An experimental case study is also presented in the end.

In Chapter 5, brief summary of the work done is given with conclusions and discussion. Advantages and drawbacks of the methods are listed and finally, suggestions for future studies are made.

CHAPTER 2

MODAL IDENTIFICATION OF NONLINEAR STRUCTURES

2.1 Introduction

The theory of modal identification of nonlinear structures using quasi-linearization of structural nonlinearities, which outlines the basis of this study, will be presented in this chapter. The underlying theory is first established by Budak and Özgüven [24, 25] and has been used by several researchers. In section 2.2 and its subsections, the basics and the extension of the method presented by Budak and Özgüven will be given. FRF measurements of nonlinear systems are discussed in section 2.3. Force amplitude and response amplitude controlled measurements applied on nonlinear structures will be explained in separate subsections. In section 2.4, the methodology of modal identification and establishment of the modal model will be presented.

2.2 Forced Harmonic Response Characteristics of Nonlinear Structures

In the following subsections, separation of the linear and nonlinear forces in a nonlinear structure and representation of the nonlinear forces as matrix multiplication will be explained. The computation of the coefficient matrix is performed by two different methods, first being the “Iterative Receptance Method” presented by Budak and Özgüven [25] and the second one being a describing function based method proposed by Tanrıku et. al. [26]. In this thesis, computation by using the second method will be given due to its relevance to the concept.

2.2.1 Representation of Nonlinear Forces by the Nonlinearity Matrix

Consider the equation of motion of a nonlinear MDOF system:

$$[M]\{\ddot{x}\} + [C]\{\dot{x}\} + [K]\{x\} + i[H]\{x\} + \{N(x, \dot{x})\} = \{f\} \quad (2.1)$$

where matrices $[M]$, $[C]$, $[H]$ and $[K]$ represent the mass, viscous damping, structural damping and stiffness matrices, respectively. Vectors $\{x\}$ and $\{f\}$ stand for the response and external force applied on the system, respectively. The vector $\{N\}$ corresponds to the nonlinear internal forces in the system. This force vector is usually a function of displacement and/or velocity response, depending on the type of nonlinearity present in the system.

Considering a sinusoidal excitation at a frequency ω and assuming that the response is also harmonic at the same frequency, the forcing and response vectors can be written as;

$$\{f\} = \{F\} e^{i\omega t} \quad (2.2)$$

and

$$\{x\} = \{X\} e^{i\omega t} \quad (2.3)$$

respectively. The vector $\{X\}$ consists of complex values to accommodate phase information. As long as the above assumption holds, the nonlinear forces can also be accepted to be harmonic with the same frequency as follows,

$$\{N\} = \{G\} e^{i\omega t} \quad (2.4)$$

where $\{G\}$ is the amplitude vector of nonlinear forces. Substituting the equations (2.2), (2.3) and (2.4) in equation (2.1) the following equation is obtained,

$$([M]\omega^2 + i[C]\omega + [K] + i[H])\{X\} + \{G\} = \{F\} \quad (2.5)$$

Budak and Özgüven [24, 25] first suggested that nonlinear forces can be expressed in a matrix form. They developed a method for the harmonic vibration analysis of nonlinear structures, by which the amplitude vector of nonlinear forces can be expressed in the form,

$$\{G\} = [\Delta]\{X\} \quad (2.6)$$

where $[\Delta]$ is the response dependent “nonlinearity matrix”. Budak and Özgüven [25] gave a formulation to obtain the elements of $[\Delta]$ for polynomial type nonlinearities. This concept is then extended by Tanrikulu *et. al.* [26] with a new formulation to different kinds of nonlinearities by using describing functions. In the following section, the computation of $[\Delta]$ by using describing functions will be presented.

2.2.2 Describing Function Approach in the Computation of Nonlinearity Matrix

The well known describing function theory [27] is used for the quasi-linearization of nonlinearities. Here the use of this theory in computation of the nonlinearity matrix will be presented. Let us consider the r^{th} element of the vector $\{N\}$, N_r . Here r stands for the coordinate of concern and N_r is the sum of the nonlinear forces acting on this coordinate. Mathematically it can be expressed as

$$N_r = \sum_{j=1}^n n_{rj} \quad (2.7)$$

where n_{rj} represents the nonlinear force element between coordinates r and j for $j \neq r$ and between the coordinate r and the ground for $j = r$. depending on the type of the nonlinearity present in the system, n_{rj} is a function of the intercoordinate displacement and/or velocity such that

$$y_{rj} = x_r - x_j, \quad r \neq j \quad (2.8)$$

$$y_{rj} = x_r, \quad r = j \quad (2.9)$$

Since x_r and x_j are harmonic functions, y_{rj} can also be represented as a harmonic function. Using complex notation,

$$x_r = X_r e^{i\omega t} \quad (2.10)$$

$$x_j = X_j e^{i\omega t} \quad (2.11)$$

$$y_{rj} = Y_{rj} e^{i\omega t} \quad (2.12)$$

the harmonic input describing function v_{rj} for n_{rj} , such that v_{rj} provides the best average of the true restoring force, can be calculated using the following integral:

$$v_{rj} = \frac{i}{\pi Y_{rj}} \int_0^{2\pi} n_{rj} e^{-i\psi} d\psi, \quad \psi = \omega t \quad (2.13)$$

Derivation of v for various nonlinearity and input types can also be found in reference [27]. Using equation (2.6), the vector $\{N\}$ can now be written as

$$\{N\} = [\Delta] \{X\} e^{i\omega t} \quad (2.14)$$

Here the elements of $[\Delta]$ are given in terms of describing functions v_{rj} as follows:

$$\Delta_{rr} = v_{rr} + \sum_{\substack{j=1 \\ j \neq r}}^n v_{rj} \quad r = 1, 2, \dots, n \quad (2.15)$$

$$\Delta_{rj} = -v_{rj} \quad r \neq j \quad r = 1, 2, \dots, n \quad (2.16)$$

When the nonlinearity considered is localized between a single coordinate and the ground, $\{N\}$ includes only one nonzero element. Consequently, the nonlinearity matrix for the system consists of only one nonzero diagonal element v_{ii} , i being the coordinate where the nonlinear element is connected.

Substituting equation (2.6) into equation (2.5), yields

$$([M]\omega^2 + i[C]\omega + [K] + i[H] + [\Delta])\{X\} = \{F\} \quad (2.17)$$

Then the receptance matrix of the system can be written as:

$$\alpha(X, \omega) = [[M]\omega^2 + i[C]\omega + [K] + i[H] + [\Delta]]^{-1} \quad (2.18)$$

From equation (2.18) it is seen that the nonlinearity can be considered as an added equivalent stiffness matrix which is a function of the response amplitude. It should be noted that the term “pseudo receptance” should be used in case of a nonlinear system as it is not possible to talk about receptance for a nonlinear system.

2.3 Measurement of FRFs in Nonlinear Structures

As mentioned earlier, “pseudo FRF” is a better expression for the FRFs of nonlinear structures since they do not satisfy the conditions for an FRF. An FRF is simply a transfer function relating the response of the system to the force applied and does not change with varying force or response levels as long as the system is linear. However, for a nonlinear system, a measured FRF is valid only for the specific force or response level maintained during the test. In the following subsections these measurements are classified and explained with respect to the control parameter.

2.3.1 Force Amplitude Controlled FRFs

In this type of measurement, a constant amplitude harmonic force is applied over a frequency range. An FRF resulting from such a measurement is invariant of the force amplitude value in a linear system. To visualize, FRFs corresponding to different forcing levels end up as the same curve when graphically represented. In case of a nonlinear system, this type of measurement produces completely

different results. When a harmonic force with constant amplitude is applied over a frequency range on a nonlinear system, the nonlinear elements in the structure will act like equivalent dampings and/or stiffnesses with different values at each frequency. In other words, at every frequency the value of equivalent damping and/or stiffness will change which violates the definition of FRF. Variation of damping and/or stiffness values over the frequency range results in the distortion of the FRF, an indicative of nonlinearity. Another sign of nonlinearity in FRFs can be observed as the amplitude of the applied force varies. Unlike linear ones, nonlinear structures generate different curves with different forcing amplitudes. These facts can also be seen in Bode plot and Nyquist plot representations of FRFs of a nonlinear structure in Figure 3 and Figure 4, respectively.

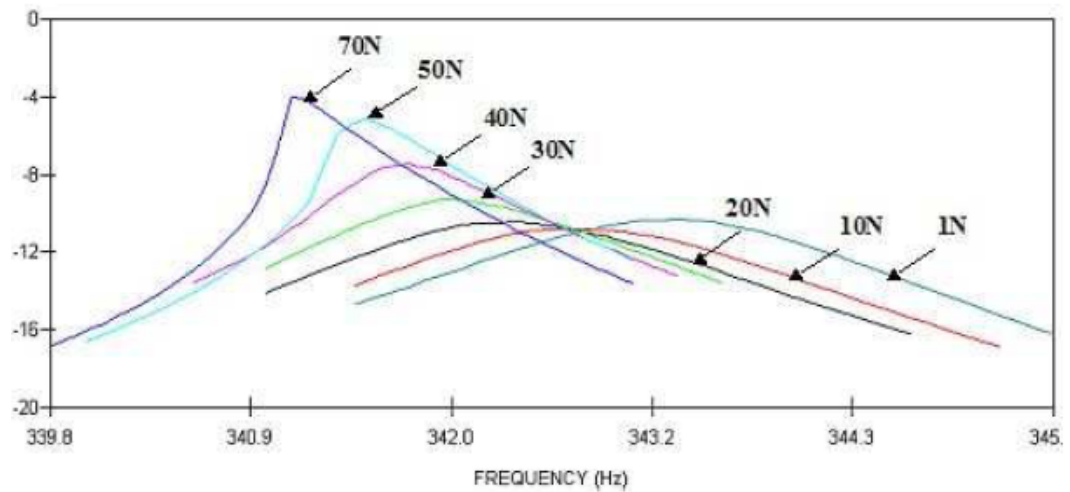


Figure 3. Bode plot representation of FRFs of a nonlinear structure at different forcing levels. [28]

This type of measurement is suitable to detect structural nonlinearity since FRF distortion is a good indicator. On the other hand, results of such a measurement are not proper for identification of modal parameters since linear analysis tools are not compatible with nonlinear systems and will give misleading results.

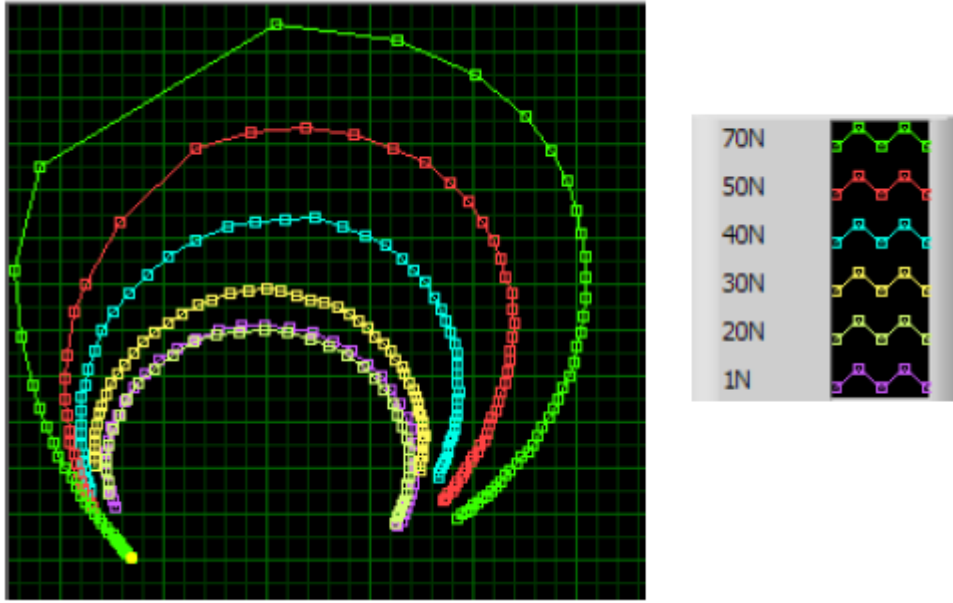


Figure 4. Nyquist plot representation of FRFs of a nonlinear structure at different forcing levels. [28]

2.3.2 Displacement Amplitude Controlled FRFs

When the response level is kept constant in a frequency sweep experiment, nonlinear elements will behave as equivalent *linear* elements, and the structure will behave linearly for that response level as discussed in [6] and experimentally shown in [28]. It can also be seen in equation (2.18) that the nonlinearity can be considered as an added equivalent stiffness matrix which is a function of the response amplitude, provided that the describing function for the nonlinearity is a function of the response amplitude only. Then, it can be concluded that response controlled measurements provide linear FRFs, each corresponding to a different response level, as can be seen in Figure 5 and Figure 6.

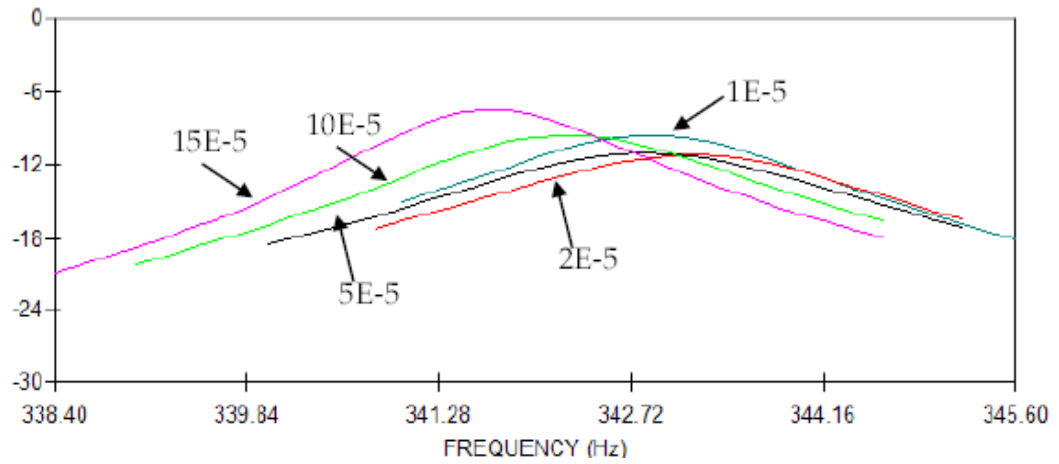


Figure 5. Bode plot representation of FRFs of a nonlinear structure at different response levels. [28]

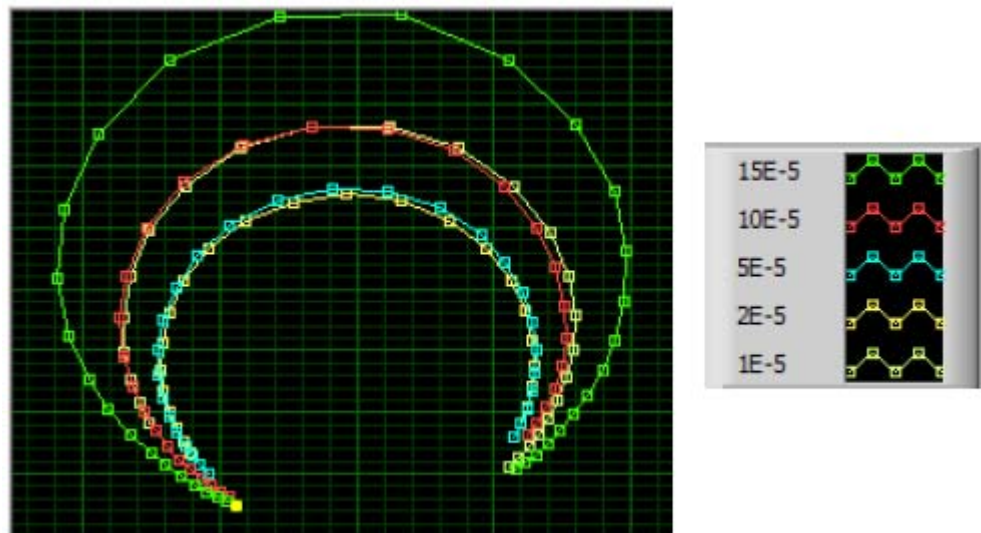


Figure 6. Nyquist plot representation of FRFs of a nonlinear structure at different response levels. [28]

Response controlled measurements can be performed by keeping the response amplitude of the nonlinear coordinate constant. Here the term “nonlinear coordinate” refers to the coordinate to which the nonlinear element is attached. If

the nonlinear element is localized between two arbitrary coordinates, the amplitude of the relative displacement between these coordinates is to be kept constant.

FRFs of linear structures are invariant of response amplitudes as well as force amplitudes. Hence, a sequence of measurement on a linear system by keeping the response amplitude constant will result in a set of overlapping curves that are indeed the same FRF.

2.4 Extraction of Modal Parameters – The Modal Model

One of the well known characteristic indicating nonlinearity in the FRF measurements is distortion especially around resonance frequencies. Linear modal identification tools are based on fitting FRF curves that show linear behavior. Consequently unreliable results are obtained. Özgüven and İmregün [15] investigated the results when linear identification is applied on a nonlinear system. Study resulted with complex modes although the system did not include nonproportional damping which is customary to assume when complex modes are encountered. In conclusion, linear identification of force amplitude controlled FRF of a nonlinear system will not present useful results other than specifying the system as nonlinear.

However, if an FRF of a nonlinear system is measured by keeping the response amplitude constant (with displacement controlled experiments), linear identification can be carried out, and a set of modal parameters for each response level can be obtained. As equation (2.18) indicates, nonlinearity in a system can be considered as an added system property matrix which is a function of the response amplitude. Therefore, the modal parameters can be expected to follow a pattern according to the nonlinearity present in the system. As the identified modal parameters vary with respect to the response amplitude Y_{rj} , they can be expressed as a function of Y_{rj} as follows

$$\omega_r = \omega_r(Y_{rj}) \quad (2.19)$$

$$\eta_r = \eta_r(Y_{rj}) \quad (2.20)$$

$${}_r A_{kl} = {}_r A_{kl}(Y_{rj}) \quad (2.21)$$

This model then can be used in harmonic response prediction of the non-linear system, as well as in coupling and modification analyses, which will be discussed in detail in next chapter.

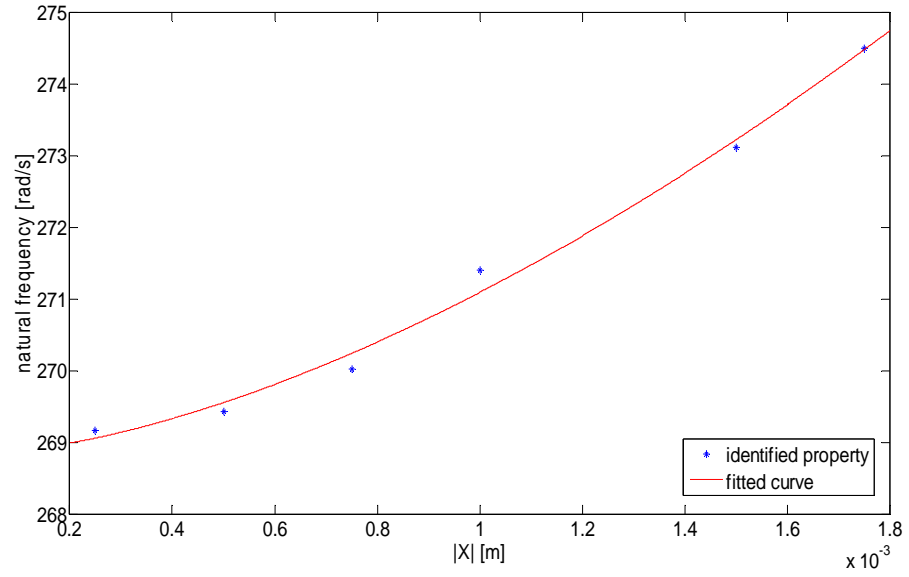


Figure 7. Natural frequencies of a nonlinear system identified at different forcing levels.

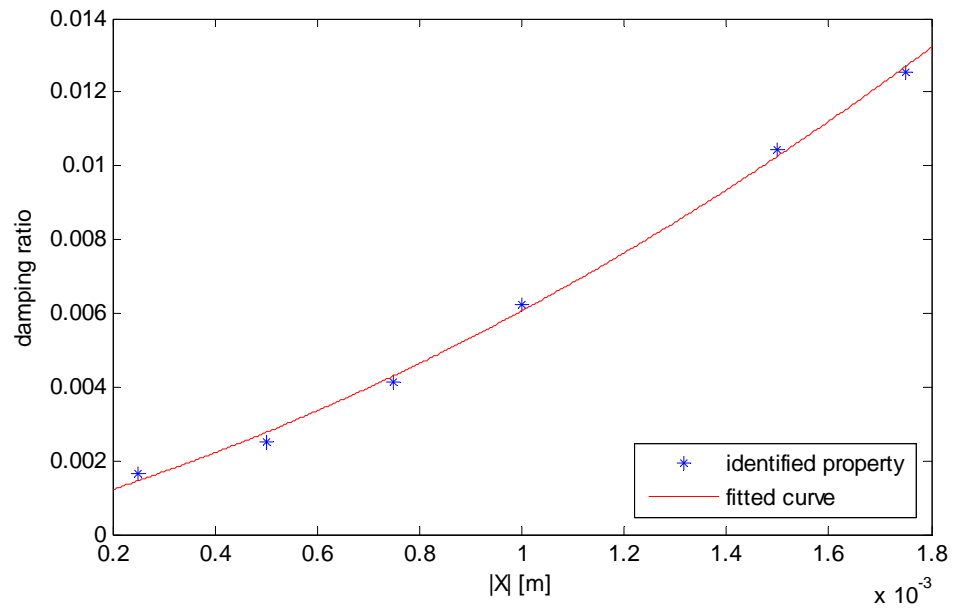


Figure 8. Damping ratios of a nonlinear system identified at different forcing levels

CHAPTER 3

HARMONIC RESPONSE ANALYSIS USING THE MODAL MODEL

In this chapter, implementation of the modal model of a nonlinear system in structural dynamic analysis will be explained in detail. In section 3.1 computation of the forced harmonic response of a nonlinear system, once its modal model is obtained, to an arbitrary force level is given. In section 3.2 response prediction of a nonlinear system coupled with a linear one using the modal model of the original nonlinear system is presented. In section 3.3 the use of the modal model in structural modification analysis of a nonlinear system is illustrated. The numerical solution method employed in these harmonic response analyses is presented in section 3.4.

3.1 Forced Harmonic Response Prediction Using the Modal Model

Once the variation of the nonlinear modal parameters with respect to the response amplitude is known, response of the system can be predicted applying an iterative solution method. In this section the theory of this approach will be given. The method is formulated with respect to the position of the nonlinear element, i.e. grounded or interconnected, in the system. In the following subsections 3.1.1 and 3.1.2 formulations for the systems possessing grounded nonlinear elements and interconnected nonlinear elements will be given, respectively.

3.1.1 Grounded Nonlinear Element

Consider a structurally damped nonlinear system in which the nonlinear element is localized between the i^{th} coordinate and ground, as shown in Figure 9.

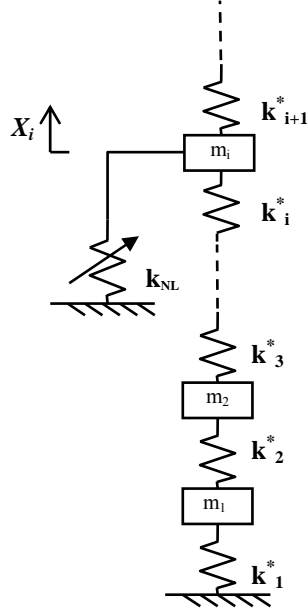


Figure 9. Discrete MDOF system possessing a grounded nonlinear element connected at the i^{th} coordinate. ($k_r^* = k_r + ih_r$).

Consider a number of harmonic vibration tests conducted on this system; each one performed by applying a harmonic force to an arbitrary coordinate while keeping X_i constant. FRFs resulting from these measurements are expected to show linear behavior, and therefore linear identification can be applied. Once the variation of the nonlinear modal parameters with respect to the response amplitude X_i is obtained as follows

$$\omega_r = \omega_r(X_i) \quad (3.1)$$

$$\eta_r = \eta_r(X_i) \quad (3.2)$$

$${}_r A_{kl} = {}_r A_{kl}(X_i) \quad (3.3)$$

they can be used to write the pseudo receptance expression of the system as a modal summation in terms of the modal parameters identified:

$$\alpha_{ij}(\omega, X_i) = \sum_{r=1}^n \frac{{}_r A_{ij}(X_i)}{(\omega_r(X_i))^2 - \omega^2 + i(\omega_r(X_i))^2 \eta_r(X_i)} \quad (3.4)$$

Then the harmonic response amplitude X_i can be written as

$$X_i = |\alpha_{ij}(\omega, X_i)| F_j \quad (3.5)$$

Here, F_j is the amplitude of the harmonic force applied at j^{th} coordinate and α_{ij} is the response level dependent receptance value. Note that the formulation above is given for a structurally damped system. In case of a system with viscous damping, damping ratio, ξ , is to be identified and included in the modal model, instead of the loss factor, η . Receptance expression for such a system also shows difference. Should the system given in Figure 9 be viscously damped, the term $2i\omega\omega_r(X_i)\zeta_r(X_i)$ in equation (3.4) will replace $i(\omega_r(X_i))^2 \eta_r(X_i)$.

For a specific value of ω , equation (3.5) becomes an implicit equation in X_i . Then, it can be solved with an iterative approach such that modal parameters are updated at each iteration step. Updating procedure is simply replacing the modal parameters with the ones corresponding to the newly obtained X_i value. Once a convergent solution is reached for X_i , then the rest of the response amplitudes X_j ($j = 1, 2, \dots, n, j \neq i$) can be calculated directly by using the modal data corresponding to the convergent response value, X_i . Note that this solution will be valid only for the case where there is a harmonic force with amplitude F_j applied at the j^{th} coordinate.

3.1.2 Interconnected Nonlinear Element

Consider a structurally damped nonlinear system possessing a nonlinear element between the coordinates r and q , as shown in Figure 10. Using complex notation,

$$x_r = X_r e^{i\omega t} \quad (3.6)$$

$$x_q = X_q e^{i\omega t} \quad (3.7)$$

where X_r and X_q are the complex response amplitudes of the coordinates r and q , respectively. Let us define a variable Y_{rq} as the amplitude of the relative displacement between the coordinates, such that

$$Y_{rq} = |X_r - X_q| \quad (3.8)$$

In order to obtain linearized FRFs of such a system so that linear identification can be applied, the relative displacement amplitude between the two coordinates, to which the nonlinear element is connected, is to be kept constant. Then the variations of the modal parameters are to be obtained with respect to the relative displacement amplitude, Y_{rq} , as follows:

$$\omega_r = \omega_r(Y_{rq}) \quad (3.9)$$

$$\eta_r = \eta_r(Y_{rq}) \quad (3.10)$$

$${}_r A_{kl} = {}_r A_{kl}(Y_{rq}) \quad (3.11)$$

Then they can be used to write the pseudo receptance expression of the system in a similar way. In this case, one needs to state two receptance expressions, since the iteration parameter is the difference of two response amplitudes.

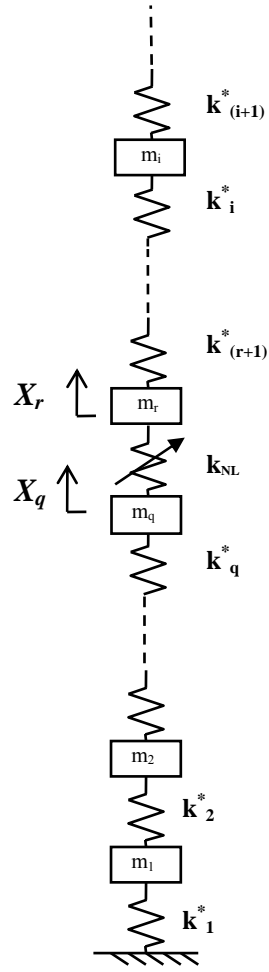


Figure 10. Discrete MDOF system possessing a nonlinear element between the coordinates q and r . ($k_r^* = k_r + i \cdot h_r$).

Consider a harmonic force of amplitude F_j applied at j^{th} coordinate. Then,

$$X_r = \alpha_{rj} F_j \quad (3.12)$$

$$X_q = \alpha_{qj} F_j \quad (3.13)$$

Using equations (3.8), (3.12) and (3.13), the relative response amplitude Y_{rq} can be written as

$$Y_{rq} = |\alpha_{rj} - \alpha_{qj}| F_j \quad (3.14)$$

where α_{rj} and α_{qj} are the response level dependent receptance values and they can be expressed in terms of the modal parameter variations as follows:

$$\alpha_{rj}(\omega, Y_{rq}) = \sum_{r=1}^n \frac{{}_r A_{rj}(Y_{rq})}{\left((\omega_r(Y_{rq}))^2 - \omega^2 + i (\omega_r(Y_{rq}))^2 \eta_r(Y_{rq}) \right)} \quad (3.15)$$

$$\alpha_{qj}(\omega, Y_{rq}) = \sum_{r=1}^n \frac{{}_r A_{rj}(Y_{rq})}{\left((\omega_r(Y_{rq}))^2 - \omega^2 + i (\omega_r(Y_{rq}))^2 \eta_r(Y_{rq}) \right)} \quad (3.16)$$

respectively.

In equation (3.14) the iteration parameter is Y_{rq} , consequently a convergent value for Y_{rq} is sought in order to obtain the response of the system for that specific forcing level. The algorithm is simply updating the modal parameters in equations (3.15) and (3.16) with respect to current Y_{rq} value and substituting in equation (3.14) to get the new Y_{rq} value. Once a convergent value for Y_{rq} is reached, then the rest of the response amplitudes can be calculated directly by using the modal data corresponding to the convergent relative response value. Note that this solution will be valid only for the case where there is a harmonic force with amplitude F_j applied at the j^{th} coordinate.

3.2 Structural Coupling Analysis Using the Modal Model

The idea presented in the preceding section can be extended so that it can be employed in dynamic analyses of nonlinear systems coupled with linear ones using the receptance coupling method. Receptance values for a linear system can be found experimentally or computationally by linear modal analysis tools. For nonlinear system, receptance values are to be constructed via modal summation by using identified response dependent modal parameters, as explained earlier.

Consider a linear and a nonlinear system with structural damping to be coupled rigidly as in Figure 11.

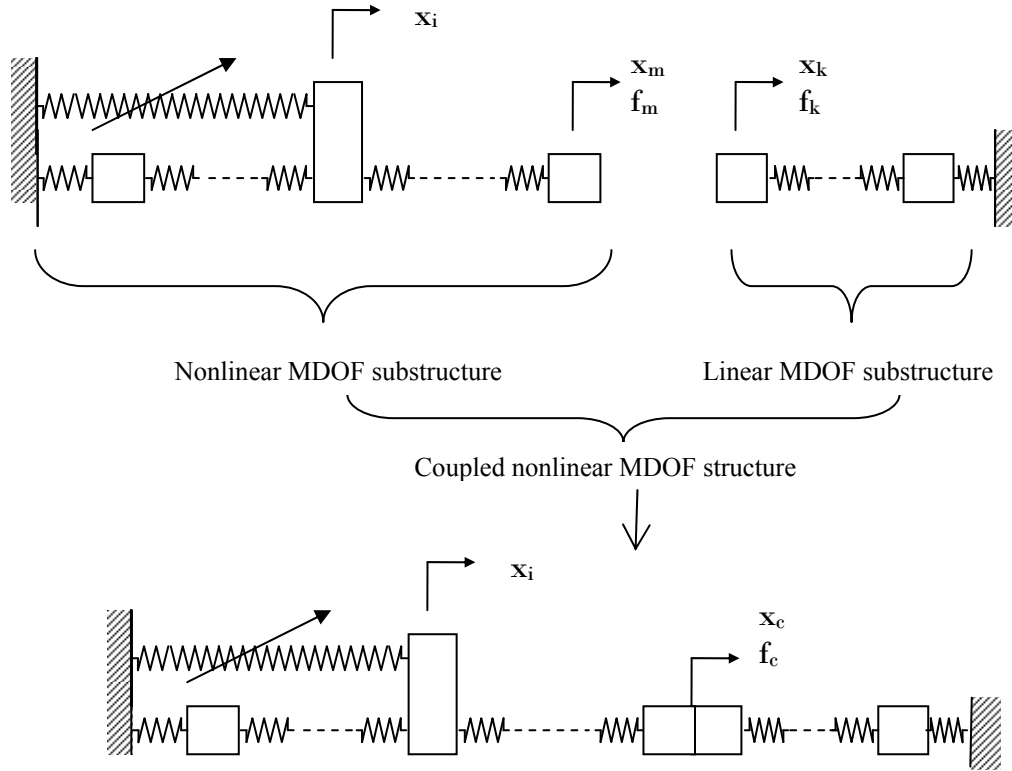


Figure 11. A nonlinear MDOF system coupled with an MDOF linear system (both systems are structurally damped).

The receptance matrices of the nonlinear and linear substructures are as follows, respectively

$$[\alpha_{NL}] = \begin{bmatrix} \alpha_{mm} & [\alpha_{mn}] \\ [\alpha_{nm}] & [\alpha_{nn}] \end{bmatrix} \quad (3.17)$$

$$[\alpha_L] = \begin{bmatrix} \alpha_{kk} & [\alpha_{kl}] \\ [\alpha_{lk}] & [\alpha_{ll}] \end{bmatrix} \quad (3.18)$$

where m and k refer to the coordinates to be coupled, n and l represent the rest of the coordinates in the nonlinear and linear systems, respectively.

For the linear substructure, the following equation can be written.

$$\{x_L\} = [\alpha_L] \{f_L\} \quad (3.19)$$

where $\{x_L\}$ and $\{f_L\}$ are the response and forcing vectors of the linear system, respectively, and $[\alpha_L]$ is the receptance matrix relating these vectors. Displacement vector in equation (3.19) is partitioned as follows

$$\{x_L\} = \begin{Bmatrix} x_k \\ \{x_l\} \end{Bmatrix} \quad (3.20)$$

Here x_k is the displacement of the single mass at the free end and $\{x_l\}$ represents the displacements of the rest of the masses. Using this partitioned displacement vector, following equations for the linear substructure can be written

$$x_k = \alpha_{kk} f_k + [\alpha_{kl}] \{f_l\} \quad (3.21)$$

$$\{x_l\} = [\alpha_{lk}] f_k + [\alpha_{ll}] \{f_l\} \quad (3.22)$$

where f_k and $\{f_l\}$ represent the external forces at the coordinates k and l .

Equations for the nonlinear system can be written similarly where the displacement vector is partitioned as

$$\{x_{NL}\} = \begin{Bmatrix} x_m \\ \{x_n\} \end{Bmatrix} \quad (3.23)$$

where x_m is the displacement of the free end of the system and $\{x_l\}$ represents the displacements of the rest of the coordinates. Note that the coordinate where the nonlinear element is connected is included in $\{x_n\}$. Then,

$$x_m = \alpha_{mm} f_m + [\alpha_{mn}] \{f_n\} \quad (3.24)$$

$$\{x_n\} = [\alpha_{nm}] f_m + [\alpha_{nn}] \{f_n\} \quad (3.25)$$

As mentioned in the preceding sections of this chapter, the receptance expressions in equations (3.24) and (3.25) can be written as a modal summation, thus they are functions of frequency and displacement amplitude of the i^{th} coordinate of the nonlinear system:

$$x_m = \alpha_{mm}(\omega, X_i) f_m + [\alpha_{mn}(\omega, X_i)] \{f_n\} \quad (3.26)$$

$$\{x_n\} = [\alpha_{nm}(\omega, X_i)] f_m + [\alpha_{nn}(\omega, X_i)] \{f_n\} \quad (3.27)$$

Recall that X_i is the amplitude of x_i , displacement of the coordinate where the nonlinear element is connected. The notation in equations (3.26) and (3.27) will not be used through the derivations, and instead the notation in equations (3.24) and (3.25) will be used for simplicity.

At the connection node, the following compatibility equations hold true when the substructures are coupled rigidly:

$$x_m = x_k \quad (3.28)$$

$$f_m = -f_k \quad (3.29)$$

Substituting equations (3.21) and (3.24) in equation (3.28) and rearranging to obtain f_m yield

$$f_m = \frac{[\alpha_{kl}] \{f_l\} - [\alpha_{mn}] \{f_n\}}{\alpha_{mm} + \alpha_{kk}} \quad (3.30)$$

Equation (3.30) can be used in equation (3.22) to obtain the following relation

$$\{x_n\} = \frac{[\alpha_{nm}][\alpha_{kl}]}{\alpha_{mm} + \alpha_{kk}} \{f_l\} + \left(\alpha_{nn} - \frac{[\alpha_{nm}][\alpha_{mn}]}{\alpha_{mm} + \alpha_{kk}} \right) \{f_n\} \quad (3.31)$$

From equation (3.31), two of the receptance expressions of the coupled system can be obtained.

$$[\alpha_{nl}^C] = \frac{[\alpha_{nm}][\alpha_{kl}]}{\alpha_{mm} + \alpha_{kk}} \quad (3.32)$$

$$[\alpha_{nn}^C] = \alpha_{nn} - \frac{[\alpha_{nm}][\alpha_{mn}]}{\alpha_{mm} + \alpha_{kk}} \quad (3.33)$$

Equation (3.30) can be rewritten to obtain f_k

$$f_k = \frac{[\alpha_{mn}]\{f_n\} - [\alpha_{kl}]\{f_l\}}{\alpha_{mm} + \alpha_{kk}} \quad (3.34)$$

Substituting equation (3.34) into equation (3.25) and reorganizing the following relation, from which the remaining receptance expressions can be extracted, is obtained:

$$\{x_l\} = \frac{[\alpha_{lk}][\alpha_{mn}]}{\alpha_{mm} + \alpha_{kk}} \{f_n\} + \left([\alpha_{ll}] - \frac{[\alpha_{lk}][\alpha_{kl}]}{\alpha_{mm} + \alpha_{kk}} \right) \{f_l\} \quad (3.35)$$

$$[\alpha_{ln}^C] = \frac{[\alpha_{lk}][\alpha_{mn}]}{\alpha_{mm} + \alpha_{kk}} \quad (3.36)$$

$$[\alpha_{ll}^C] = [\alpha_{ll}] - \frac{[\alpha_{lk}][\alpha_{kl}]}{\alpha_{mm} + \alpha_{kk}} \quad (3.37)$$

Equations (3.32), (3.33), (3.36) and (3.37) can be combined to form the complete receptance matrix of the coupled system.

$$\begin{bmatrix} \alpha^c \end{bmatrix} = \begin{bmatrix} \begin{bmatrix} \alpha_{nn}^c \end{bmatrix} & \begin{bmatrix} \alpha_{nl}^c \end{bmatrix} \\ \begin{bmatrix} \alpha_{ln}^c \end{bmatrix} & \begin{bmatrix} \alpha_{ll}^c \end{bmatrix} \end{bmatrix} \quad (3.38)$$

In equations (3.26) and (3.27), response dependency of the receptance expressions of the nonlinear system was shown. As those equations are used throughout the derivation, it is obvious that the final receptance matrix of the coupled system is also X_i dependent.

$$\begin{bmatrix} \alpha^c \end{bmatrix} = \begin{bmatrix} \alpha^c(\omega, X_i) \end{bmatrix} \quad (3.39)$$

Once the receptance matrix of the assembled system is written in terms of X_i as in equation (3.39), response of the system at any force level can be found by the same methodology explained in this section.

In the coupling analysis presented up to here, the formulation for two single coordinates to be coupled is given for simplicity. However, the extension of the formulations for coupling of multiple coordinates is also straightforward. Let the number of coordinates to be coupled be r . Then the partitioning of response vectors, given with equations (3.20) and (3.23) are performed with the same approach, only x_k and x_m being vectors of size r instead of single values. Consequently, the size of the receptance expressions will also change and the terms in the denominator in above formulation will appear as matrix inversion and multiplication.

In the coupling analysis explained above, an important point is not to take the coordinate where the nonlinear element is connected as a connection node. This restriction is due to the nature of receptance coupling method. In receptance coupling method, information related to the coupling nodes are not available in the receptance matrix of the coupled system. This is an undesired situation in this study since the displacement amplitude of the coordinate where the nonlinear element is connected is needed in order to carry out the dynamic analysis of the system. Ferreira [29] presented a ‘‘Refined Formulation of FRF Coupling’’ which

enables to keep the information related to the coupling nodes. Employment of the algorithm can remove the restriction of coupling node selection.

3.3 Structural Modification Analysis Using the Modal Model

The basic methodology presented in section 3.1 can also be implemented in structural modification problems. In this section, the formulation of this implementation is given. The theory is closely related to the work presented by Özgüven [30]. For simplicity, the theory for linear systems [30] will be given first.

Consider a MDOF linear system subject to modification as shown in Figure 12.

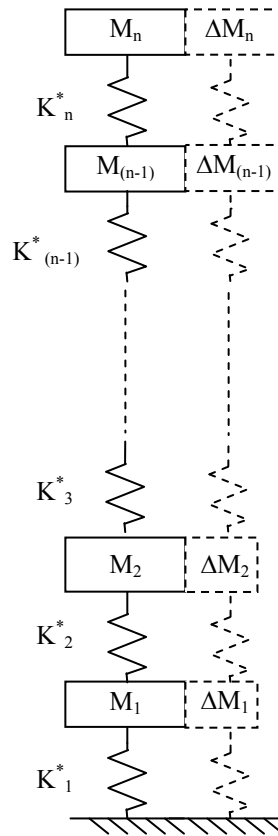


Figure 12. A discrete MDOF linear system subject to modification.

Receptance matrix, $[\alpha]$ of the original (before modification) system can be written as:

$$[\alpha] = [K - \omega^2 [M] + i[H]]^{-1} \quad (3.40)$$

where $[K]$, $[M]$ and $[H]$ are the stiffness, mass and structural damping matrices of the system, respectively. When this system is modified without increasing the total degrees of freedom of the system, the receptance matrix $[\gamma]$ of the modified structure can be written as:

$$[\gamma] = [K + [\Delta K] - \omega^2 [M + [\Delta M]] + i[H + [\Delta H]]]^{-1} \quad (3.41)$$

where $[\Delta K]$, $[\Delta M]$ and $[\Delta H]$ represent the stiffness, mass and damping matrices of the modifying structure, respectively. Inverting both sides of equations (3.40) and (3.41), and then combining them yields

$$[\gamma]^{-1} = [\alpha]^{-1} + [D] \quad (3.42)$$

where $[D]$ denotes the dynamic structural modification matrix and is expressed as

$$[D] = [\Delta K] - \omega^2 [\Delta M] + i[\Delta H] \quad (3.43)$$

When all terms of the equation (3.42) are premultiplied by $[\alpha]$ and postmultiplied by $[\gamma]$, the following relation is obtained:

$$[\alpha] = [\gamma] + [\alpha][D][\gamma] \quad (3.44)$$

Using this relation, $[\gamma]$ can be obtained as:

$$[\gamma] = [I + [\alpha][D]]^{-1} [\alpha] \quad (3.45)$$

Now if we apply the same modification method to a nonlinear system, then $[\alpha]$ in equation (3.45) will be the pseudo receptance matrix of the nonlinear system which can be obtained by modal synthesis by using identified response dependent modal parameters of the nonlinear system. Response dependent modal parameters are to be identified from the FRFs of unmodified nonlinear system, measured at different response levels as discussed in section 2.4.

The response dependent pseudo receptance of the modified system will then be given by

$$\left[\gamma(\omega, X_i) \right] = \left[[I] + [\alpha(\omega, X_i)][D] \right]^{-1} [\alpha(\omega, X_i)] \quad (3.46)$$

Once the receptance matrix of the modified system is written in terms of X_i as in equation (3.46), i being the coordinate where the nonlinear element is connected, response of the system at any force level can be found by the same methodology explained in this chapter.

3.4 Numerical Solution Technique

In the methods presented in this chapter, an implicit equation is reached so it can be solved iteratively with a proper numerical solution method for a given ω and the response of the system for that particular forcing can be achieved. In this thesis, the fixed point iteration method is used for the numerical solution of this final equation. For simplicity, the algorithm for the solution for a SDOF nonlinear system with is given first.

The implicit equation obtained in the end of the response prediction procedure can be expressed as

$$(X)_{p+1} = \left| \alpha(\omega, (X)_p) \right| \cdot F \quad (3.47)$$

where $(X)_{p+1}$ is the response amplitude of the nonlinear coordinate at $(p+1)^{th}$ iteration step and $\alpha(\omega, (X)_p)$ is the pseudo receptance expression at frequency ω and p^{th} iteration step. In equation (3.47), $\alpha(\omega, (X)_p)$ is expressed in terms of the modal parameters corresponding to the p^{th} iteration step as follows:

$$\alpha(\omega, (X)_p) = \frac{A((X)_p)}{\left(\left(\omega_n((X)_p) \right)^2 - \omega^2 + i \left(\omega_n((X)_p) \right)^2 \eta((X)_p) \right)} \quad (3.48)$$

for a structurally damped system, where ω_n is the natural frequency of the system.

The pseudo receptance expression given by equation (3.48) is updated at every iteration step. Iterations are to be repeated until a specified tolerance is reached. The convergence criteria is specified as

$$e_p = \frac{|(X)_{p+1} - (X)_p|}{|(X)_p|} \times 100 \quad (3.49)$$

The starting value for the iterations is taken as the linear solution of the system at the first frequency value. For the following frequencies, the convergent X value corresponding to the previous frequency point is used as the initial value. Similarly, the solution is carried out starting from the last frequency point and continuing with decreasing frequency values. If the nonlinearity in the system involves multiple solutions for certain frequency ranges, simply known as jump phenomena, it can be observed in the system when the solution of equation (3.47) is performed for both frequency sweep directions.

In case the system to be analyzed is a MDOF system with a grounded nonlinear element connected at i^{th} coordinate, the equation of concern is written as:

$$X_i = |\alpha_{ij}(\omega, X_i)| \cdot F_j \quad (3.50)$$

where X_i is the harmonic response amplitude of the i^{th} coordinate, ω is the frequency, F_j is the amplitude of the harmonic force applied at j^{th} coordinate and α_{ij} is the response level dependent receptance value. In this case, α_{ij} is expressed as a modal summation where the all the modal parameters corresponding to the p^{th} iteration step are used in the calculation, as follows:

$$\alpha_{ij}(\omega, (X_i)_p) = \sum_{r=1}^n \frac{r A_{ij}((X_i)_p)}{\left(\left(\omega_r((X_i)_p) \right)^2 - \omega^2 + i \left(\omega_r((X_i)_p) \right)^2 \eta_r((X_i)_p) \right)} \quad (3.51)$$

At the frequencies where the system shows linear behavior, convergence is achieved rapidly. However, at other frequencies which are near resonance, convergence can be difficult to obtain with the plain fixed point iteration method. In such cases, convergence is obtained by using a weighted average displacement, $(X_i)_{p+1}^*$, instead of $(X_i)_{p+1}$, in calculating $(\alpha_{ij})_{p+1}$, as follows:

$$(X_i)_{p+1}^* = \lambda (X_i)_{p+1} + (1 - \lambda) (X_i)_p \quad (3.52)$$

In equation (3.52), λ is a weighting factor that is assigned a value between 0 and 2. For the values of λ between 0 and 1, previous value is weighted more and this is called underrelaxation. It is employed to make a non-convergent system to converge or hasten convergence by dampening out oscillations. For the values of λ between 1 and 2, present value is weighted more and this is called overrelaxation. This type of weighting is designed to accelerate the convergence of an already convergent system.

CHAPTER 4

CASE STUDIES

In this chapter, case studies to demonstrate the validity and efficiency of the presented methods are given.

4.1 Forced Harmonic Response Prediction

In this section, implementation of the method presented in section 3.1 on systems with different types of nonlinear elements is given.

4.1.1 Case Study 1

A 5-DOF structurally damped system with a grounded cubic stiffness element, as shown in

Figure 13, under harmonic forcing is examined.

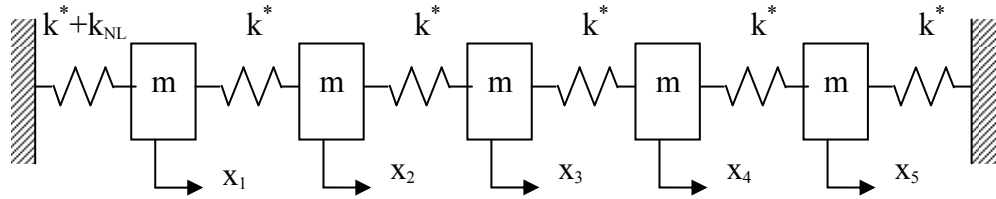


Figure 13. Five DOF system with grounded cubic stiffness.

System parameters for the given discrete system are as follows:

$$m = 1 \text{ kg}, k^* = 50000(1 + i0.01) \text{ N/m}, k_{NL} = bx_1^2, b = 10^7 \text{ N/m}^3$$

As explained in section 2.4, FRFs obtained by displacement controlled tests are identified to construct the modal model of the system. 8 FRFs are generated theoretically, each corresponding to a simulated test performed with a different displacement amplitude. The values of the displacement amplitude, X_1 , start with 1 cm and continue with 0.5 cm increment. In Figure 14 and Figure 15, point and transfer FRFs corresponding to these values are presented, respectively. Limited number of the FRFs are shown in the figure for simplicity. It is possible to observe the linear behavior of each curve and also the trend in shifting of resonance peaks which is an indication of hardening stiffness.

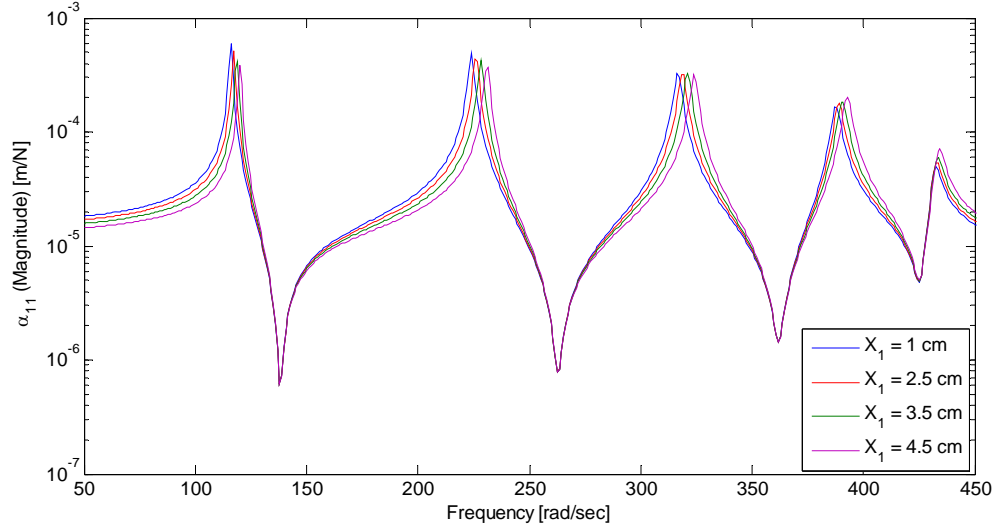


Figure 14. Point FRFs generated at constant displacement amplitudes

Modal parameters corresponding to each FRF are extracted using modal identification. As mentioned earlier, linear identification can be easily used with these FRFs since they show linear behavior. Identification of the modal parameters is performed by the formulation presented by Richardson and Formenti [31]. They introduced a least squared error parameter estimation

technique based on the fact that the frequency response measurement of a linear, second order dynamical system can be represented as a ratio of two polynomials. Natural frequencies, damping ratios and modal constants of the system are obtained using this technique. Magnitude and phase of the modal constant are identified as two separate parameters, as modal constant is a complex quantity for a damped system.

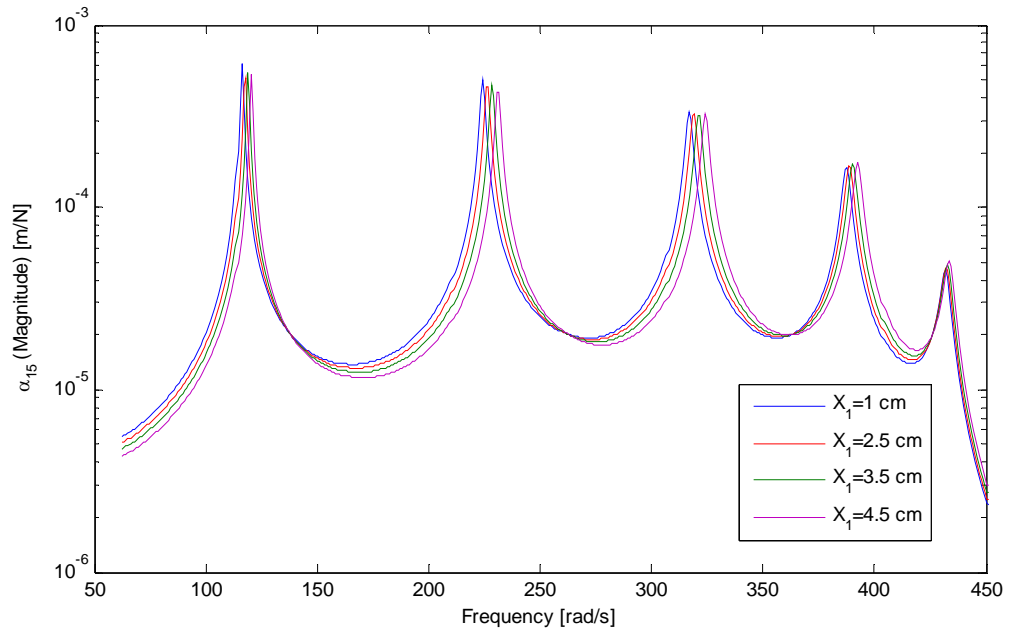


Figure 15. Transfer FRFs generated at constant displacement amplitudes

Identified modal parameters corresponding to the first mode for each set of FRFs are listed in Table 1 and Table 2 to set an example for the variation of parameters with response amplitude.

Table 1. Modal parameters obtained by identification of constant displacement point FRFs (α_{11})

Displacement amplitude [mm]	Natural frequency [rad/s]	Damping ratio [%] (structural damping model)	Modal constant	
			Magnitude	Phase (degrees)
10	116.02	1.0051	0.0817	-0.7639
15	116.35	0.9991	0.0798	-0.7525
20	116.79	0.9930	0.0771	-0.7379
25	117.33	0.9836	0.0739	-0.7192
30	117.97	0.9748	0.0702	-0.6983
35	118.67	0.9661	0.0662	-0.6731
40	119.43	0.9567	0.0619	-0.6459
45	120.22	0.9476	0.0575	-0.6175

Table 2. Modal parameters obtained by identification of constant displacement transfer FRFs (α_{15})

Displacement amplitude [mm]	Natural frequency [rad/s]	Damping ratio [%] (structural damping model)	Modal constant	
			Magnitude	Phase (degrees)
10	116.02	0.9962	0.0828	-0.2966
15	116.34	0.9908	0.0821	-0.2906
20	116.79	0.9937	0.0812	-0.2823
25	117.33	0.9855	0.0800	-0.2717
30	117.96	0.9666	0.0786	-0.2590
35	118.66	0.9574	0.0769	-0.2445
40	119.42	0.9484	0.0751	-0.2283
45	120.21	0.9400	0.0731	-0.2107

It can be seen in Table 1 and Table 2 that modal parameters follow a visible pattern which allows fitting proper functions for every set of parameters with respect to displacement amplitude. It is also possible to observe that natural frequencies and damping ratios are approximately the same for both FRF sets whereas modal constants are different. This is an expected result since natural frequency and damping ratio are modal parameters independent of the identified FRF but modal constant is not and needed to be identified for each element of the FRF matrix. Identification of sets of both point and transfer FRFs are necessary in order to calculate the desired pseudo FRF since the corresponding modal constants are required.

Graphical representation of the identified parameters from point FRFs and the fitted curves are shown in Figures 15 – 19, each set in a figure corresponding to a mode.

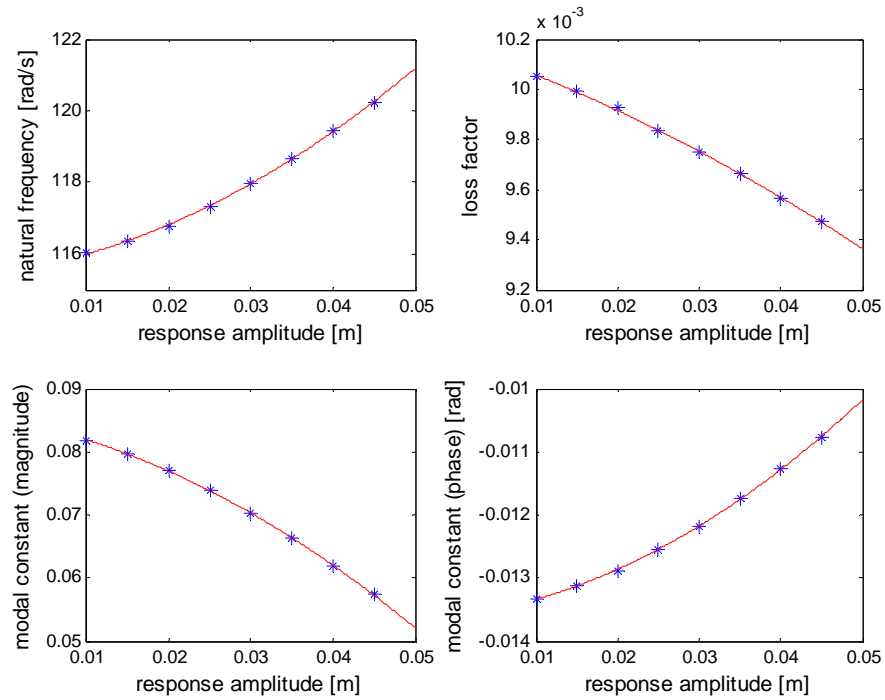


Figure 16. Variation of the modal parameters of the first mode with respect to response amplitude, X_1 . (* identified parameters, — fitted curve)

As can be seen from the figures, modal parameters of the nonlinear system follow a trend and therefore they can be expressed in terms of proper mathematical functions that fit to the corresponding data points. In practical applications points are expected to be scattered due to measurement errors. Since analytical expressions are fit to modal data points, it is expected that having scattered data does not affect the results significantly.

For the system in this case study, relation between the identified modal parameters and the response amplitude of the first coordinate are finely represented with second order polynomials. This can be taken as a result of the form of describing function for cubic stiffness type nonlinearity.

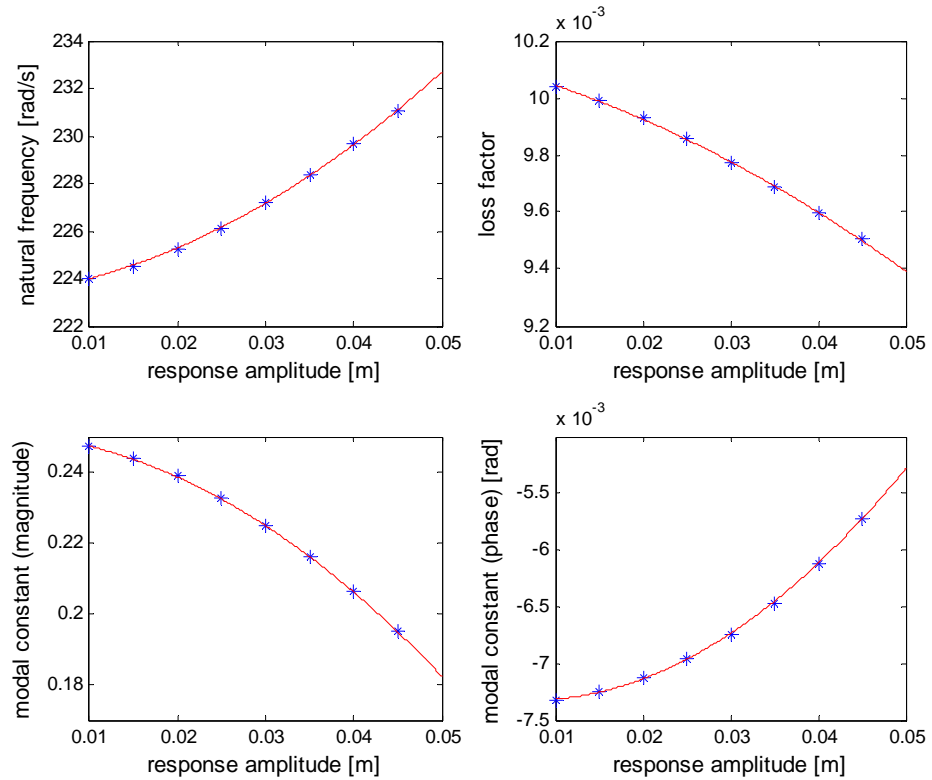


Figure 17. Variation of the modal parameters of the second mode with respect to response amplitude, X_1 . (* identified parameters, — fitted curve)

A typical result of hardening stiffness can be obtained from natural frequency versus displacement amplitude curves, in which the natural frequency increases with increasing displacement amplitude. Should the system have softening stiffness, simply a negative nonlinear stiffness coefficient, the natural frequencies would decrease with increasing displacement amplitude.

One should be observant in selection of the displacement amplitudes to be set in constant displacement amplitude tests in order to obtain a set of modal parameters that describe the behavior of the nonlinear system well enough. If the range of displacement amplitudes is kept narrow, resulting modal parameters are expected to be approximate, which prevents the observation of the trend of the parameters clearly to fit a proper function. This fact, however, may require performance of harmonic vibration tests with relatively large displacement amplitudes and is a drawback of this method.

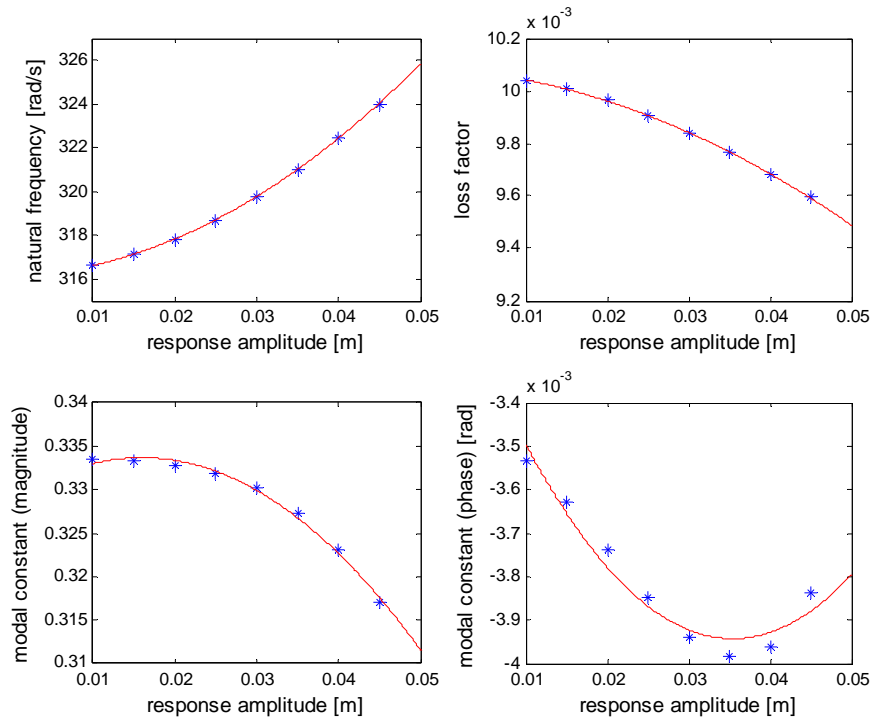


Figure 18. Variation of the modal parameters of the third mode with respect to response amplitude, X_1 . (* identified parameters, — fitted curve)

The functions that are fit to the modal data are used in pseudo receptance expression of the system by modal summation as explained in section 3.1. Frequency response of the system at different forcing levels is calculated by using the modal model.

Pseudo point receptance values calculated for forcing level of 100 N by using the modal parameters identified are presented in Figures 20 – 22. The force is applied at the first mass to which the nonlinear element is connected. The match of the responses obtained from the modal model with those calculated by harmonic balance method demonstrates the validity of the modal model and the approach suggested. Note that both approaches are valid if the basic assumption (harmonic excitation results in harmonic response at the same frequency) holds true.

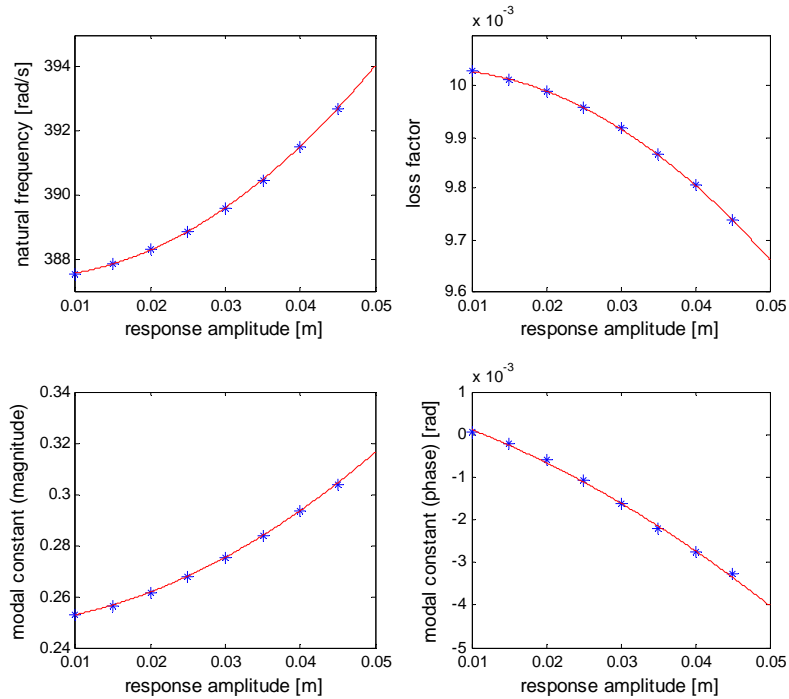


Figure 19. Variation of the modal parameters of the fourth mode with respect to response amplitude, X_1 . (* identified parameters, — fitted curve)

Figure 21 and Figure 22 show solutions for increasing and decreasing frequency sweeps with that of harmonic balance solution, respectively. Slight differences are observed between the results of this study and the harmonic balance method only around jump frequency, and it is believed that they are due to expressing of modal parameters with analytical functions unlike exact describing functions as in the harmonic balance method.

In Figure 23 a close up view of first two modes of the pseudo point receptance of the system for forcing level of 100 N calculated with both frequency sweep directions is shown. Similarly in Figure 24, response of the system to a force level of 250 N covering the frequencies of the third and fourth modes calculated with both sweep directions are presented. In both figures, a jump phenomenon is apparent.

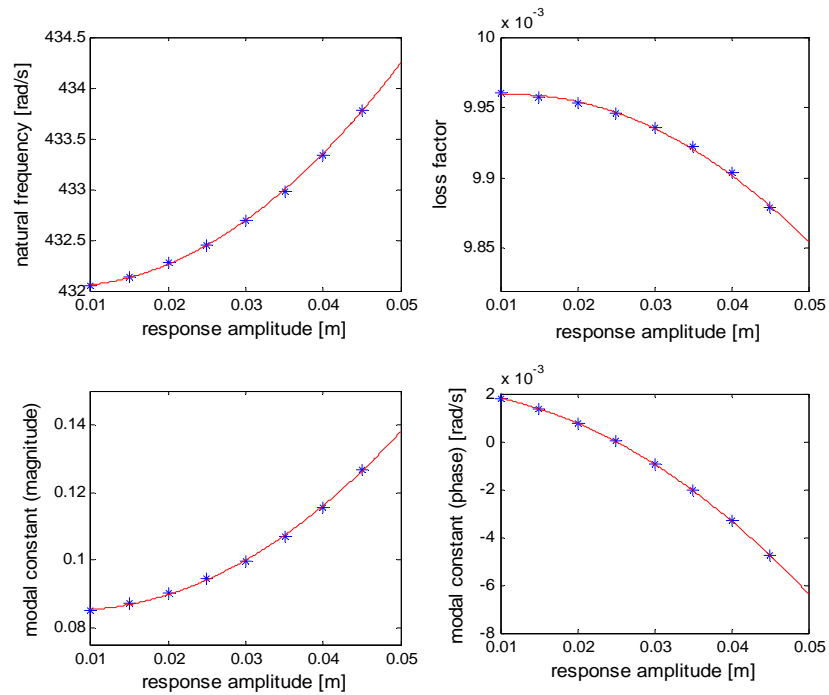


Figure 20. Variation of the modal parameters of the fifth mode with respect to response amplitude, X_1 . (* identified parameters, — fitted curve)

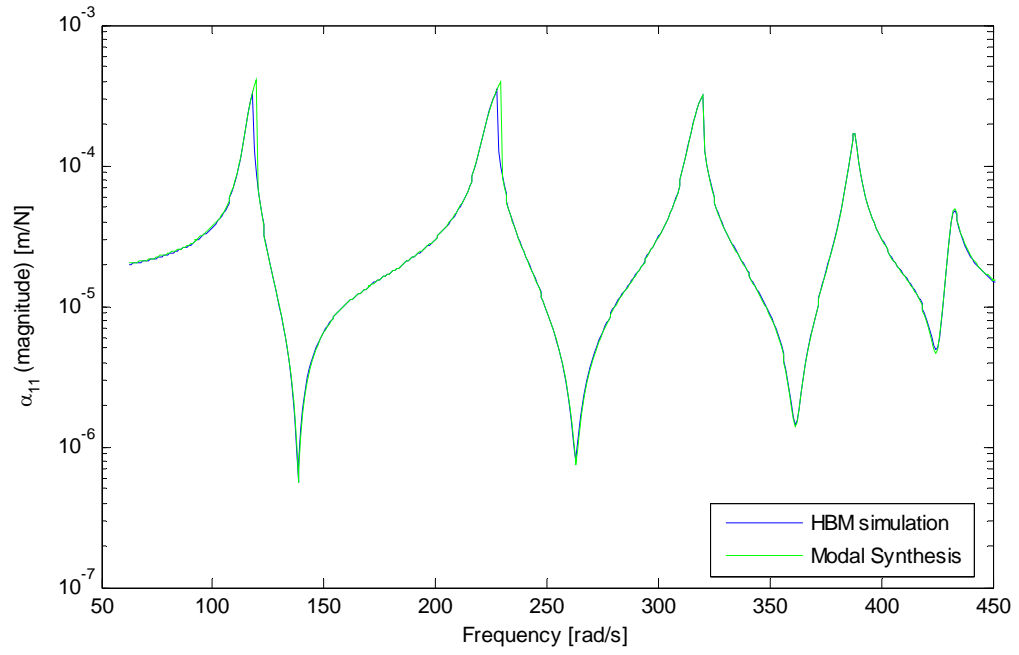


Figure 21. Frequency response of the system in Case Study 1 to a force level of $F_1 = 100$ N with increasing frequency sweep.

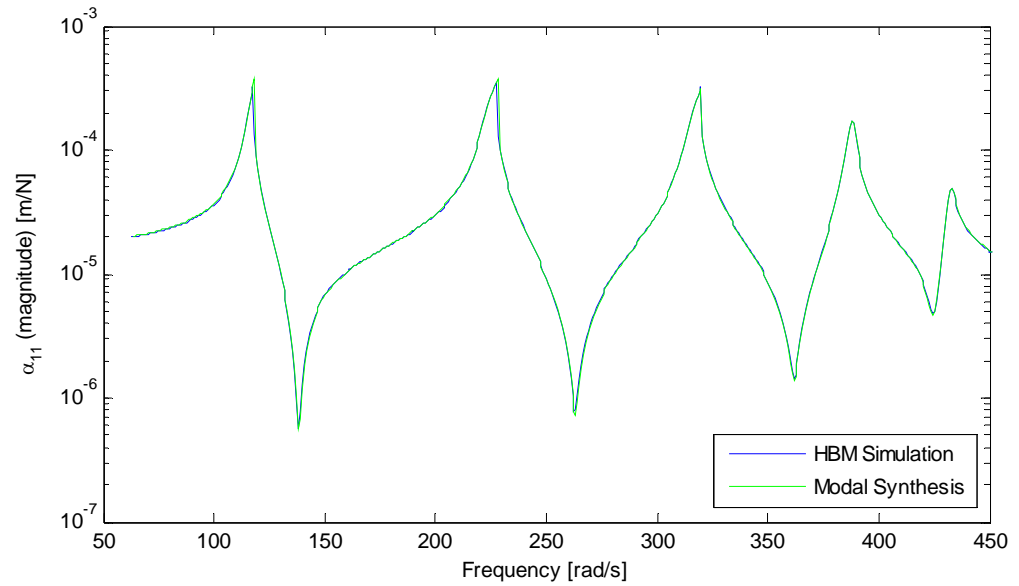


Figure 22. Frequency response of the system in Case Study 1 to a force level of $F_1 = 100$ N with decreasing frequency sweep.

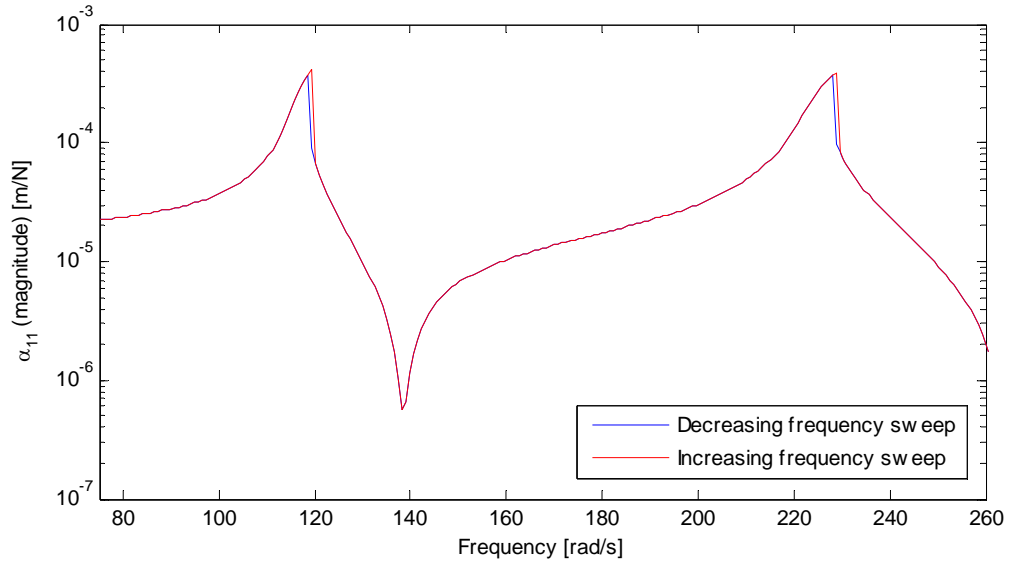


Figure 23. Frequency response of the system in Case Study 1 to a force level of $F_1 = 100$ N with both increasing and decreasing frequency sweep.

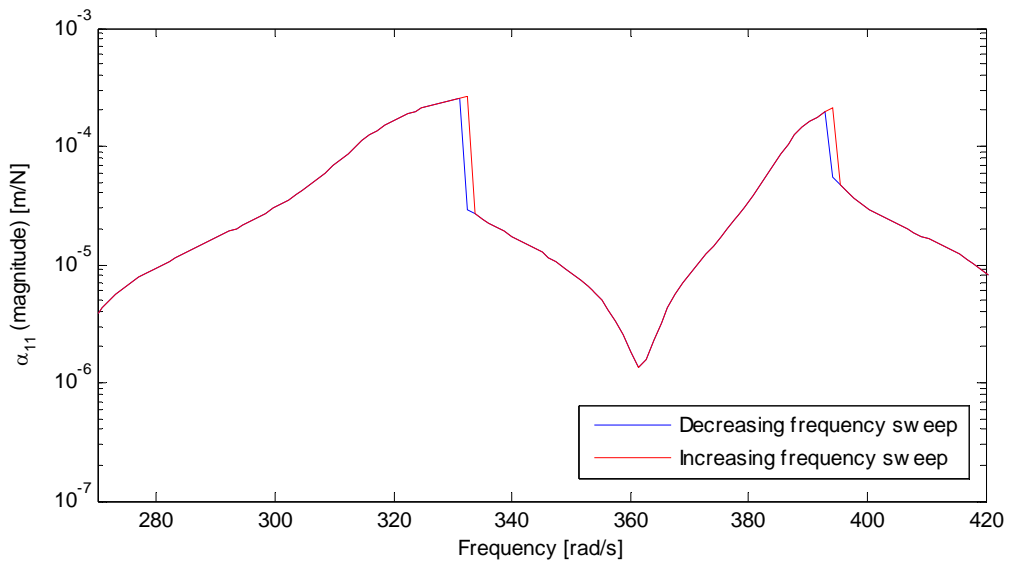


Figure 24. Frequency response of the system in Case Study 1 to a force level of $F_1 = 250$ N with both increasing and decreasing frequency sweep.

As mentioned earlier, it is also possible to calculate transfer FRFs of a nonlinear system by using the correspondent modal parameter variations. In order to illustrate this, transfer FRFs of the same system shown in Figure 15 are subjected to the same procedure of identification and curve fitting. The functions that are fit to the modal data are used to express the pseudo transfer receptance between the first and the fifth coordinates. The force is applied at the fifth mass and the response is measured at the first coordinate to which the nonlinear element is connected. In Figure 25 and Figure 26 solutions for increasing and decreasing frequency sweeps with that of harmonic balance solution are shown, respectively. Solutions match in the same way as reached in the point FRFs.

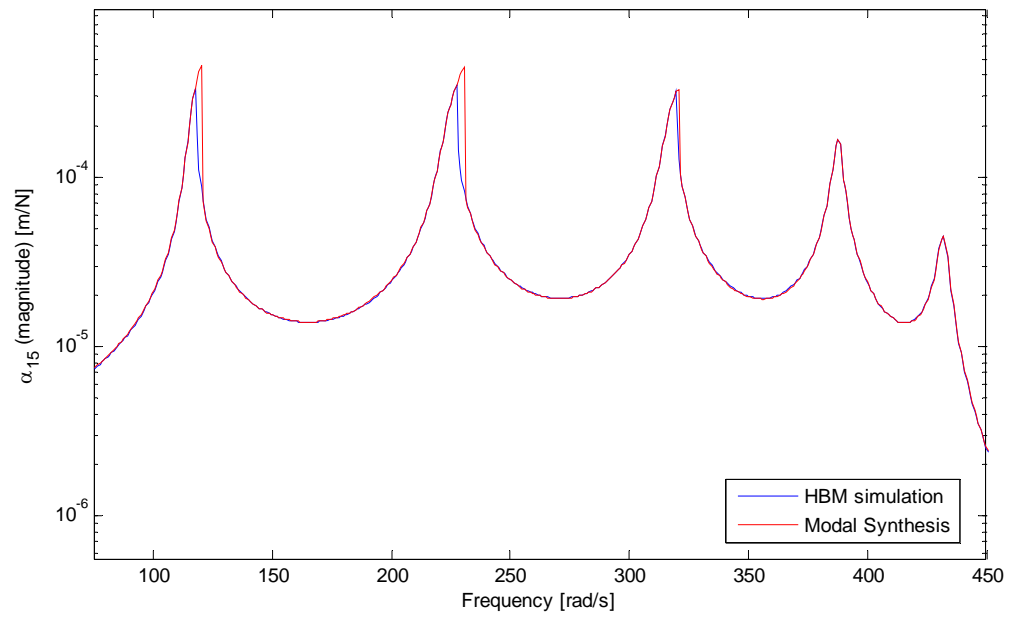


Figure 25. Frequency response of the system in Case Study 1 to a force level of $F_5 = 100$ N with increasing frequency sweep.

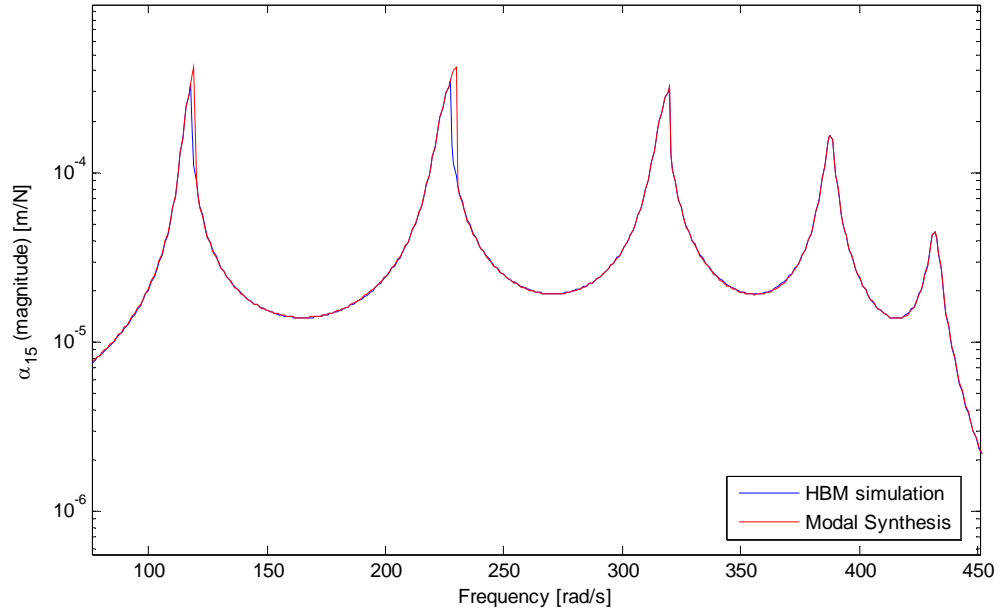


Figure 26. Frequency response of the system in Case Study 1 to a force level of $F_5 = 100$ N with decreasing frequency sweep.

4.1.2 Case Study 2

In order to investigate the effect of noise in test results, the same system in Case Study 1 is examined by polluting the FRFs obtained by simulation. FRFs shown in Figure 14 are polluted by multiplying each receptance value with a random number such that the mean value is 1 and the standard deviation is 0.05. One of the polluted FRFs is shown in Figure 27.

Modal parameters obtained by the identification of the polluted FRFs are presented in Figures 27 – 29, corresponding to first, second and fifth modes respectively. It can be observed that natural frequencies and modal constants are not much affected by pollution but loss factor values and modal constant phase angles are rather scattered. However, it is still possible to fit a proper curve for each parameter set presenting the trend.

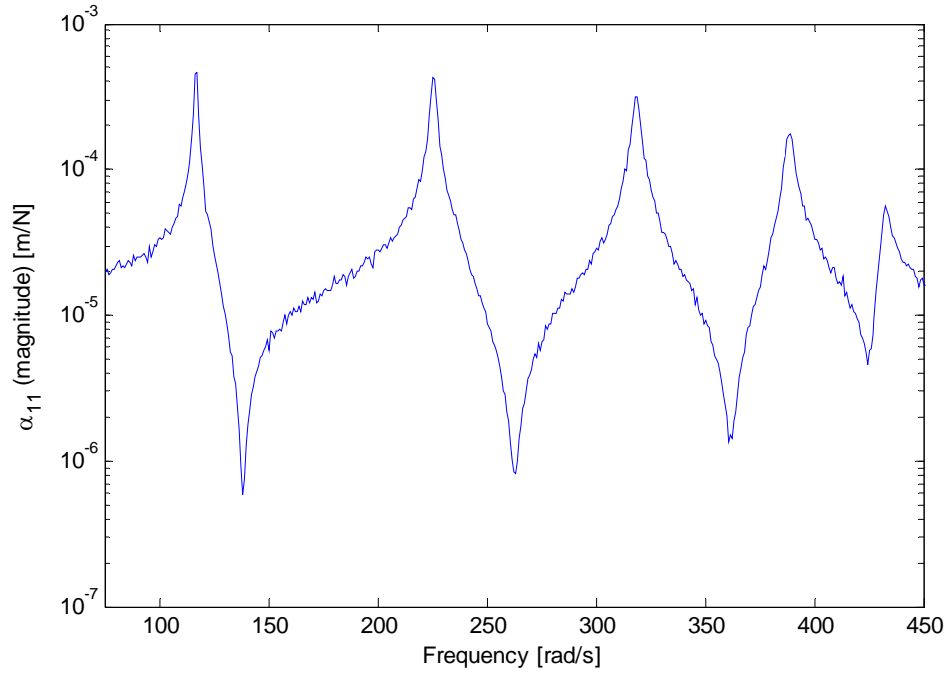


Figure 27. Polluted point FRF of the system in Case Study 1, obtained for $X_1 = 2.5$ cm.

Pseudo point receptance values calculated for forcing level of 100 N by using the modal parameters identified are presented in Figure 31 and Figure 32, corresponding to increasing and decreasing frequency sweep, respectively. The force is applied at the first mass to which the nonlinear element is connected. The responses obtained from the modal model with those calculated by harmonic balance method finely match, which demonstrates the validity of the modal model and the robustness of the proposed method to experimental errors and noise.

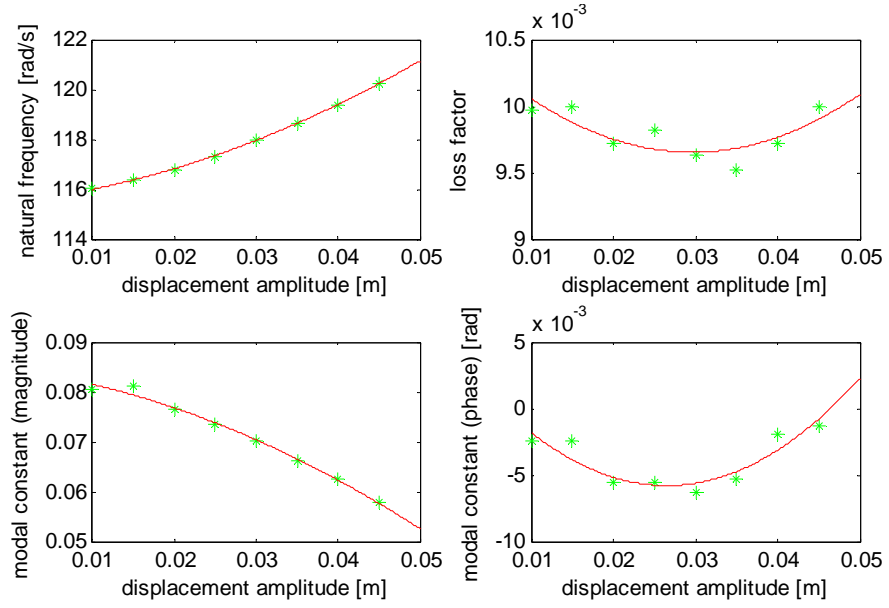


Figure 28. Variation of the modal parameters of the first mode with respect to response amplitude, X_1 . (* identified parameters, — fitted curve)

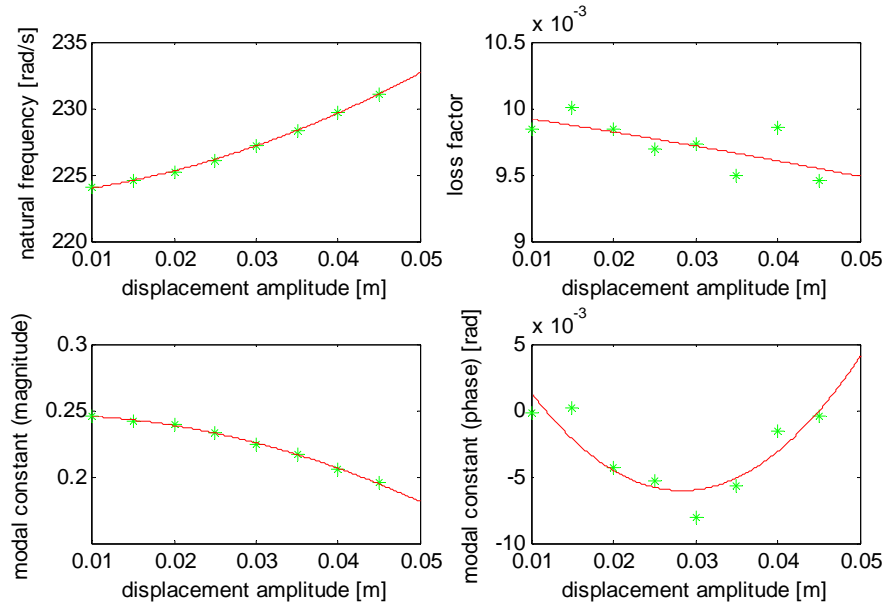


Figure 29. Variation of the modal parameters of the second mode with respect to response amplitude, X_1 . (* identified parameters, — fitted curve)

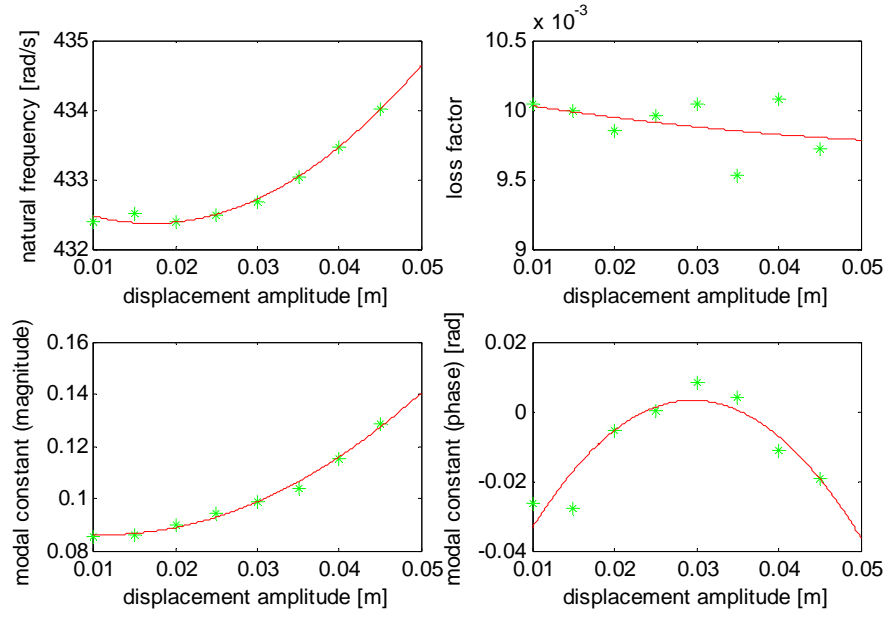


Figure 30. Variation of the modal parameters of the fifth mode with respect to response amplitude, X_1 . (* identified parameters, — fitted curve)

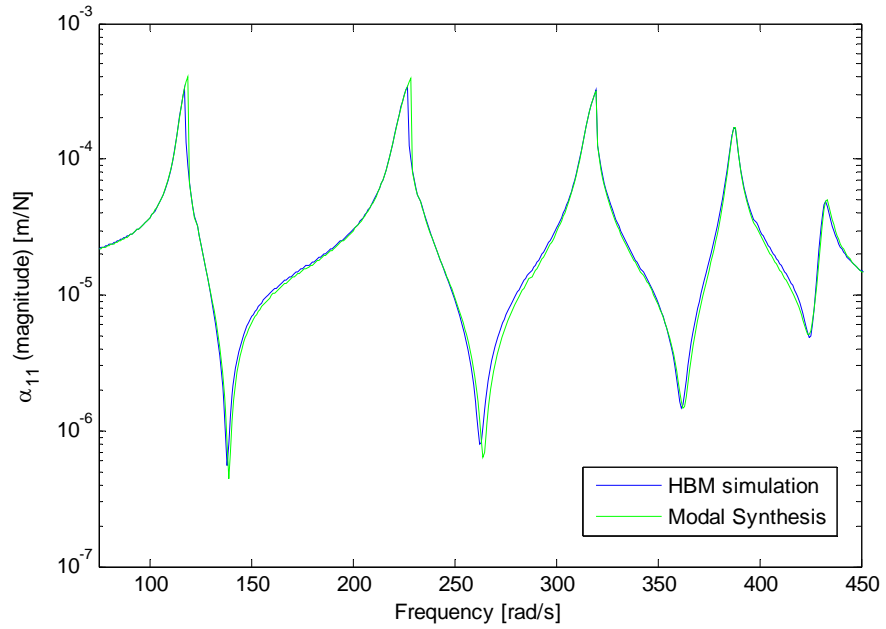


Figure 31. Frequency response of the system in Case Study 2 to a force level of $F_1 = 100$ N with increasing frequency sweep.

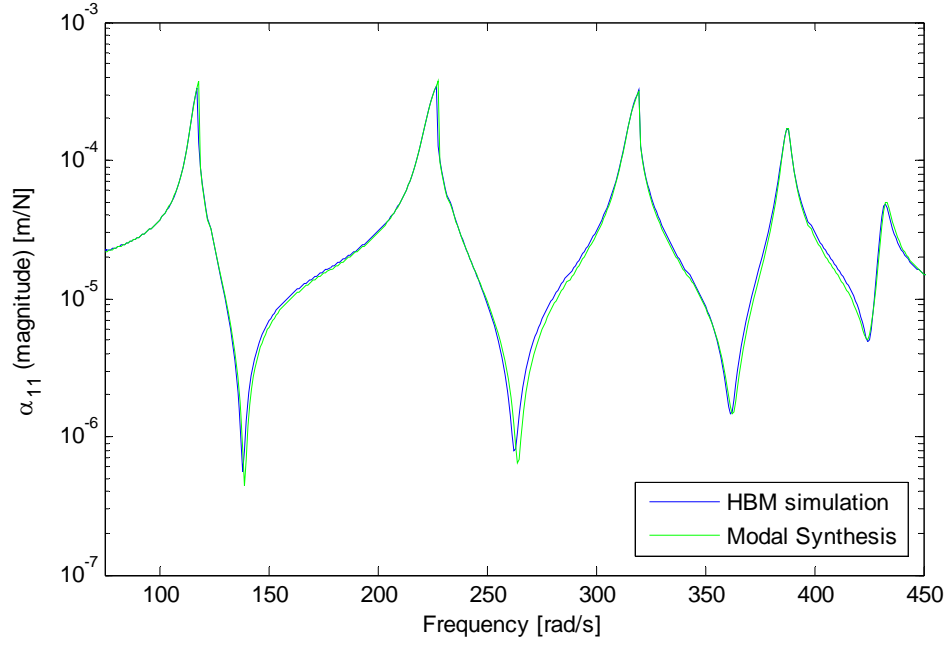


Figure 32. Frequency response of the system in Case Study 2 to a force level of $F_1 = 100$ N with decreasing frequency sweep.

4.1.3 Case Study 3

A 5-DOF viscously damped system with a grounded velocity squared damping element, as shown in Figure 33, under harmonic forcing is examined. System parameters are given as follows:

$$m = 1 \text{ kg}, k = 50000 \text{ N/m}, c = (3 \times 10^{-5} k) \text{ Ns/m}, c_{NL} = b |\dot{x}_1| \dot{x}_1, b = 1 \text{ Ns}^2/\text{m}^2$$

6 theoretical FRFs are generated, corresponding to series of simulated tests performed with constant displacement amplitude, X_1 . The values of the displacement amplitude are evenly distributed between 5 cm and 10 cm. In Figure 34, FRFs corresponding to first four of these values are presented. It is possible to observe the linear behavior of each curve and also the shift in resonance peaks which is the indication of the damping nonlinearity.

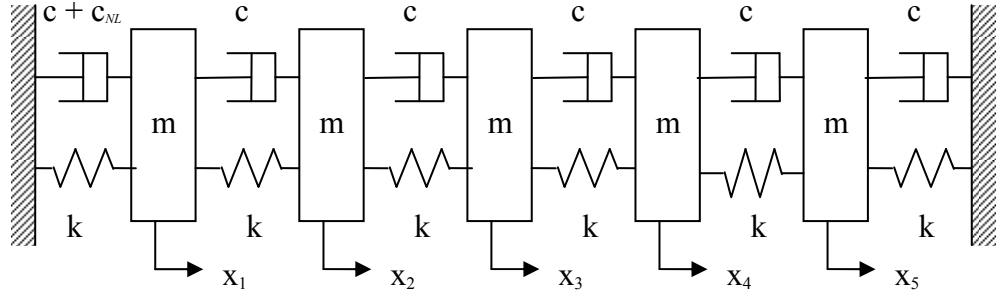


Figure 33. 5 - DOF viscously damped system with grounded velocity squared nonlinearity.

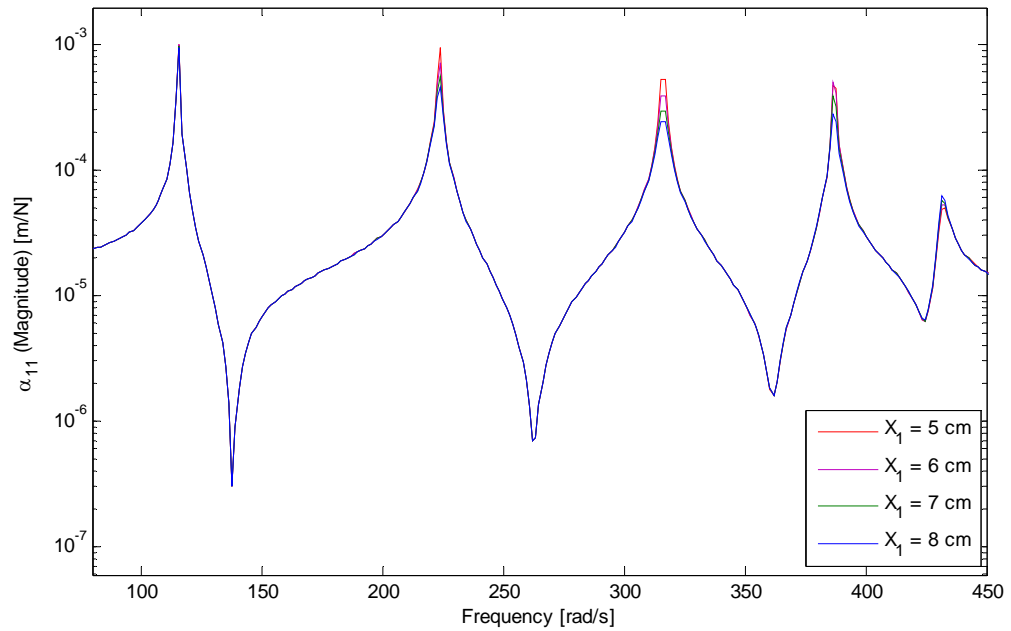


Figure 34. FRFs generated at constant displacement amplitudes

Modal parameters obtained from the identification of these FRFs are shown in Figures 28 – 30, corresponding to first, third and fifth modes respectively. Characteristics of damping nonlinearity can be observed in variation trends of modal parameters. It can be observed that, unlike stiffness nonlinearity as in the

previous case, natural frequency values remain almost constant. This is an expected result since damping nonlinearity does not cause a shift in resonance frequency but the FRF values at resonant frequency change. It can also be observed in Figure 34.

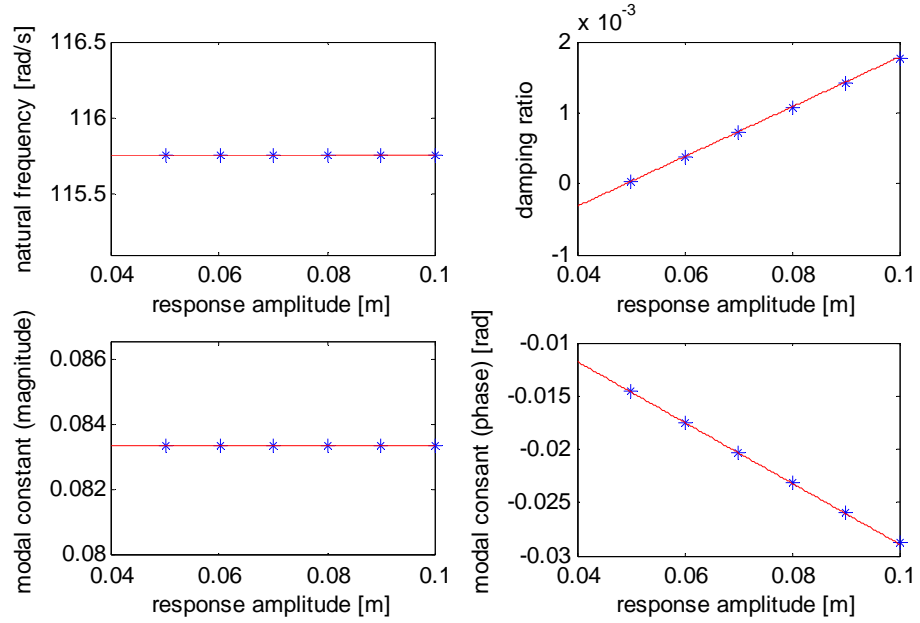


Figure 35. Variation of the modal parameters of the first mode with respect to response amplitude, X_1 . (* identified parameters, — fitted curve)

The same statement can also be made for modal constants, as they also remain constant. On the other hand, damping ratios spread through a large range. This is the most apparent property of a system with damping nonlinearity. Since natural frequency and modal constant magnitude values deviate around a certain value, they are taken as constant.

Considering the differences of the modal parameter variation characteristics between cubic stiffness and velocity squared damping nonlinearities, it can be

concluded that modal parameter variations can also be used to have an idea on the type of the nonlinearity in the system.

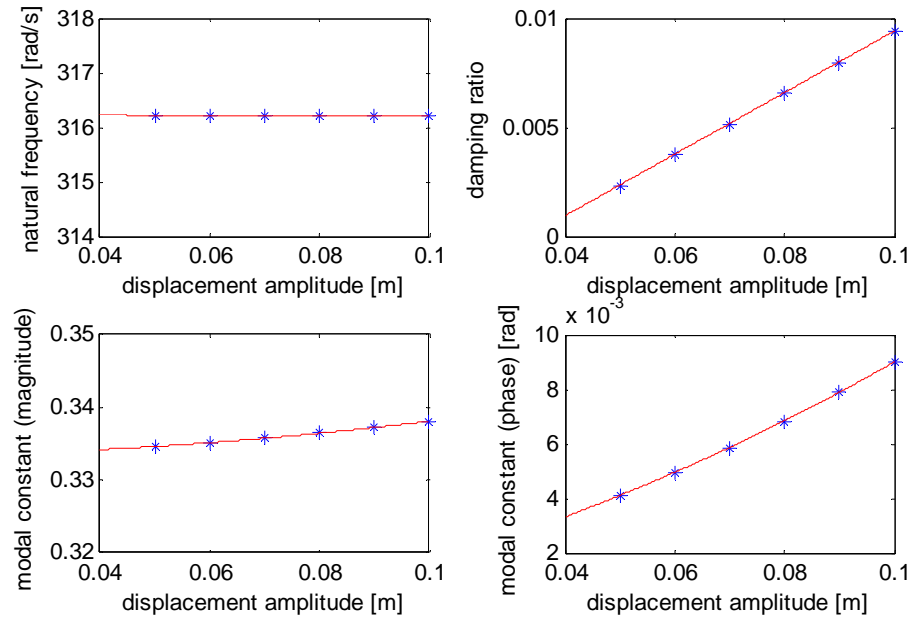


Figure 36. Variation of the modal parameters of the third mode with respect to response amplitude, X_1 . (* identified parameters, — fitted curve)

The functions that are fit to the modal data are used in the calculation of pseudo receptance of the system. Pseudo point receptance values calculated for forcing level of 100 N and 200 N are presented in Figure 37 and Figure 38. The force is applied at the first mass to which the nonlinear element is connected.

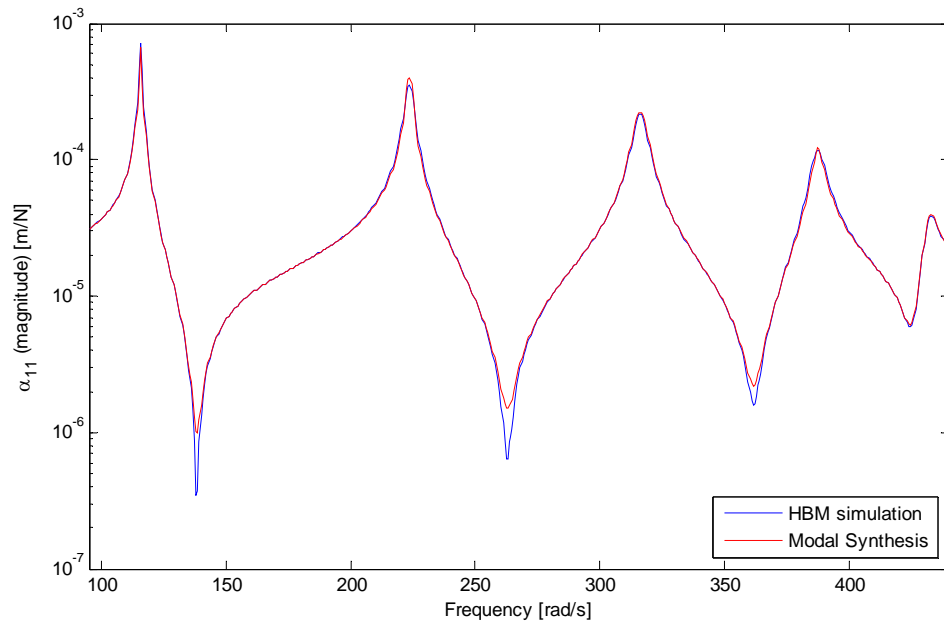


Figure 37. Frequency response of the system in Case Study 3 to a force level of $F_1 = 100$ N

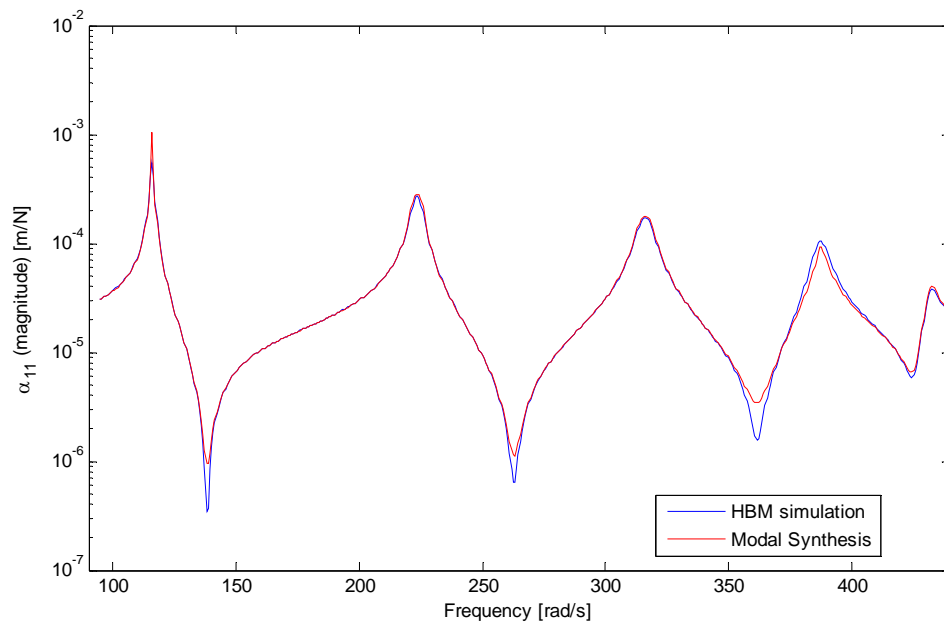


Figure 38. Frequency response of the system in Case Study 3 to a force level of $F_1 = 200$ N

4.1.4 Case Study 4

The same system in Case Study 3 is examined by polluting the FRFs obtained by simulation. FRFs shown in Figure 34 are polluted by multiplying each receptance value with a random number. Random numbers are normally distributed with their mean value of 1 and the standard deviation of 0.05. One of the polluted FRFs is shown in Figure 39.

Modal parameters are obtained by the identification of the polluted FRFs. Modal parameter variations of the first, second and fifth modes are presented in Figures 39 – 41, respectively. The same characteristics of a nonlinear system with damping nonlinearity can also be observed in the identified modal parameters.

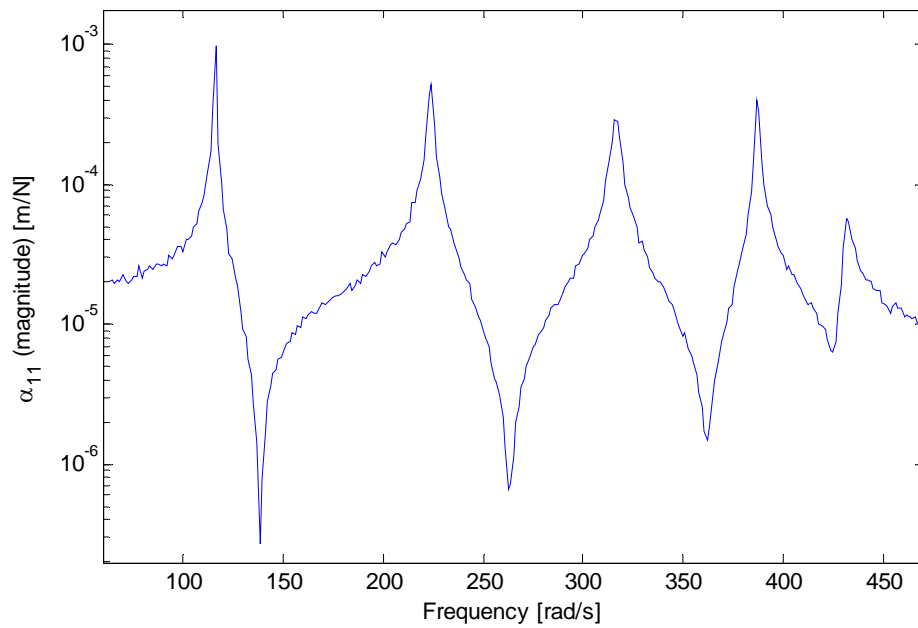


Figure 39. Polluted point FRF of the system in Case Study 3, obtained for $X_1 = 0.07$ m

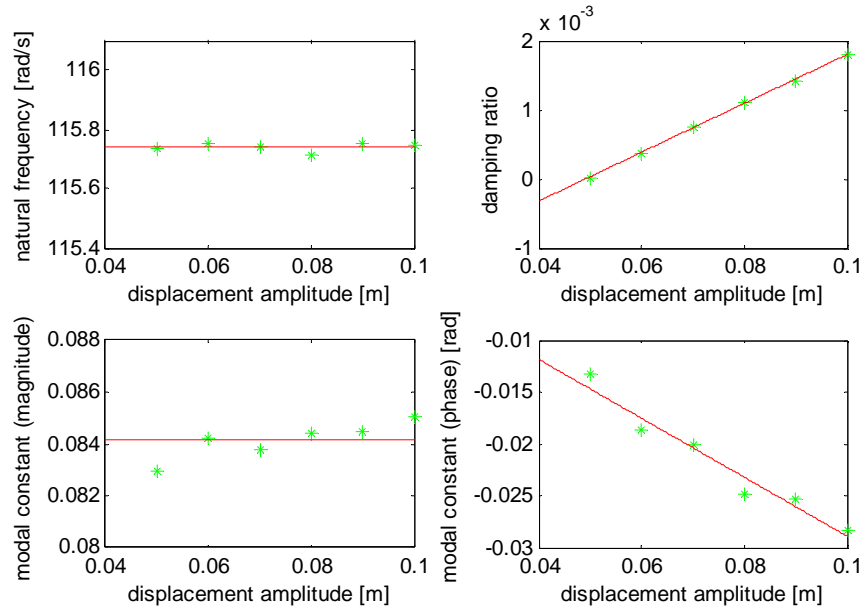


Figure 40. Variation of the modal parameters of the first mode with respect to response amplitude, X_1 . (* identified parameters, — fitted curve)

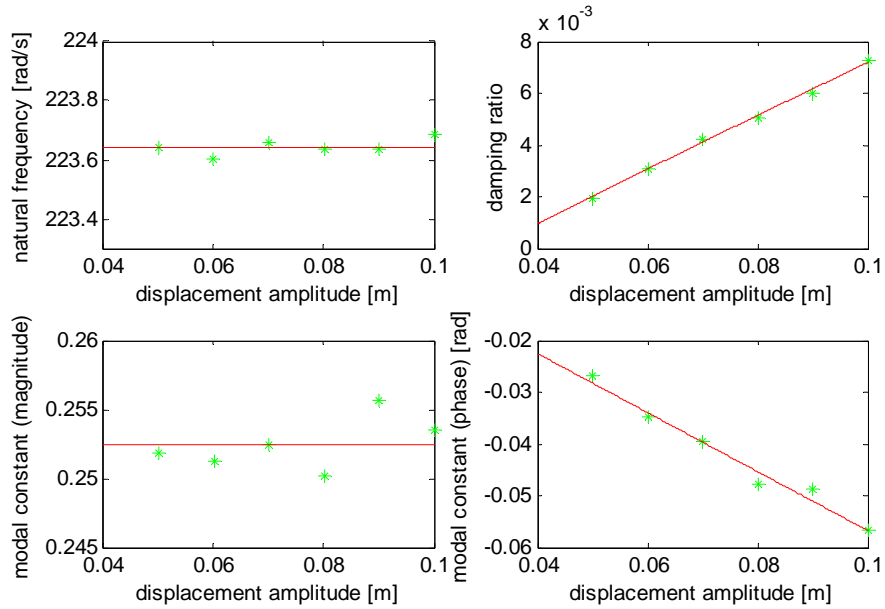


Figure 41. Variation of the modal parameters of the second mode with respect to response amplitude, X_1 . (* identified parameters, — fitted curve)

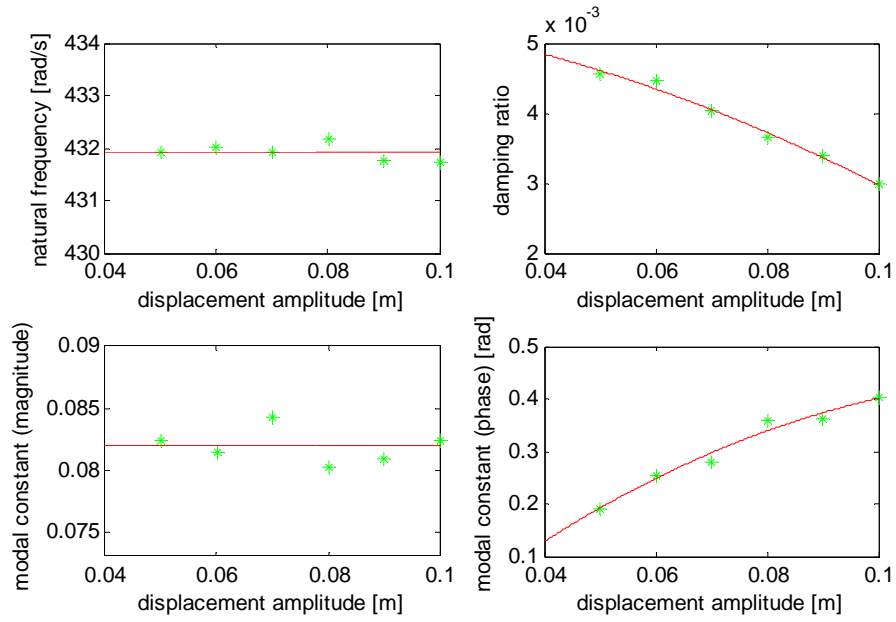


Figure 42. Variation of the modal parameters of the fifth mode with respect to response amplitude, X_1 . (* identified parameters, — fitted curve)

Pseudo point receptance values calculated for forcing level of 200 N and 500 N covering the first three modes by using the modal parameters identified are presented in Figure 43 and Figure 44, respectively. The force is applied at the first mass to which the nonlinear element is connected. The responses obtained from the modal model with those calculated by harmonic balance method show a good match demonstrating the validity of the modal model and the robustness of the proposed method to experimental errors and noise.

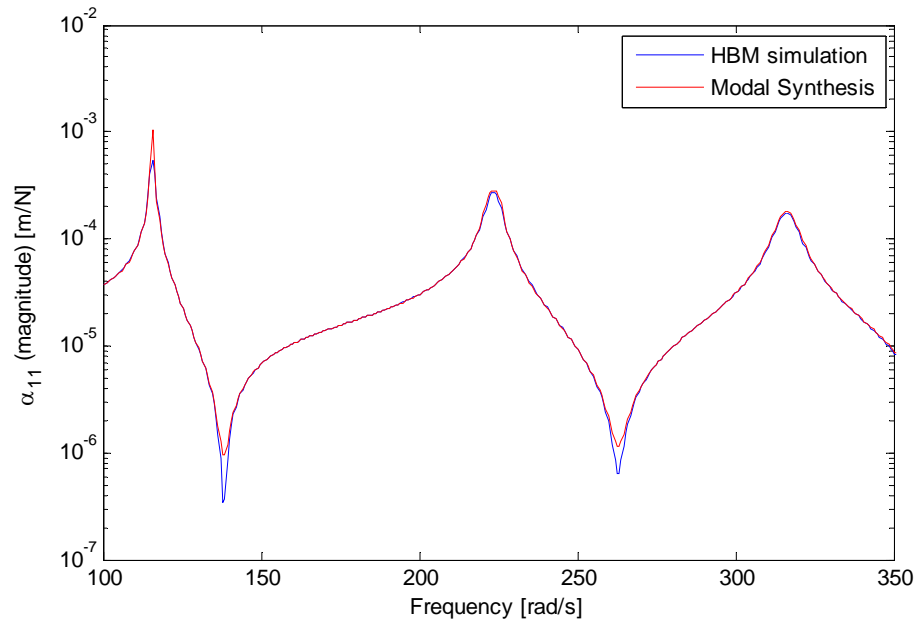


Figure 43. Pseudo receptance of the system in Case Study 4 to a forcing level
 $F_1 = 200 \text{ N}$

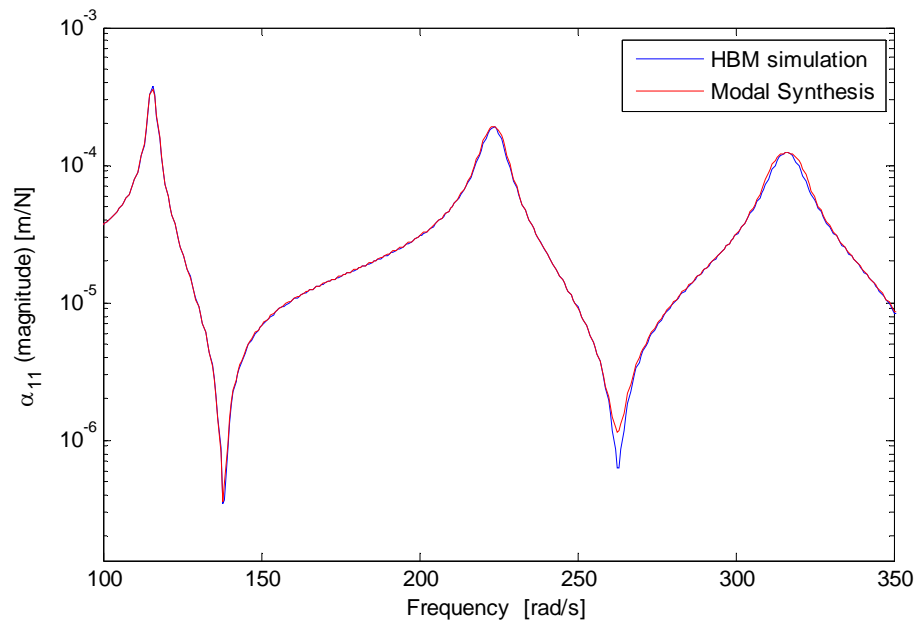


Figure 44. Pseudo receptance of the system in Case Study 4 to a forcing level
 $F_1 = 500 \text{ N}$

4.1.5 Case Study 5

The same system in Case Study 3 is examined with the nonlinear damping element inserted between the first and the second mass. As explained in section 3.1.2, for this type of nonlinear systems harmonic vibrations tests are to be carried out such that the relative displacement amplitude between the coordinates at which the nonlinear element is connected is kept constant. Furthermore, measurements of a set of both point and transfer FRFs are required.

For this system, FRFs are generated for relative displacement amplitudes evenly distributed between 1 cm and 5 cm. The relative displacement amplitude of concern is designated with Y_{12} , standing for the relative displacement between the first and second coordinates. A number of FRFs are shown in Figure 45 and Figure 46 for a frequency range covering the last three modes.

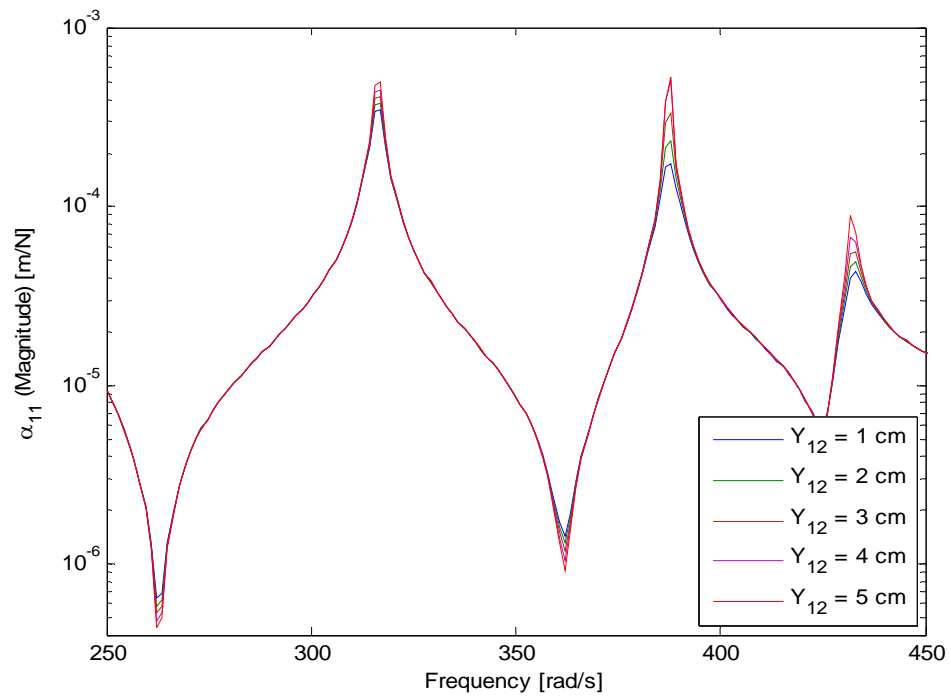


Figure 45. Point FRFs generated at constant displacement amplitudes

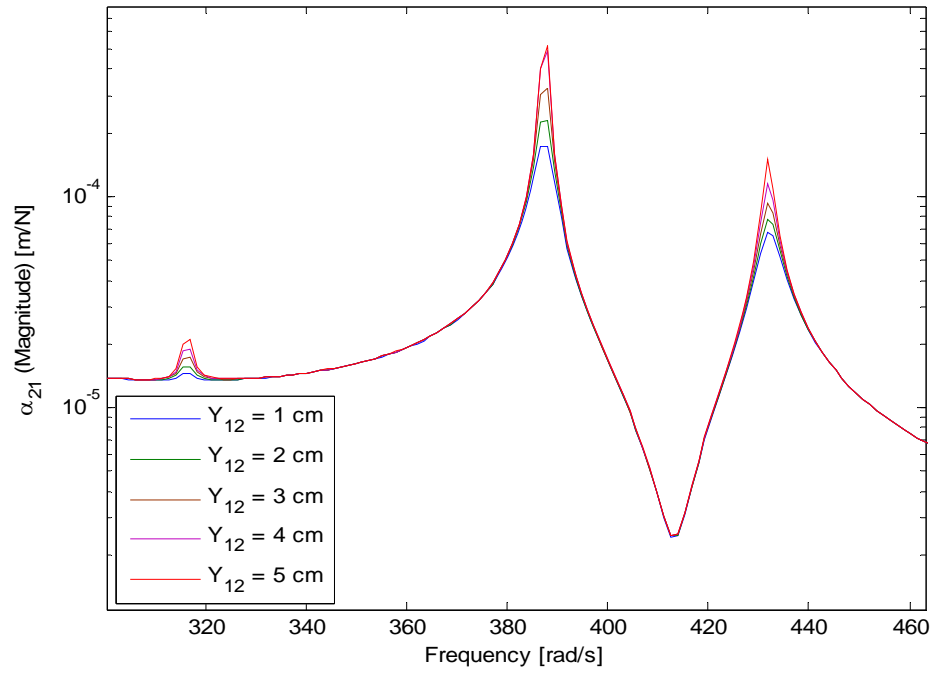


Figure 46. Transfer FRFs generated at constant displacement amplitudes

Modal parameters obtained from the identification of the point and transfer FRFs are presented in Figures 34 – 39. Figures 34 – 36 represent the modal parameters of the last three modes of the point FRFs while Figures 37 – 39 show the modal parameter variations of the same modes of the transfer FRFs. The obtained variations are used in the computation of the response of the system to different forcing levels. Pseudo point FRF of the system for forcing levels of 100N, 200N and 500 N applied on the first mass are shown in Figure 54.

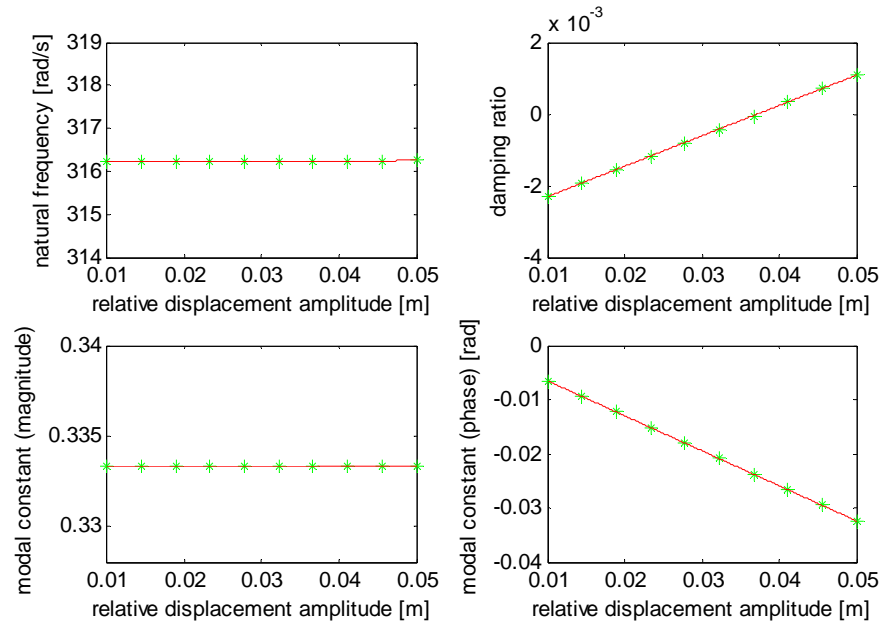


Figure 47. Variation of the modal parameters of the third mode with respect to relative response amplitude, Y_{12} . (* identified parameters, — fitted curve)

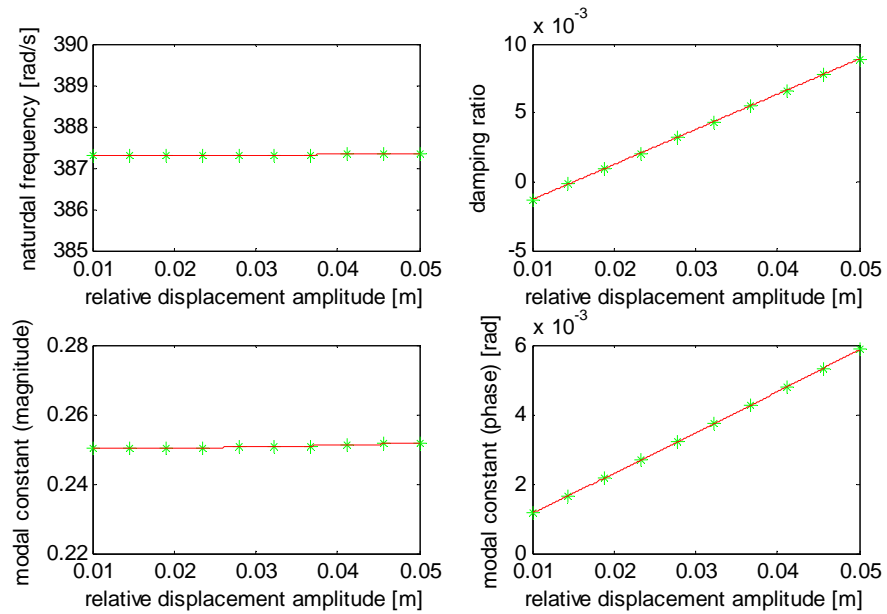


Figure 48. Variation of the modal parameters of the fourth mode with respect to relative response amplitude, Y_{12} . (* identified parameters, — fitted curve)

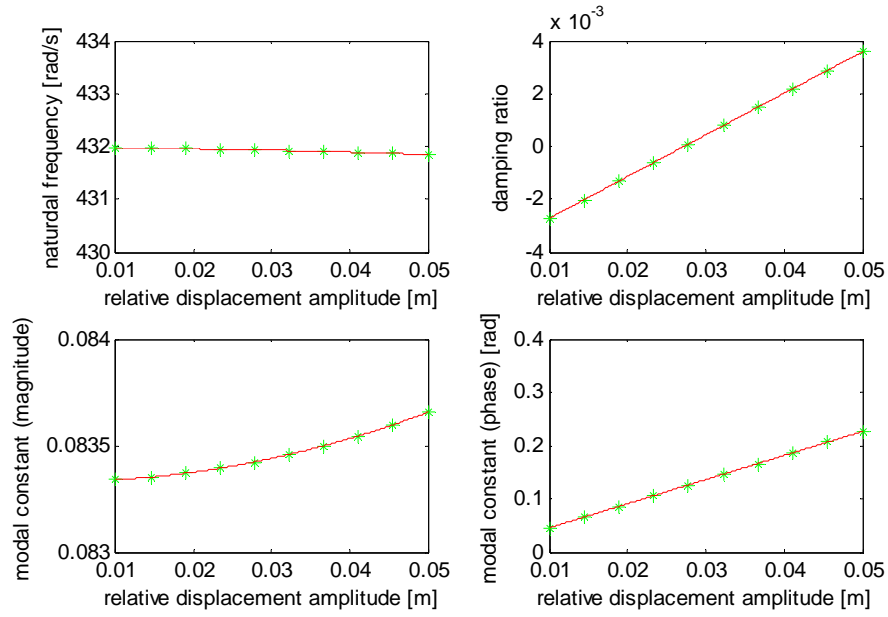


Figure 49. Variation of the modal parameters of the fifth mode with respect to relative response amplitude, Y_{12} . (* identified parameters, — fitted curve)

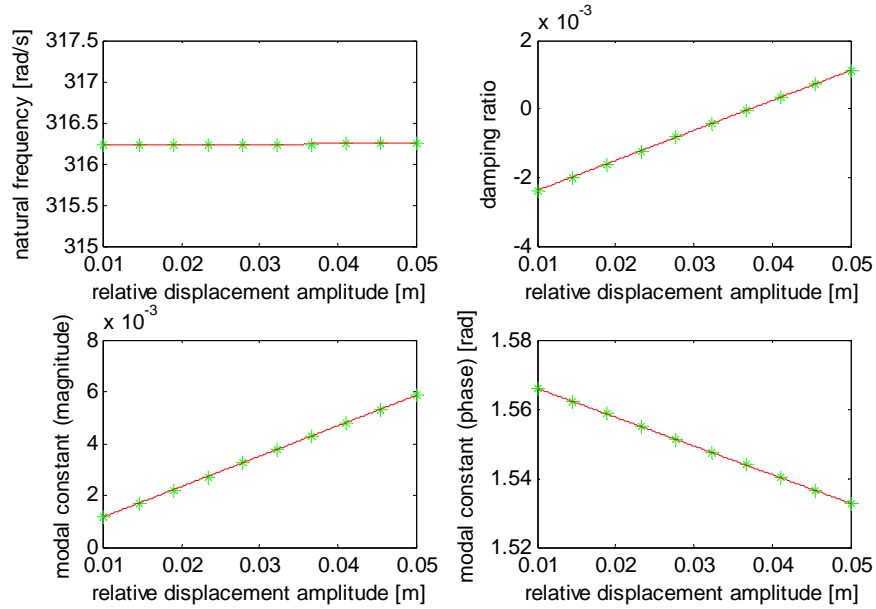


Figure 50. Variation of the modal parameters of the third mode with respect to relative response amplitude, Y_{12} . (* identified parameters, — fitted curve)

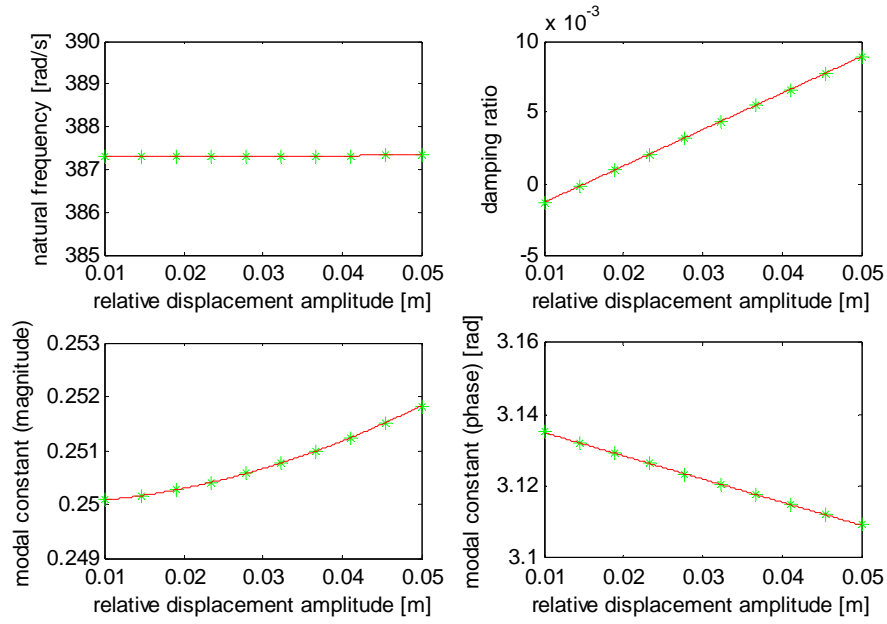


Figure 51. Variation of the modal parameters of the fourth mode with respect to relative response amplitude, Y_{12} . (* identified parameters, — fitted curve)

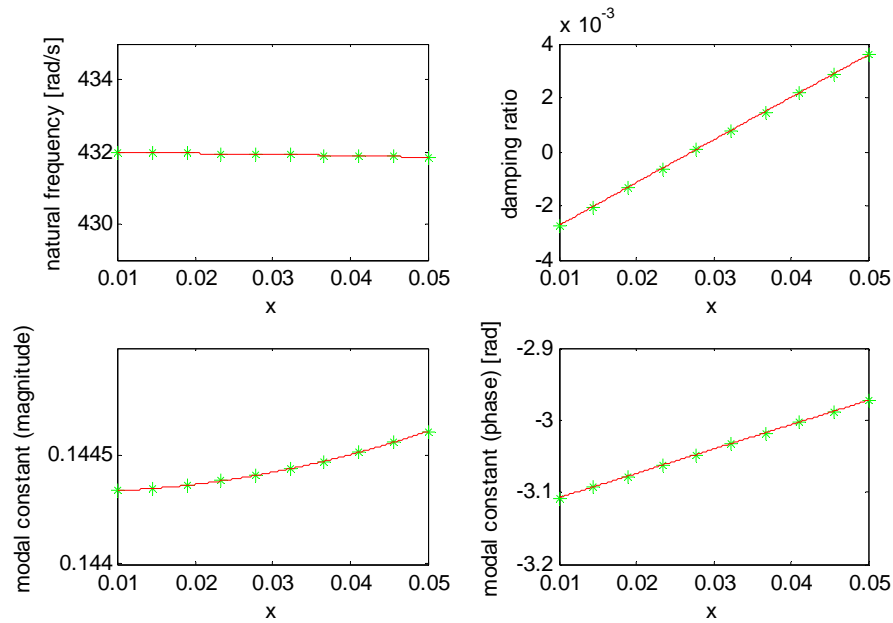


Figure 52. Variation of the modal parameters of the fifth mode with respect to relative response amplitude, Y_{12} . (* identified parameters, — fitted curve)

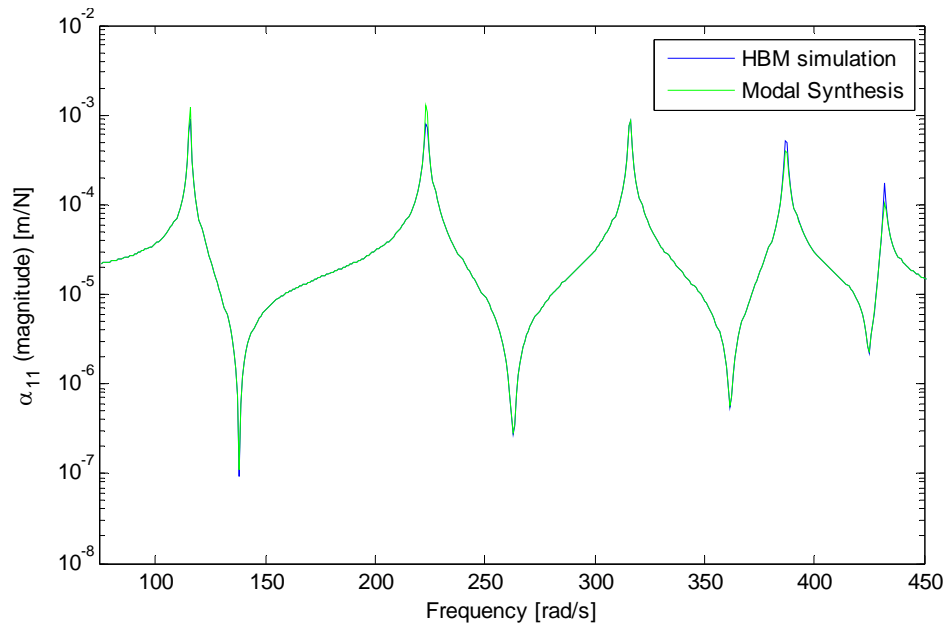


Figure 53. Pseudo receptance of the system in Case Study 5 to forcing level,
 $F_1 = 100 \text{ N}$

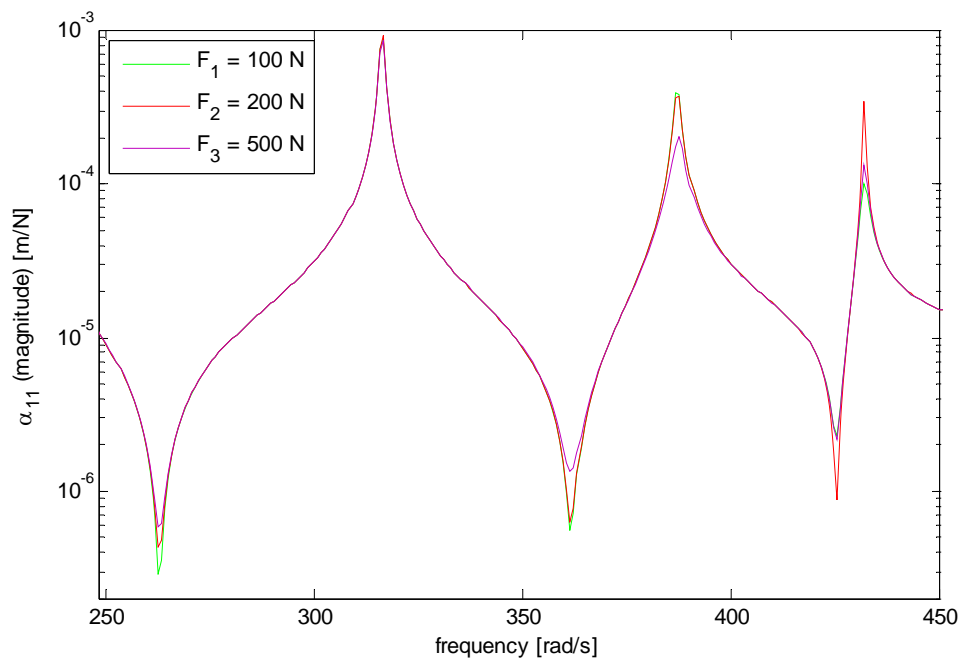


Figure 54. Pseudo receptance of the system in Case Study 5 to forcing levels of
 $F_1 = 100 \text{ N}, 200 \text{ N}, 500 \text{ N}$

4.2 Coupling of Nonlinear Systems by Using Modal Model

In this section, implementation of the proposed method in coupling analysis is given. In the following case studies, a nonlinear system is coupled with a linear system and the response of the coupled system is calculated using the modal model of the nonlinear system. Displacement controlled simulated tests are performed on the nonlinear system and the modal parameters are identified to construct the modal model. FRFs of the linear subsystem to be coupled with the nonlinear system are formed by using the system properties. In practical applications, FRFs of the linear system can be obtained by a single force controlled or response controlled test, since FRFs of linear systems are independent of the force or response level.

4.2.1 Case Study 6

In this case study, a three – DOF system with grounded cubic nonlinearity is rigidly coupled with a two – DOF linear system as shown in Figure 55.

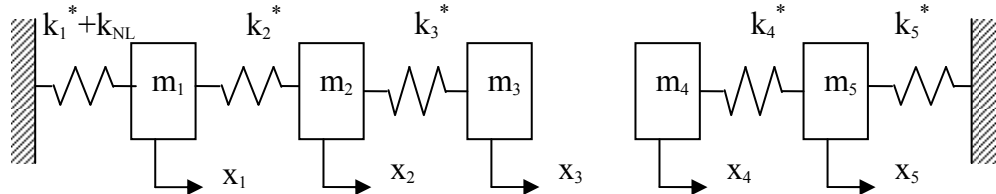


Figure 55. Nonlinear system to be rigidly coupled with a linear system.

System parameters for the given discrete systems are as follows:

$$m_1 = m_2 = m_3 = m_4 = 1 \text{ kg}, m_5 = 2 \text{ kg},$$

$$k_1^* = k_2^* = 1000(1 + 0.02i) \text{ N/m}, k_3^* = k_4^* = k_5^* = 10000(1 + 0.02i) \text{ N/m}$$

$$k_{NL} = bx_1^2, \quad b = 10^7 \text{ N/m}^3$$

Displacement amplitude controlled simulated tests are generated for the nonlinear substructure and the results are used to calculate the response of the coupled system. 8 FRFs are theoretically generated in which the displacement amplitude, X_1 , is evenly distributed between 1 cm and 4.5 cm. Modal parameters obtained from the identification of these FRFs are presented in Figure 57 and Figure 58.

As explained in section 3.2, FRFs of the linear subsystem to be coupled with the nonlinear system are also required in the analysis. In this case study, transfer and point FRFs of the linear system is obtained by matrix inversion and are shown in Figure 56.

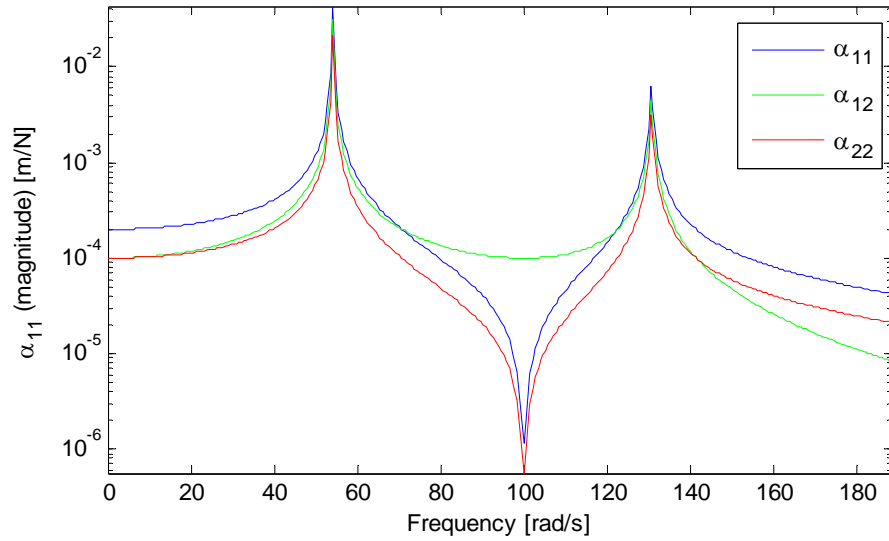


Figure 56. Transfer and point FRFs of the linear subsystem in Case Study 6.

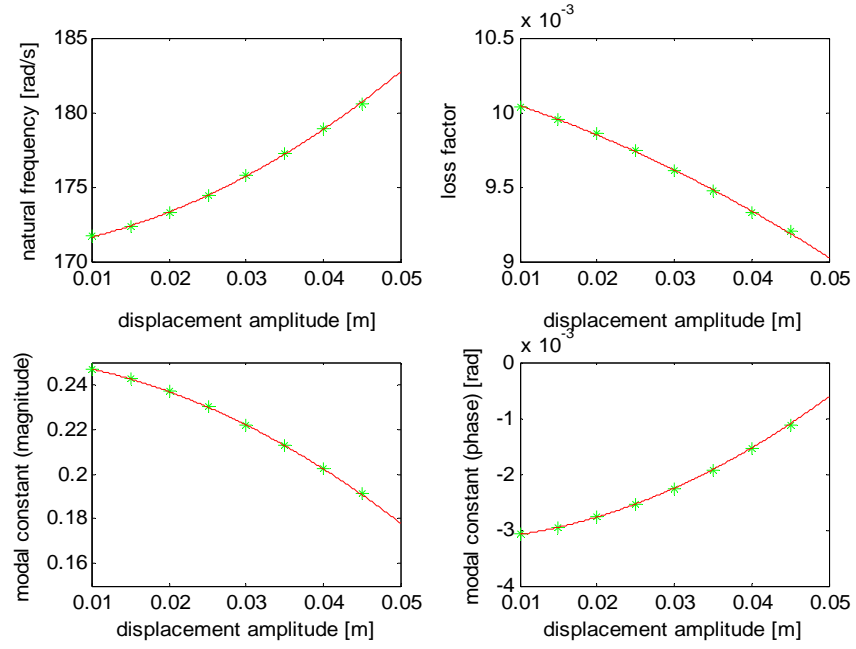


Figure 57. Variation of the modal parameters of the first mode with respect to response amplitude, X_1 . (* identified parameters, — fitted curve)

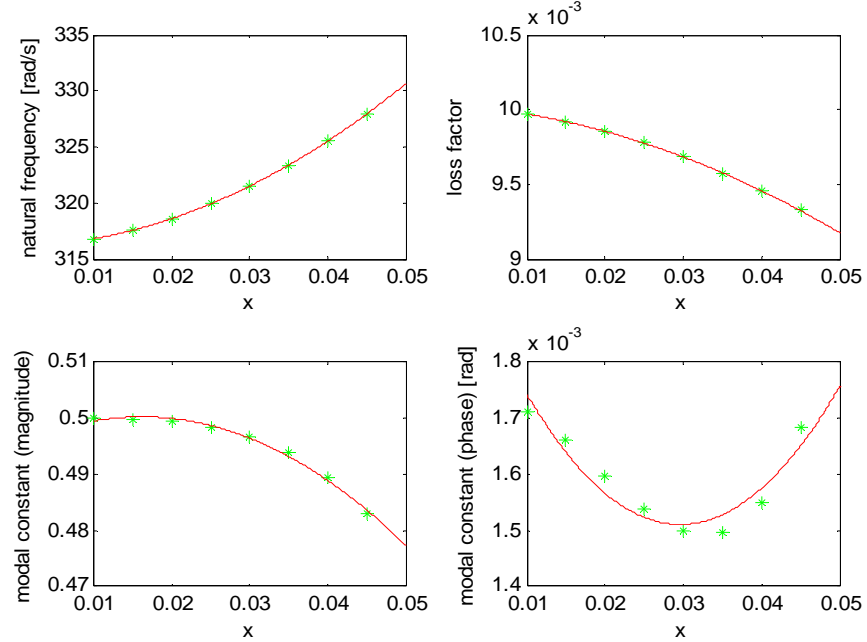


Figure 58. Variation of the modal parameters of the second mode with respect to response amplitude, X_1 . (* identified parameters, — fitted curve)

The pseudo receptance of the coupled system is computed by using the modal parameter variations of the nonlinear subsystem and the FRFs of the linear subsystem, as explained in section 3.2. The pseudo receptance is obtained around the first two resonances. Figure 59 shows the pseudo receptance obtained by using only 2 modes and compares it with the solution obtained by harmonic balance method using all 5 modes, for low to high frequency sweep. The corresponding response for decreasing frequency sweep is plotted in Figure 60, with the increasing frequency sweep solution.

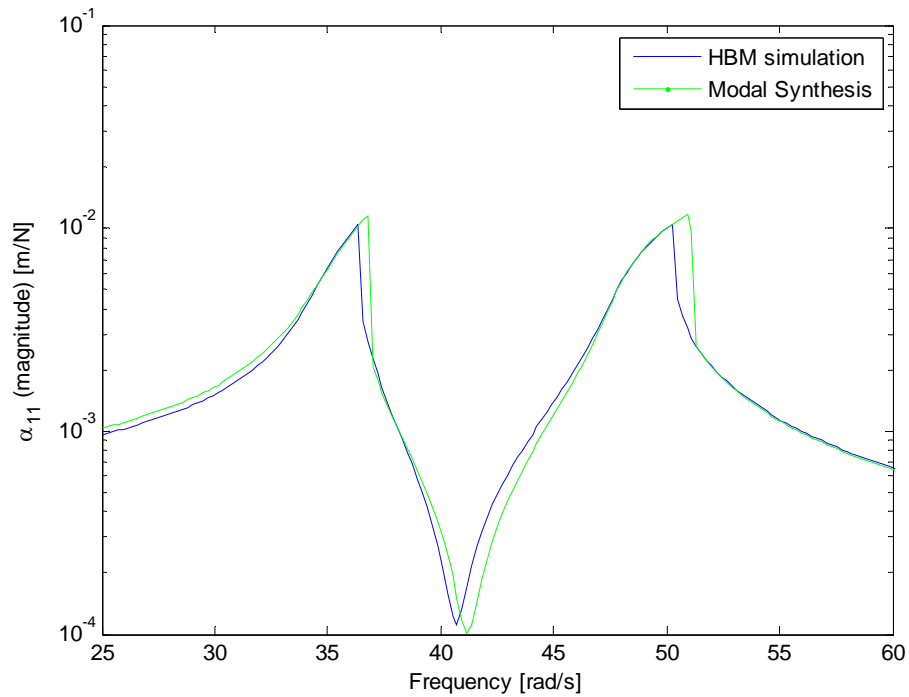


Figure 59. Pseudo receptance of the coupled system in Case Study 6 for a forcing level, $F_1 = 2$ N.

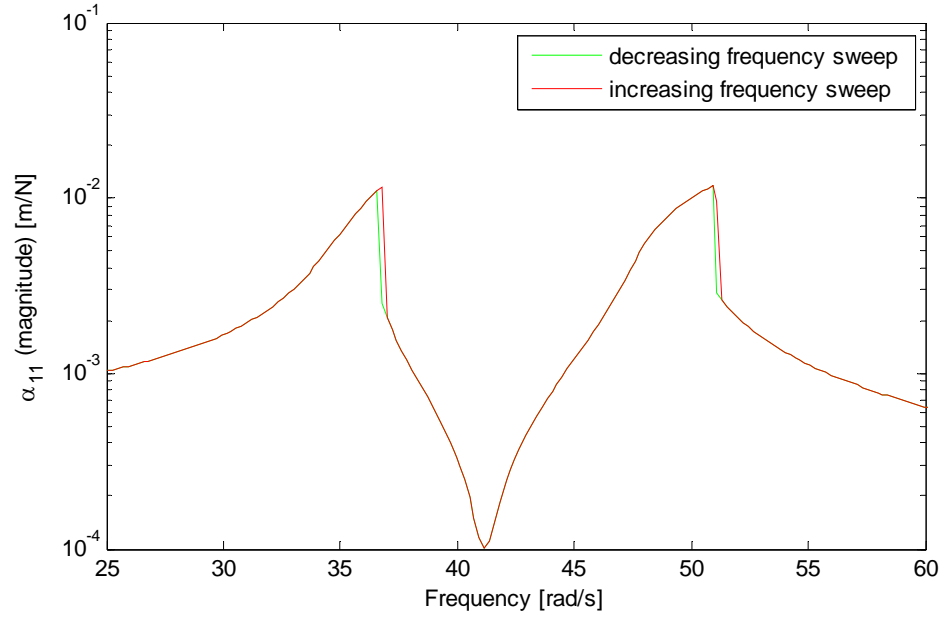


Figure 60. Pseudo receptance of the coupled system in Case Study 6 for a forcing level, $F_1 = 2$ N.

4.2.2 Case Study 7

In this case study, a three – DOF viscously damped system with interconnected velocity squared damping nonlinearity is rigidly coupled with a 2 – DOF viscously damped, linear system as shown in Figure 61.

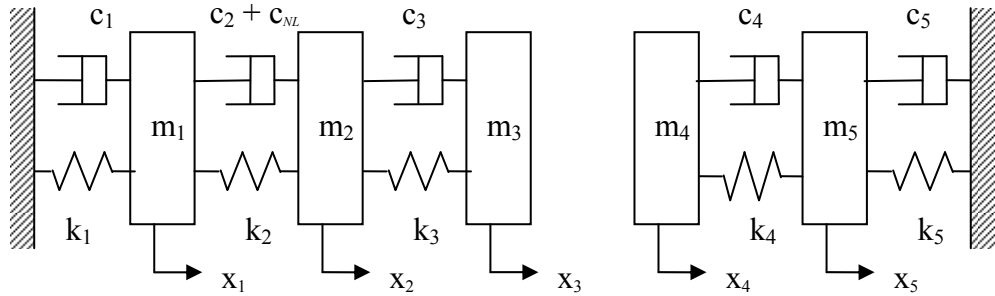


Figure 61. A nonlinear system to be rigidly coupled with a linear system.

System parameters for the given discrete systems are as follows:

$$m_1 = m_2 = m_3 = m_4 = 1 \text{ kg}, m_5 = 2 \text{ kg},$$

$$k_1 = k_2 = 1000 \text{ N/m}, k_3 = k_4 = k_5 = 10000 \text{ N/m}$$

$$c_i = 0.00003k_i \text{ Ns/m}, i = 1, 2, 3, 4, 5$$

$$c_{NL} = b|\dot{y}_{12}|\dot{y}_{12}, b = 1 \text{ Ns}^2/\text{m}^2$$

In this case study, FRFs of the nonlinear system are generated for relative displacement amplitudes evenly distributed between 1 cm and 5 cm. Modal parameters obtained from the identification of the point and transfer FRFs are presented in Figures 60 – 65. Figures 60 – 62 represent the modal parameters of the point FRFs while Figures 63 – 65 show the modal parameter variations of the transfer FRFs. Transfer and point FRFs of the linear system is obtained by matrix inversion and are shown in Figure 62.

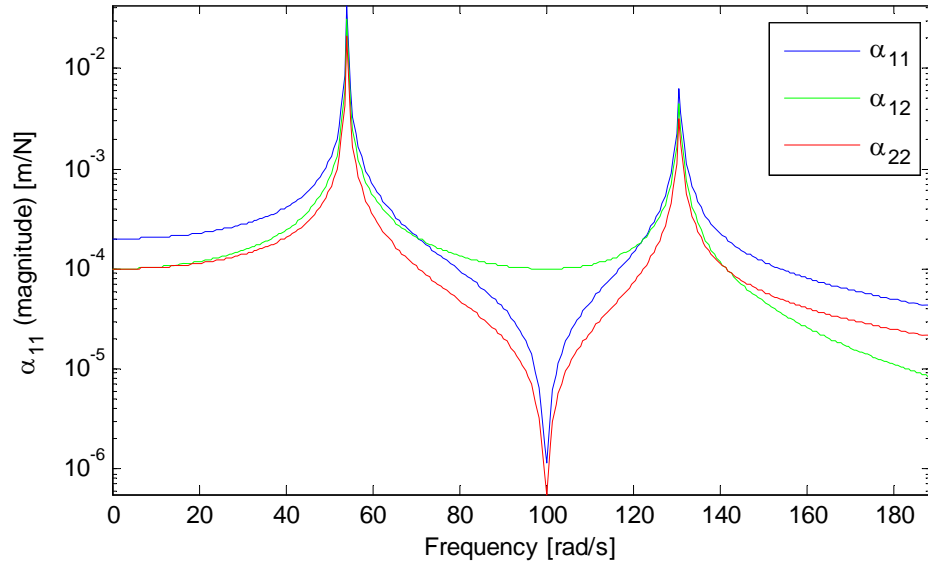


Figure 62. Point and transfer FRFs of the linear subsystem in Case Study 7.

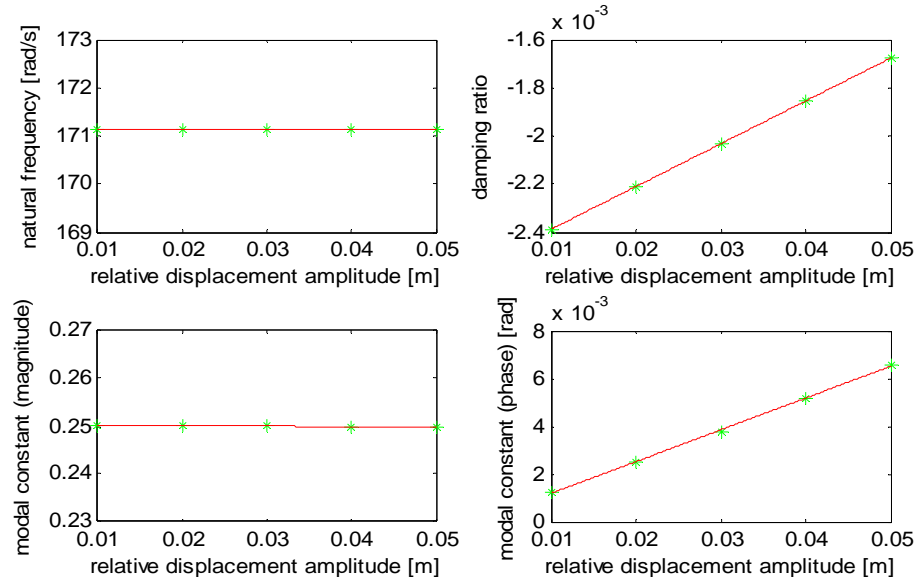


Figure 63. Variation of the modal parameters of the first mode with respect to relative response amplitude, Y_{12} . (* identified parameters, — fitted curve)

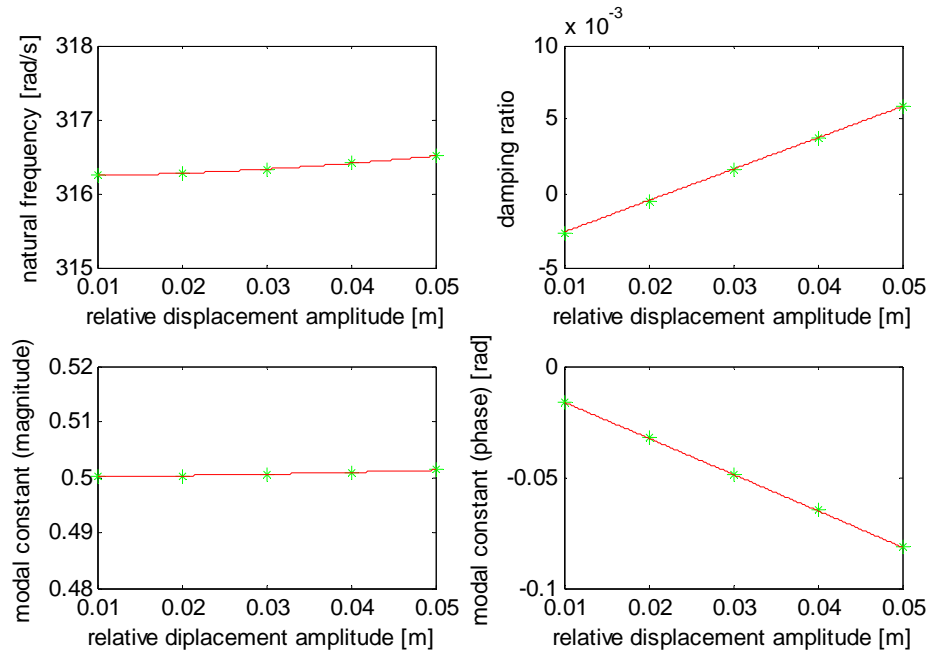


Figure 64. Variation of the modal parameters of the second mode with respect to relative response amplitude, Y_{12} . (* identified parameters, — fitted curve)

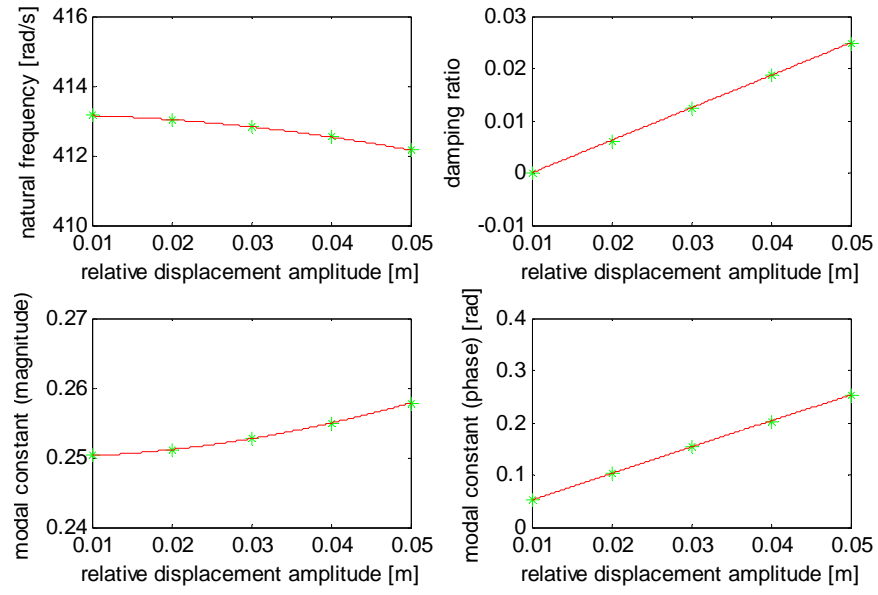


Figure 65. Variation of the modal parameters of the third mode with respect to relative response amplitude, Y_{12} . (* identified parameters, — fitted curve)

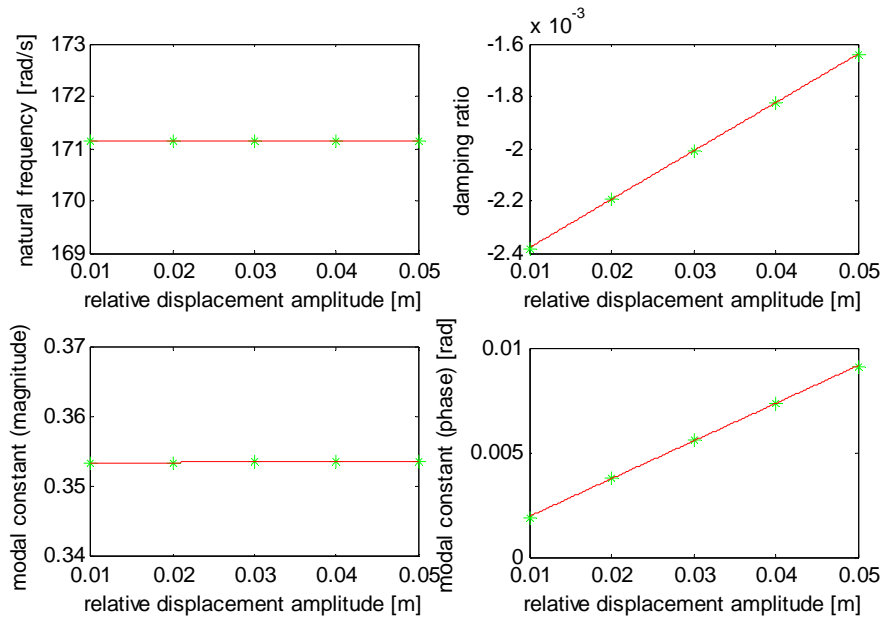


Figure 66. Variation of the modal parameters of the first mode with respect to relative response amplitude, Y_{12} . (* identified parameters, — fitted curve)

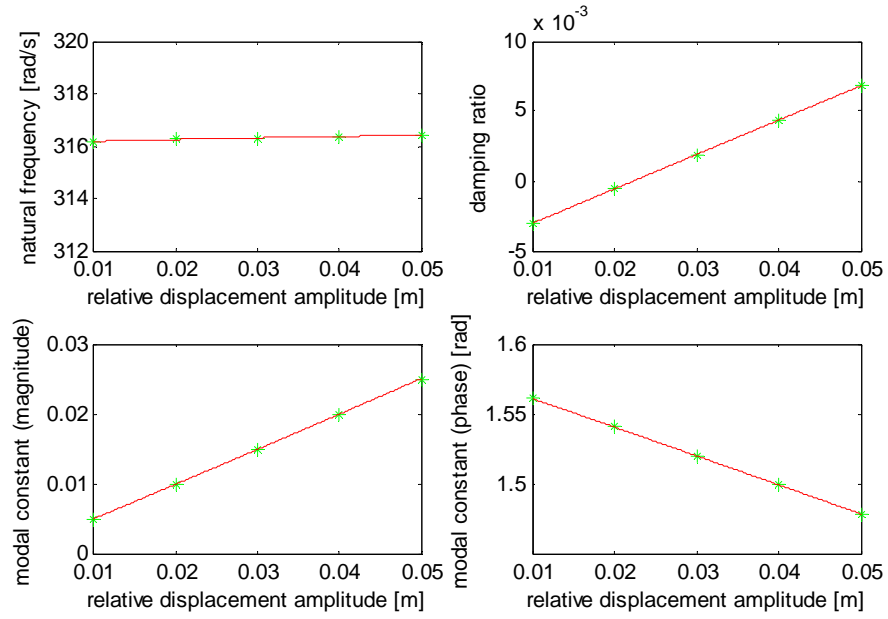


Figure 67. Variation of the modal parameters of the second mode with respect to relative response amplitude, Y_{12} . (* identified parameters, — fitted curve)

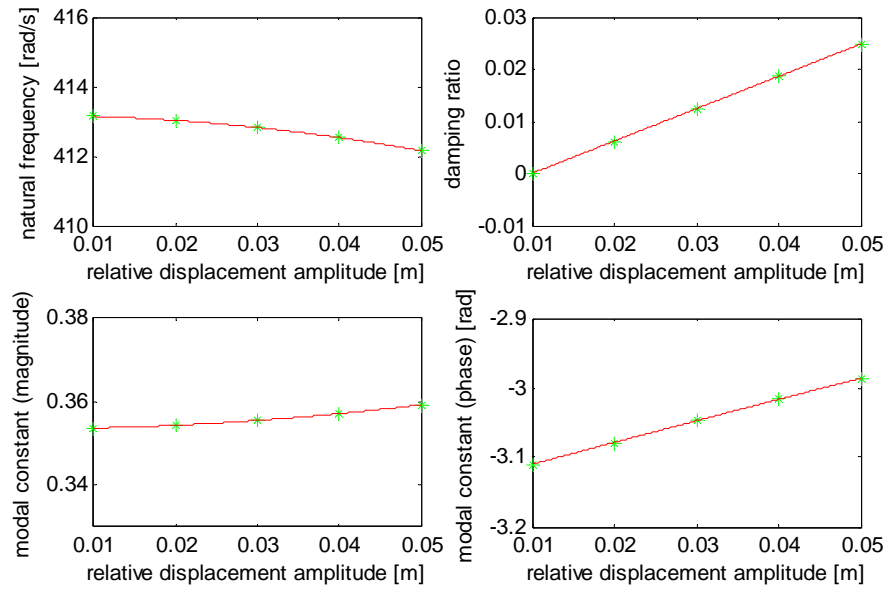


Figure 68. Variation of the modal parameters of the third mode with respect to relative response amplitude, Y_{12} . (* identified parameters, — fitted curve)

The obtained parameter variations and FRFs of the linear subsystem are used in the computation of the response of the system to different forcing levels as explained in section 3.2. Pseudo point FRFs of the system for forcing levels of 1 N, 2 N and 5 N applied on the first mass are shown in Figure 69.

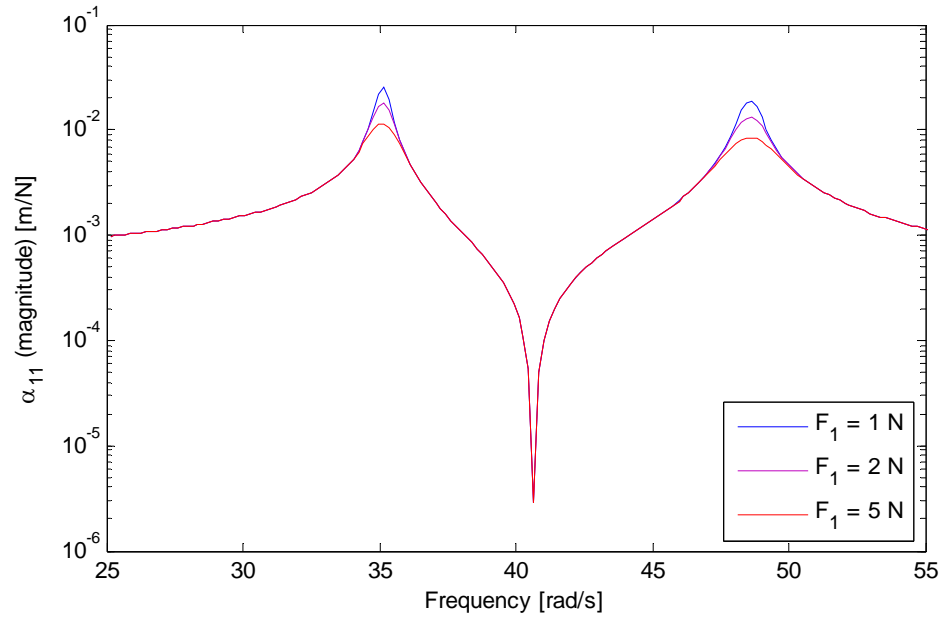


Figure 69. Pseudo receptance of the system in Case Study 7 to different forcing levels.

4.3 Structural Modification in a Nonlinear System by Using Modal Model

In this section, implementation of the proposed method in structural modification analysis of nonlinear systems is given. In each of the following case studies, a nonlinear system is modified with linear elements and the response of the modified system is calculated by using the modal model of the original nonlinear system. The model is constructed with the modal parameters identified from the displacement controlled simulated FRFs of the original nonlinear system.

4.3.1 Case Study 8

In this case study, the nonlinear substructure in Case Study 6 is taken as the system to be modified. Modal parameters of the original nonlinear system are already given in Figure 57 and Figure 58. The system is modified as follows:

$$[\Delta M] = \begin{bmatrix} 1 & 0 & 0 \\ 0 & 0 & 0 \\ 0 & 0 & 1 \end{bmatrix} \text{ kg}, [\Delta K] = 10^5 \times \begin{bmatrix} 1 & -0.5 & 0 \\ -0.5 & 1 & -0.5 \\ 0 & -0.5 & 1 \end{bmatrix} \text{ N/m},$$

$$[\Delta H] = 0.02[\Delta K] \text{ N/m}$$

The variations of modal parameters and the linear modification matrices are used in the iterative solution of the modified system as given in section 3.3. The pseudo point FRF of the modified system for forcing level of 100 N applied on the first mass and the point FRF of the original system is shown in Figure 70.

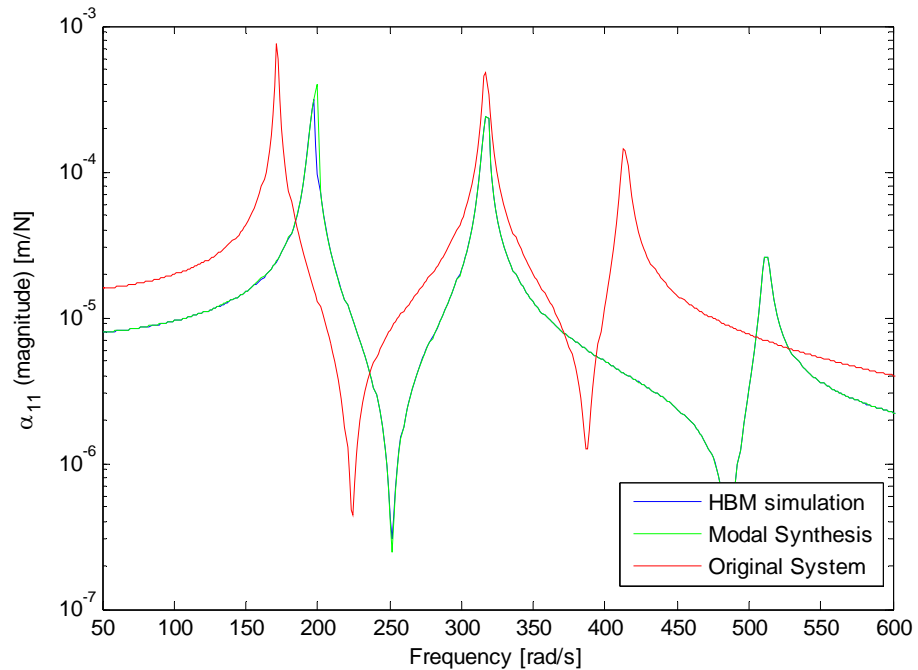


Figure 70. Pseudo receptance of the system in Case Study 8 to a forcing level

$$F_1 = 100\text{N}.$$

4.3.2 Case Study 9

In this case study the three – DOF nonlinear system in Case Study 5 is modified as follows:

$$[\Delta M] = \begin{bmatrix} 1 & 0 & 0 \\ 0 & 0 & 0 \\ 0 & 0 & 1 \end{bmatrix} \text{ kg}, [\Delta K] = 10^5 \times \begin{bmatrix} 1 & -0.5 & 0 \\ -0.5 & 1 & -0.5 \\ 0 & -0.5 & 1 \end{bmatrix} \text{ N/m},$$

$$[\Delta C] = 0.00003[\Delta K] \text{ Ns/m}$$

Modal parameters of the original nonlinear system are already given in Figures 63 - 68. The identified modal parameters of the original nonlinear system and the modification matrices are used in the computation of the response of the modified system. Pseudo point FRF of the system for forcing levels of 100 N, 200 N and 500 N and the corresponding FRF of the original system are shown in Figure 71. The force is applied on the first mass of the modified system.

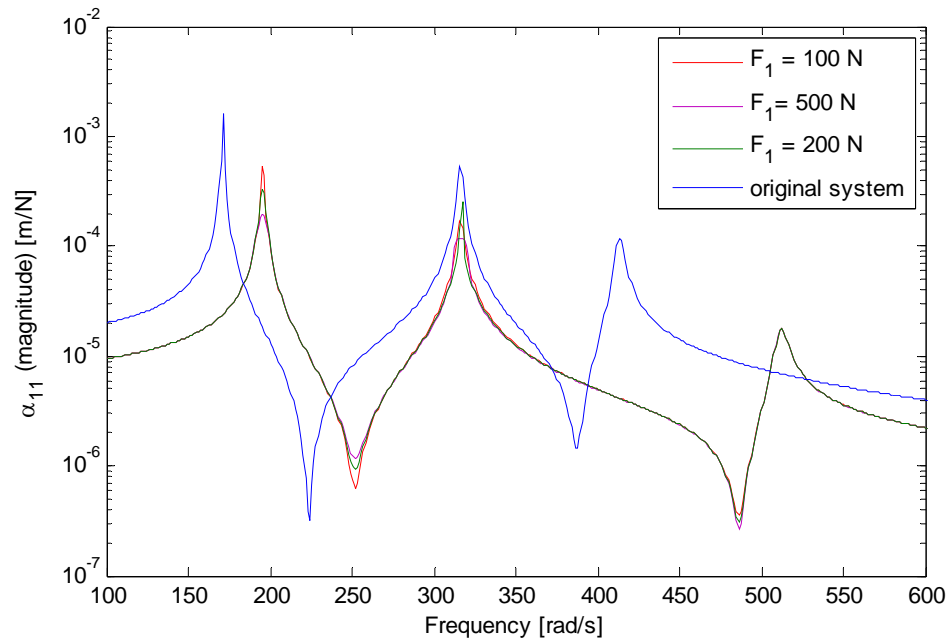


Figure 71. Response of the system in Case Study 9 to different forcing levels.

4.4 Experimental Case Study

For the validation of the method developed in this study in application to a real system, the results of a nonlinear modal test conducted by Aykan in a recent study [32] are used. The setup is similar to the one previously used by Ferreira [29] and later by Elizalde Siller [23].

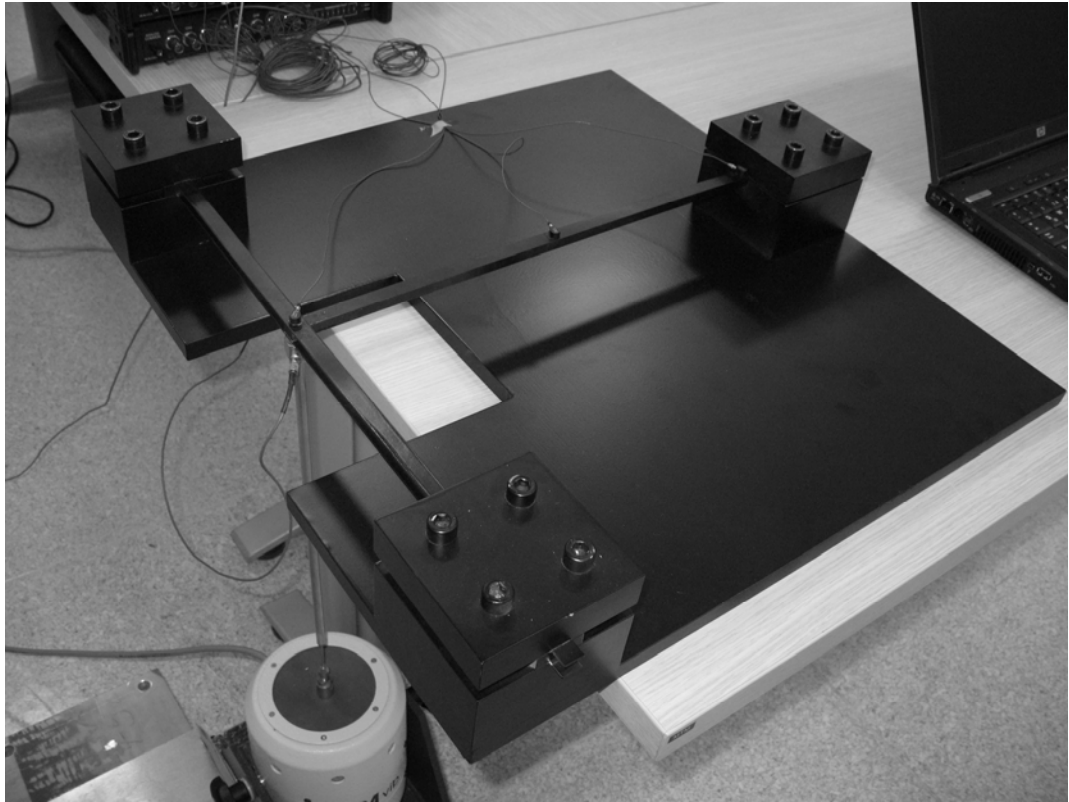


Figure 72. Experimental Setup

The setup consists of a linear cantilever beam with its free end held between two thin identical beams which generate the cubic spring effect.

Before the dynamic tests, a static test has been conducted in order to establish the stiffness characteristics of the setup. The results of this test are presented as a

force versus deflection curve shown in Figure 73. When the curve is examined, cubic stiffness characteristics can easily be observed in the system, which clearly show that nonlinearity is present in the setup.

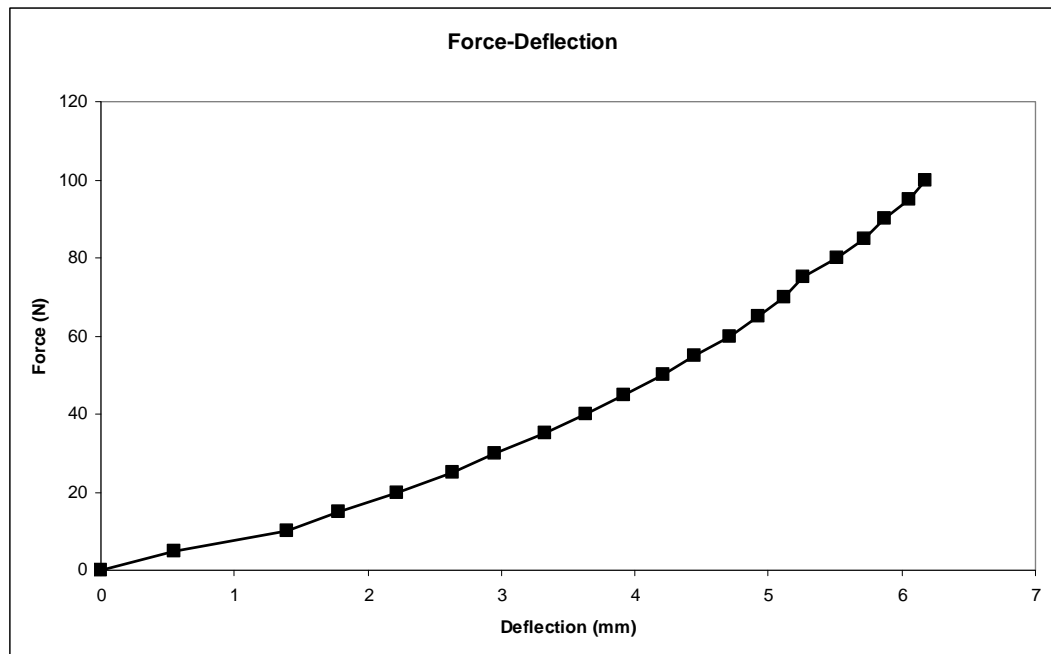


Figure 73. Stiffness characteristics of the experimental setup

The vibration tests are divided into two groups: constant force testing and constant displacement testing. In order to simplify the analyses and validate the model, only the driving point FRF's were considered in the tests. The FRF results obtained for the constant force and constant displacement tests are shown in Figure 74 and Figure 75, respectively.

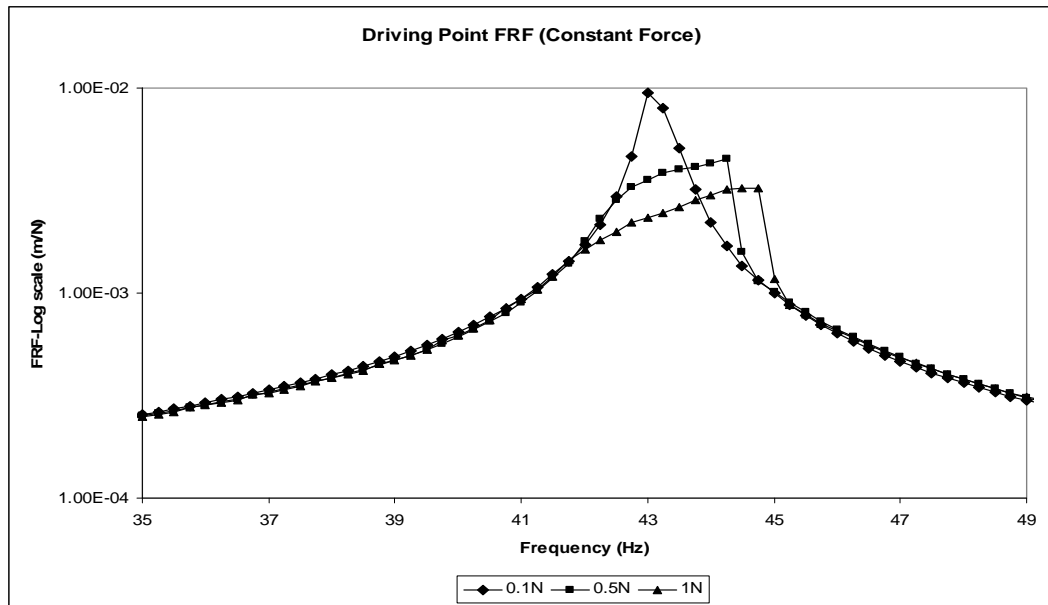


Figure 74. FRFs obtained from force controlled tests

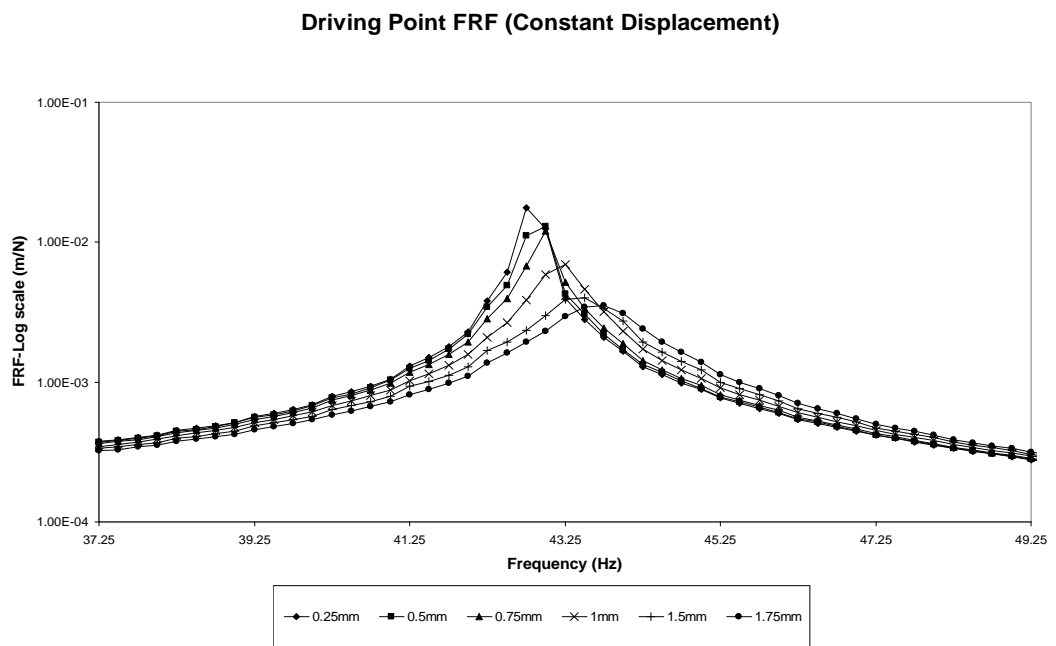


Figure 75. FRFs obtained from displacement controlled tests

The FRFs obtained by displacement controlled tests were identified to construct the modal model of the system. 6 tests were performed with different displacement amplitudes. Modal parameters corresponding to each FRF are extracted to use as the model of the system and are shown in Table 3 and represented in Figure 76. A good agreement between the measured and regenerated FRFs with identified parameters is achieved.

Table 3. Modal parameters obtained by identification of constant displacement FRFs

Displacement amplitude [mm]	Natural frequency [rad/s]	Damping ratio (viscous damping model)	Modal constant	
			Magnitude	Phase angle (degrees)
0.25	269.11	0.00190	6.5061	2.5281
0.50	269.48	0.00285	6.7166	1.7540
0.75	270.14	0.00430	6.9004	1.7826
1.00	271.43	0.00558	6.4468	-2.3939
1.50	272.84	0.01043	6.8385	5.5669
1.75	274.31	0.01243	6.6291	-2.8006

A proper function is fitted to every set of parameters with respect to displacement amplitude. One can observe that the values for the magnitude modal constant do not follow a proper trend but fluctuate around a nominal value. On this reason, their mean value is taken as if it is the actual value instead of fitting a curve.

The model is used to predict the response of the system at 4 different forcing levels. Results are compared with that of the force controlled tests measured at the same forcing levels. FRFs used for identification were measured for a frequency range limited to one resonance peak only. Synthesis of FRFs was also performed for this frequency range.

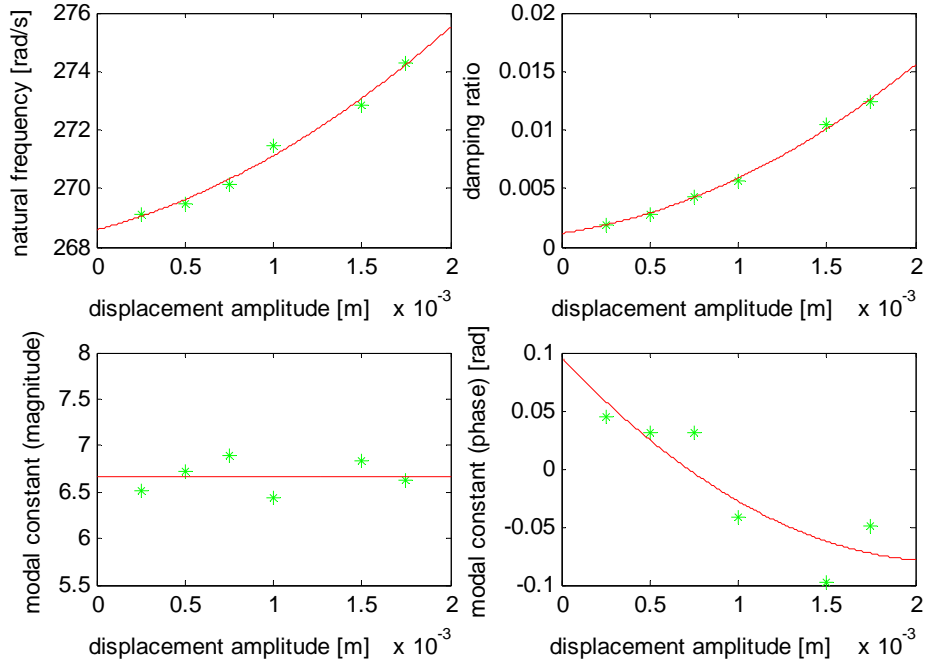


Figure 76. Variation of the modal parameters with respect to response amplitude.

(* identified parameters, — fitted curve)

Frequency response of the system at forcing levels of 0.1 N, 0.2 N, 0.5 N and 1 N are calculated by using the modal model and presented in Figures 74 – 77. The consistency of the pseudo receptance values obtained from the modal model with constant force FRFs demonstrates the validity of the modal model. Differences are observed between the results around the frequency range through which constant displacement measurements are carried. It is believed it is due to force dropouts that were encountered during constant force tests at the resonance zone. Another possible reason is that the displacement amplitude controlled FRFs were carried out for a frequency range covering a single mode which prevents the inclusion of the effect of out of range modes on the identified modal parameters.

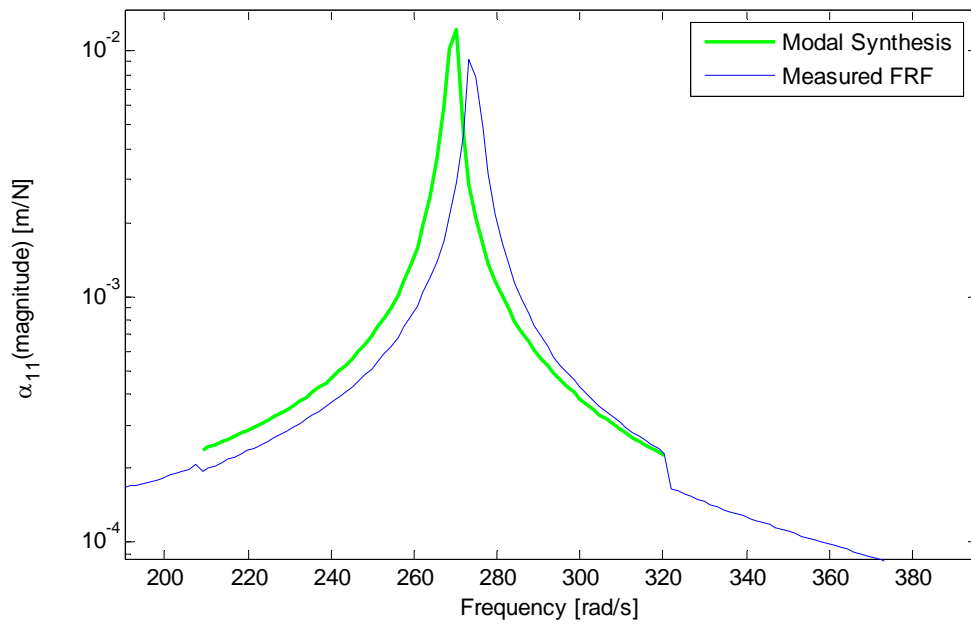


Figure 77. Pseudo receptance of the system to $F = 0.1$ N

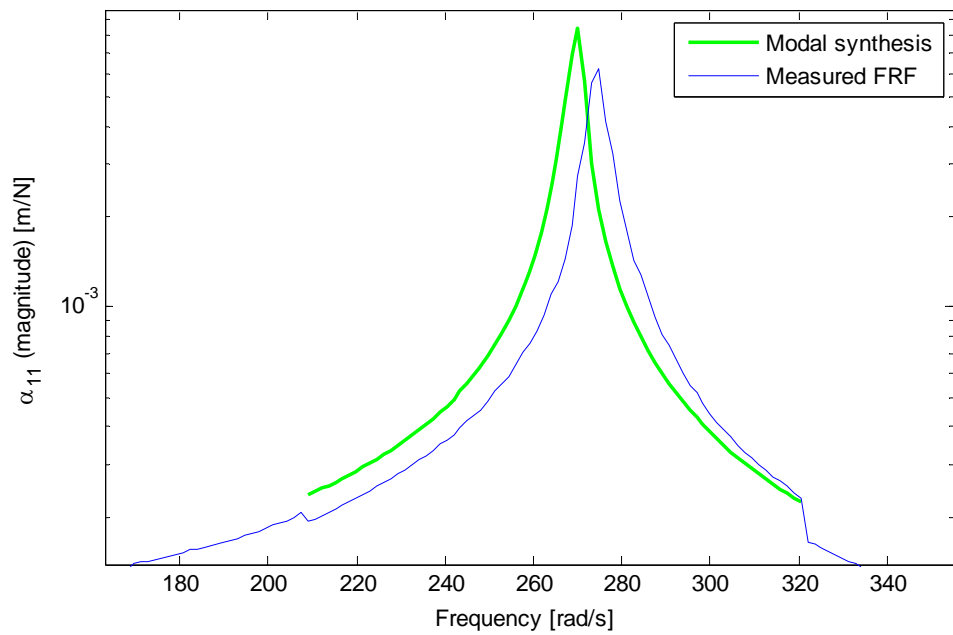


Figure 78. Pseudo receptance of the system to $F = 0.2$ N

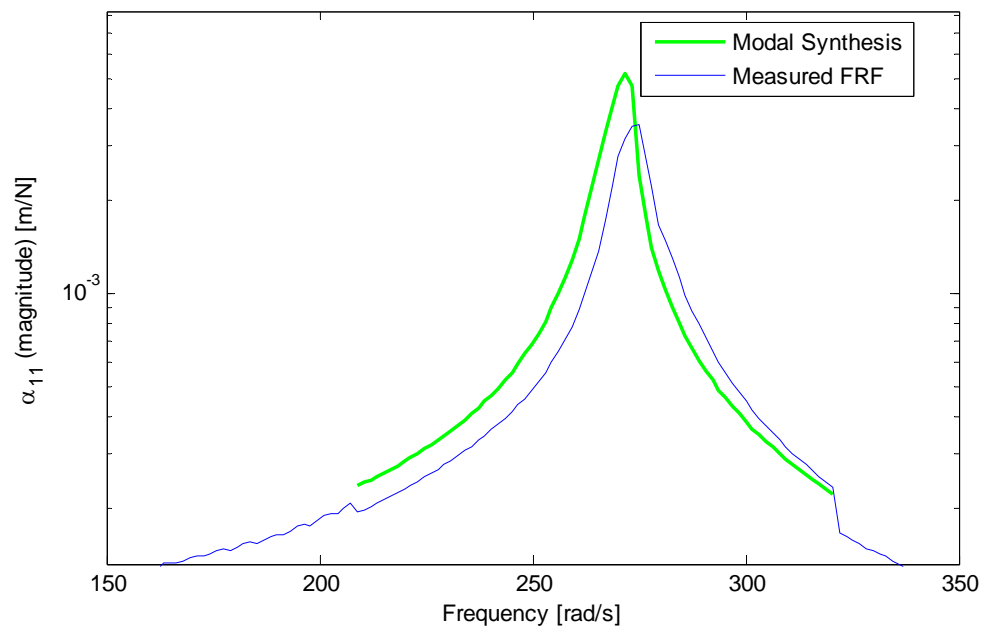


Figure 79. Pseudo receptance of the system to $F = 0.5$ N

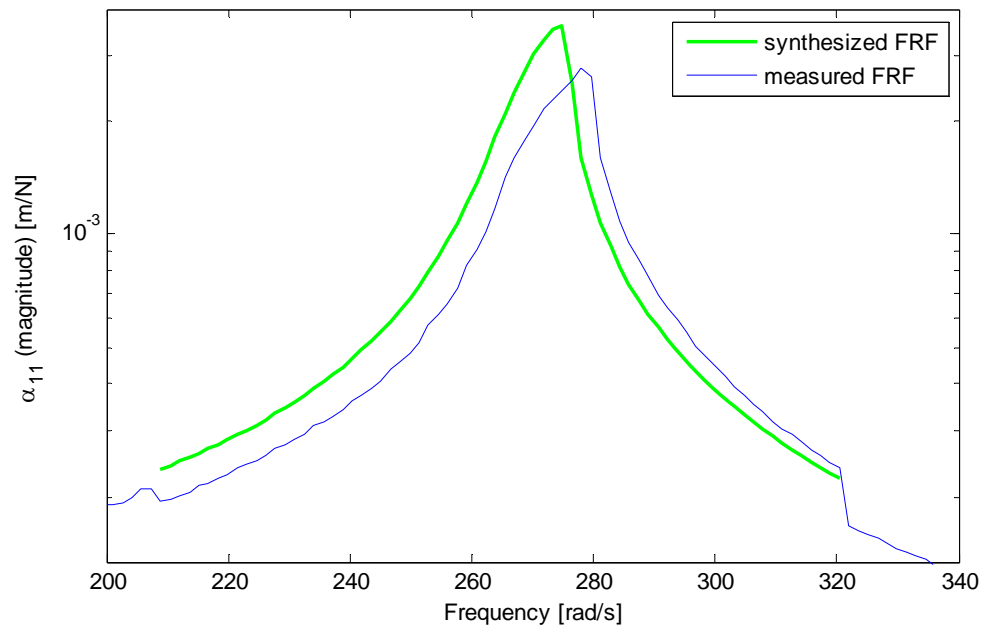


Figure 80. Pseudo receptance of the system to $F = 1$ N

CHAPTER 5

CONCLUSIONS

In this thesis a new approach for modal identification and modal analysis of nonlinear systems is proposed. The modal model of a nonlinear system is obtained by identifying modal parameters from the linear FRFs obtained for constant displacement amplitude of the nonlinear coordinate (the coordinate where nonlinear element is connected), or for constant relative displacement amplitude between the nonlinear coordinates for interconnected nonlinear elements. Repeating the identification for different response amplitudes, identified modal parameters can be expressed as functions of the related response amplitude. Here, the fact that nonlinear systems exhibit linear behavior under certain conditions is used and this made the use of linear identification methods on nonlinear systems possible.

It is demonstrated with case studies that the modal model can successfully be employed in the nonlinear response prediction of the system at any forcing level. The uses of a modal model in dynamic coupling of the identified nonlinear system with a linear system, and also in the dynamic modification analysis of a nonlinear system are also formulated and validated by case studies. In order to validate the results, comparison with the solutions of the same case study with harmonic balance method is used.

In order to investigate the effect of actual conditions such as experimental errors and noise, two of the case studies are used with polluted data. Data pollution is performed by multiplication of FRF values with random numbers. It was observed that modal parameters are generally not affected considerably and the results still show considerable match with the solution of harmonic balance method.

It was also observed that the variation of modal parameters may be used to identify the characteristics of the nonlinearity in the structure. For instance, natural frequency values of a structure with stiffness nonlinearity spread around a moderate range whereas those of a structure with damping nonlinearity remain almost constant. In such cases where the parameters do not follow an apparent trend but deviate around a nominal value, mean value of the modal parameters is used instead of fitting a curve to the identified parameters. It is possible to use this observation as a tool to determine the type of the nonlinearity in a system. Therefore, for a further research it can be recommended to use the relations between the nonlinearity type and modal parameter variations in nonlinear modal identification.

As the modal parameters are represented as functions of the response itself, an iterative solution is required in each analysis. Fixed point iteration is used as the numerical solution method, and a weighting coefficient is employed in order to provide convergence at frequencies near resonance, especially with systems involving jump phenomena.

The agreement observed between the frequency responses obtained by using the method proposed in this study with those of the harmonic balance method demonstrated the validity of the modal model and the method suggested, provided that the basic assumption “harmonic excitation results in harmonic response at the same frequency” holds true, as both approaches base on this assumption. However, a slight mismatch is observed between the solutions of this study and those of HBM only around frequencies where jump occurs.

In order to investigate the validity of the proposed method in real structures, data obtained from a nonlinear modal test conducted in a recent study [32] are also studied and the results are presented as an experimental case study. Solutions obtained by the proposed method are compared to the results of force controlled tests that are also presented in the same recent study for validity. The results are found consistent in a good extent.

The methods suggested are applicable to nonlinear systems where nonlinearity is localized and therefore can be modeled as a single element, either grounded or between any two coordinates. However, it is observed that the methods work more effectively for grounded nonlinear elements. Improvement of the solution with interconnected nonlinear elements is suggested as future work. Furthermore, feasibility of performing constant displacement amplitude vibration tests should also be investigated.

For future work, comparison and validation of the results with time domain solutions can be performed. This can be useful in terms of investigating the mismatch between the solutions obtained with the proposed method and the harmonic balance method.

Considering the proposed method is applied on small scale systems with local nonlinearity, implementation of the proposed method for large systems possessing nonlocal nonlinearity is also suggested as future work.

REFERENCES

- [1] Ewins, D.J., “Modal Testing: Theory and Practice”, Research Studies Press, Letchworth and Wiley, N.Y, 1984.
- [2] Worden, K., Tomlinson, G.R., “Nonlinearity in Structural Dynamics: Detection, Identification and Modeling”, IoP Publishing, 2001.
- [3] He, J., “Identification of Structural Dynamic Characteristics”, Phd Thesis, Imperial College of Science, Technology and Medicine, 1987.
- [4] Goge, D., Sinapius, M., Fullekrug, U., Link, M., “Detection and Description of Nonlinear Phenomena in Experimental Modal Analysis via Linearity Plots”, International Journal of Nonlinear Mechanics, Volume 40, Issue 1, Nonlinear Fluid Mechanics, 27-48, 2005.
- [5] Mertens, M., Van der Auweraer, H., Vanherck, P., Snoeys, R., “Detection of Nonlinear Dynamic Behaviour of Mechanical Structures”, 4th International Modal Analysis Conference, Los Angeles, California, USA, 712-719, 1986.
- [6] He, J., Ewins, D. J., "A Simple Method of Interpretation for the Modal Analysis of Nonlinear Systems," 5th International Modal Analysis Conference, London, England, 626-634, 1987.
- [7] Lin, R. M., Ewins, D. J., “On the Location of Structural Nonlinearity from Modal Testing - A Feasibility Study”, 8th International Modal Analysis Conference, 497-515, 1990.
- [8] Lin, R. M., “Identification of the Dynamic Characteristics of Nonlinear Structures”, Phd Thesis, Imperial College of Science, Technology and Medicine, 1990.

- [9] Vakakis, A. F., Ewins, D. J., “Effects of Weak Nonlinearities on Modal Analysis”, 10th International Modal Analysis Conference, San Diego, California, USA, 73-78, 1992.
- [10] Benhafi, Y., Penny, J. E. T., Friswell, M.I., "A Method of System Identification for Nonlinear Vibrating Structures", 8th International Modal Analysis Conference, Kissimmee, Florida, USA, 1284-1290, 1990
- [11] Benhafi, Y., Penny, J. E. T., Friswell, M.I., "A Parameter Identification Method for Discrete Nonlinear Systems Incorporating Cubic Stiffness Elements", International Journal of Analytical and Experimental Modal Analysis, Volume 7, Issue 3, 179-196, 1992.
- [12] Özer, M. B., Özgüven, H. N., “A New Method for Localization and Identification of Nonlinearities in Structures”, 6th Biennial Conference on Engineering Systems Design and Analysis, İstanbul, Turkey, 2002.
- [13] M.Bü. Özer, et al., Identification of structural non-linearities using describing functions and the Sherman–Morrison method, Mechanical Systems and Signal Processing (2008), doi:[10.1016/j.ymssp.2007.11.014](https://doi.org/10.1016/j.ymssp.2007.11.014)
- [14] Song, H. W., Wang, W. L., “Nonlinear System Identification Using Frequency Domain Measurement Data”, 16th International Modal Analysis Conference, Santa Barbara, California, USA, 746-752, 1998.
- [15] Özgüven, H. N., İmregün, M., “Complex Modes Arising from Linear Identification of Nonlinear Systems”, The International Journal of Analytical and Experimental Modal Analysis, Volume 8, Issue 2, 151-164, 1993.
- [16] Setio, S., Setio, H. D., Jézéquel, L., “Modal Analysis of Nonlinear Multi-degree-of-freedom Structures”, International Journal of Analytical and Experimental Modal Analysis, Volume 7, Issue 2, 75-93, 1992.

- [17] Ferreira, J. V., Ewins, D. J., “Nonlinear Receptance Coupling Approach Based on Describing Functions”, 14th International Modal Analysis Conference, Dearbourn, February, 1996.
- [18] Richard, C. M., Singh, R., “Feasibility of Identifying Nonlinear Multi-Degree-of-Freedom Systems with Unknown Polynomial Forms”, 18th International Modal Analysis Conference, San Antonio, Texas, February 7-10, 2000.
- [19] Chong, Y. H., İmregün, M., “Modal Parameter Extraction Methods for Nonlinear Systems”, 16th International Modal Analysis Conference, Santa Barbara, California, USA, 728-735, 1998.
- [20] Chong, Y. H., İmregün, M., “Variable Modal Parameter Identification for Nonlinear MDOF Systems – Parts I & II”, Journal of Shock and Vibration, Volume 8, Issue 4, 217-227, 2000.
- [21] Chong, Y. H., İmregün, M., “Coupling of Nonlinear Substructures Using Variable Modal Parameters”, Mechanical Systems and Signal Processing, Volume 14, Issue 5, 731-746, 2000.
- [22] Chong, Y. H., İmregün, M., “Development and Application of a Nonlinear Modal Analysis Technique for MDOF Systems”, Journal of Vibration and Control, Issue 7, 167 – 179, 2001
- [23] Elizalde Siller, H. R., “Nonlinear Modal Analysis Methods for Engineering Structures”, Phd Thesis, Imperial College of Science, Technology and Medicine, 2004.
- [24] Budak, E., Özgüven, H. N., “A Method for Harmonic Response of Structures with Symmetrical Nonlinearities”, 15th International Seminar on Modal Analysis, Leuven, Belgium, 901–915, 1990.

- [25] Budak, E., Özgüven, H. N., “Iterative Receptance Method for Determining Harmonic Response of Structures with Symmetrical Nonlinearities”, *Mechanical Systems and Signal Processing*, 75–87, 1993.
- [26] Tanrikulu, Ö, Kuran, B., Özgüven, H. N. and Imregun, M., “Forced Harmonic Response Analysis of Nonlinear Structures”, *AIAA Journal*, Volume 31, 1313 - 1320, 1993.
- [27] Gelb, A., and Vander Velde, W. E., “Multiple-Input Describing Functions and Nonlinear System Design”, McGraw Hill, 1968.
- [28] Perinpanayagam, S., Robb., D., Ewins., D. J., Barragan, J. M., “Non-linearities in an Aero-engine Structure: From Test to Design”, 2004 International Conference on Modal Analysis Noise and Vibration Engineering, Leuven, Belgium, 3167–3182, 2004.
- [29] Ferreira, J. V., “Dynamic Response Analysis of Structures with Nonlinear Components”, Phd Thesis, Imperial College of Science, Technology and Medicine, 1998.
- [30] Özgüven, H. N., “Structural Modifications Using Frequency Response Functions”, *Mechanical Systems and Signal Processing*, Volume 4, Issue 1, 53-63, 1987.
- [31] Richardson, M., Formenti, D., “Parameter Estimation from Frequency Response Measurements Using Rational Fraction Polynomial”, 1st International Modal Analysis Conference, Orlando, Florida, 1982.
- [32] Arslan, Ö., Aykan, M., Özgüven, H. N., “An Experimental Study on Identification of Nonlinear Systems”, in preparation.

APPENDIX A

HARMONIC INPUT DESCRIBING FUNCTIONS

Mathematical expressions and the corresponding harmonic input describing functions for the nonlinearities considered in this work are listed below:

- Cubic Stiffness:

$$n = bx^3$$

$$\nu = \frac{3}{4}bX^2$$

- Velocity Squared Damping

$$n = b\dot{x}|\dot{x}|$$

$$\nu = \frac{8b\omega^2 X}{3\pi}$$

- Piecewise Linear Stiffness

$$n = k_1 x, \quad |x| < \delta$$

$$n = (k_1 - k_2)\delta + k_2 x, \quad |x| \geq \delta$$

$$\nu = k_1, \quad X < \delta$$

$$\nu = \frac{2(k_1 - k_2)}{\pi} \left[\sin^{-1} \left(\frac{\delta}{X} \right) + \left(\frac{\delta}{X} \right) \sqrt{1 - \left(\frac{\delta}{X} \right)^2} \right] + k_2, \quad X \geq \delta$$

APPENDIX B

Modal Identification of Non-Linear Structures and the Use of Modal Model in Structural Dynamic Analysis

Özge Arslan and H. Nevzat Özgüven
Department of Mechanical Engineering
Middle East Technical University
Ankara 06531, TURKEY

Email: arslan@me.metu.edu.tr, ozguven@metu.edu.tr

NOMENCLATURE

$[D]$	Dynamic structural modification matrix
$\{f\}$	Generalized external forcing vector
$\{F\}$	Amplitude vector of harmonic external forcing
i	Unit imaginary number
$[H]$	Linear structural damping matrix
$[I]$	Identity matrix
$[K]$	Linear stiffness matrix
$[M]$	Linear mass matrix
$\{N\}$	Internal non-linear forcing vector
n	Number of degrees of freedom
v	Describing function
$\{x\}$	Displacement vector
$\{X\}$	Complex amplitude vector of steady state harmonic displacements
$[\alpha]$	Receptance matrix
$[\Delta]$	Non-linearity matrix
$[\Delta C]$	Viscous damping matrix of modifying system
$[\Delta K]$	Stiffness matrix of modifying system
$[\Delta M]$	Mass matrix of modifying system
$[\gamma]$	Receptance matrix of modified system
ω	Excitation frequency

ABSTRACT

One of the major problems in structural dynamics is to identify nonlinearity, which is usually local in large structural systems, and to conduct dynamic analysis of the non-linear system. In this work, a new approach is suggested for modal identification of a non-linear system. Modal parameters obtained through modal identification are used in harmonic response prediction at different forcing levels. The response at only the fundamental harmonic is considered. The model can also be used to predict the response of the non-linear system coupled with a linear system and/or subjected to structural modification. An iterative solution method is used in structural dynamic analyses. The identification method proposed is for systems where nonlinearity is between a single coordinate and the ground. Response dependent modal parameters of the non-linear system are obtained via modal testing at different response levels. The method presented is verified through case studies. In the case studies presented, a subsystem with cubic stiffness type non-linearity is considered and the simulated FRFs of the subsystem generated for various response levels are used as pseudo experimental values.

1. INTRODUCTION

Nonlinearity is a generally encountered phenomenon in mechanical structures. Although structures in general have some amount of nonlinearity, response amplitudes are so small that non-linear forces are not excited in most cases. Therefore a linear model will be sufficient for dynamic analysis. However in some cases, especially when there are joints introducing high nonlinearity or when the response level is so high that non-linear forces are comparable to linear forces, a linear model will not suffice and a non-linear analysis will be required.

There exist a variety of studies in non-linear structural dynamics area, most of which concentrate on detection, localization, and identification of nonlinearity [1 - 8]. In recent years studies on modeling and identification of nonlinearity have also increased. However, construction of reliable models for non-linear structures is still an uncertain issue in this field. Former studies [9 - 11] show that linear identification of non-linear systems causes misleading results. In [9] Özgüven and Imregün applied linear modal analysis on classically damped non-linear systems. The results showed highly complex modes that indicate non-linear behavior since the initial damping was proportional. This indicated that linear identification methods can reveal nonlinearity in a structure but they fail to provide a reliable modal model. As linear modal analysis tools are not compatible with the non-linear theory, majority of the studies in this field [11 - 13] focus on development of non-linear modal analysis techniques. Chong and Imregün [14 - 15] suggested a non-linear modal analysis for a multi-degree-of-freedom system by first identifying modal parameters from measured response. For verification they used simulated non-linear response data. They were able to predict the non-linear response of the system for other excitation levels by using the modal parameter variations with respect to modal displacement.

The approach proposed in this study bases on the fact that non-linear structures exhibit linear behavior under certain conditions, which makes the use of linear modal identification methods possible. Modal parameters identified under these conditions are used to construct a modal model for the non-linear system to be analyzed. In that respect, this study follows a similar approach with that of Chong and Imregün [14 - 15]. However, in the present study physical displacements are used, unlike in references [14] and [15] in which modal displacements were employed. Furthermore, the present work uses a semi analytical approach for the modal model, and also extends the use of the modal model in structural modification problems in addition to response prediction and dynamic coupling analysis.

2. THEORY

When a constant amplitude harmonic force is applied over a frequency range, the non-linear elements in a structure will act like equivalent dampings and/or stiffnesses with different values at each frequency. However, when the response level is kept constant in a frequency sweep experiment, non-linear elements will behave as equivalent *linear* elements, and the structure will behave linearly for that response level as discussed in [2] and experimentally shown in [16]. Then if an FRF of a non-linear system is measured by keeping the response amplitude constant (with displacement controlled experiments), a linear identification can be carried out, and a set of modal parameters for each response level can be obtained. Then, the modal parameters identified at several response levels can easily be employed in harmonic response analyses.

2.1 Modal Identification of Non-linear Structures from Response Level Controlled FRFs – Modal Model of a Non-linear Structure

Consider the equation of motion of a non-linear MDOF system:

$$[M]\{\ddot{x}\} + [K]\{x\} + i[H]\{\dot{x}\} + \{N(x, \dot{x})\} = \{f\} \quad (1)$$

where matrices $[M]$, $[H]$ and $[K]$ represent the mass, structural damping and stiffness matrices, respectively. Vectors $\{x\}$ and $\{f\}$ stand for the response and external force applied on the system, respectively. The vector $\{N\}$ corresponds to the non-linear internal forces in the system. This force vector is usually a function of displacement and/or velocity response, depending on the nonlinearity present in the system. In this study the nonlinearity between a single coordinate and the ground is considered, therefore $\{N\}$ includes only one nonzero element.

Considering a sinusoidal excitation at a frequency ω and assuming that the response is also harmonic at the same frequency, the forcing and response vectors can be written as;

As the nonlinearity considered in this study is between a single coordinate and the ground, $\{N\}$ includes only one nonzero element. Consequently, the nonlinearity matrix for the system consists of only one nonzero diagonal element v_{ii} as can be seen from Eq. (6).

Substituting Eqs. (2), (3) and (5) into Eq. (1), yields

$$\left(-\omega^2[M] + [K] + i[H] + [\Delta(x, \dot{x})]\right)\{X\} e^{i\omega t} = \{F\} e^{i\omega t} \quad (8)$$

Then the receptance matrix of the system can be written as:

$$\alpha(\omega, X) = \left[-\omega^2[M] + [K] + i[H] + [\Delta(x, \dot{x})]\right]^{-1} \quad (9)$$

From Eq. (6) it is seen that the nonlinearity can be considered as an added equivalent stiffness matrix which is a function of the response amplitude, provided that the describing function for the nonlinearity is a function of only the response amplitude. Then, it can be concluded that response controlled measurements provide linear FRFs, each corresponding to a different response level. Response controlled measurements are to be performed by keeping the response amplitude of the non-linear coordinate constant. Here the term "non-linear coordinate" refers to the coordinate to which the non-linear element is attached. Identification by using these FRFs results in a set of modal parameters for the system, each set corresponding to a specific response amplitude value. The above derivation is for a system with structural damping, and it can easily be extended to a viscously damped system.

As the identified modal parameters vary with respect to the response amplitude X_i , identified modal parameters can be expressed as a function of X_i as follows

$$\omega_r = \omega_r(X_i) \quad (10)$$

$$\eta_r = \eta_r(X_i) \quad (11)$$

$$r A_{kl} = r A_{kl}(X_i) \quad (12)$$

This model then can be used in harmonic response prediction of the non-linear system, as well as in coupling and modification analyses, which will be discussed in detail below.

2.2 Harmonic Response Prediction in Non-linear Structures by Modal Superposition

Once the variation of the non-linear modal parameters with respect to the response amplitude is known, the harmonic response amplitude X_i can be written as

$$X_i = \left| \alpha_{ij}(\omega, X_i) \right| \cdot F_j \quad (13)$$

Here, F_j is the amplitude of the harmonic force applied at j^{th} coordinate and α_{ij} is the response level dependent receptance value. Note that, α_{ij} should actually be called "pseudo receptance" as it is not possible to talk about receptance for a non-linear system. The pseudo receptance expression in Eq. (13) can be written as a modal summation in terms of modal parameters identified above, as follows

$$\alpha_{ij}(\omega, X_i) = \sum_{r=1}^n \frac{r A_{ij}(X_i)}{\left(\left(\omega_r(X_i) \right)^2 - \omega^2 + i \left(\omega_r(X_i) \right)^2 \eta_r(X_i) \right)} \quad (14)$$

Then, the solution of Eq. (13) requires iteration. Once a convergent solution is obtained for X_i then the rest of the response amplitudes X_j ($j = 1, 2, \dots, n, j \neq i$) can be calculated directly by using the modal data corresponding to the convergent response value, X_i .

Eq. (13) is an implicit equation in X_i so it can be solved iteratively with a proper numerical solution method for a given ω . In this study the fixed point iteration method is used for the numerical solution, and a weighting

coefficient is employed in order to provide convergence at frequencies near resonance. Note that this solution will be valid only for the case where there is a harmonic force with amplitude F_j applied at the j^{th} coordinate.

2.3 Structural Coupling by Using Modal Model

The modal model obtained above can also be employed in dynamic analyses of the non-linear system coupled with linear ones by using the receptance coupling method. Receptance values for the linear system can be found experimentally or computationally by linear modal analysis tools, whereas, the pseudo receptance values of the non-linear system are calculated from the modal model as explained above.

Let us consider a non-linear system coupled rigidly with a linear system as shown in Figure 2.

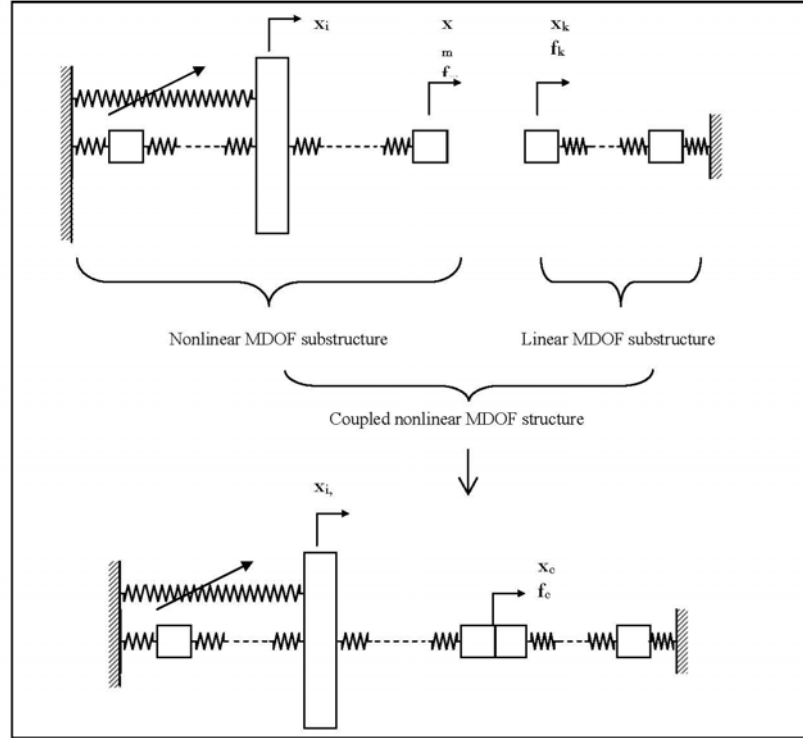


Figure 2. Non-linear system coupled rigidly with a linear system

The receptance matrices of the non-linear and linear substructures can be partitioned as follows

$$[\alpha_{NL}] = \begin{bmatrix} \alpha_{mm} & [\alpha_{mn}] \\ [\alpha_{nm}] & [\alpha_{nn}] \end{bmatrix} \quad (15)$$

$$\begin{bmatrix} \alpha_L \end{bmatrix} = \begin{bmatrix} \alpha_{kk} & \alpha_{kl} \\ \alpha_{lk} & \alpha_{ll} \end{bmatrix} \quad (16)$$

Here subscripts m and k refer to the coordinates to be coupled, and subscripts n and l represent the rest of the coordinates in the non-linear and linear systems, respectively.

By using classical receptance coupling techniques, the receptance matrix of the coupled system can be obtained as

$$\begin{bmatrix} \alpha^C \end{bmatrix} = \begin{bmatrix} \alpha_{nm}^C & \alpha_{nl}^C \\ \alpha_{ln}^C & \alpha_{ll}^C \end{bmatrix} \quad (17)$$

where

$$\alpha_{nl}^C = \frac{\alpha_{nm} \alpha_{kl}}{\alpha_{nm} + \alpha_{kk}} \quad (18)$$

$$\alpha_{nn}^C = \alpha_{nn} - \frac{\alpha_{nm} \alpha_{mn}}{\alpha_{nm} + \alpha_{kk}} \quad (19)$$

$$\alpha_{ln}^C = \frac{\alpha_{lk} \alpha_{mn}}{\alpha_{nm} + \alpha_{kk}} \quad (20)$$

$$\alpha_{ll}^C = \alpha_{ll} - \frac{\alpha_{lk} \alpha_{kl}}{\alpha_{nm} + \alpha_{kk}} \quad (21)$$

As the elements of α_{NL} are response level dependent pseudo receptances, so are the receptance values in α^C :

$$\alpha^C = \alpha^C(\omega, X_i) \quad (22)$$

Then α_{ij}^C from Eq. (22) can be substituted in Eq. (13) to find the response of the system to a harmonic forcing applied at the j^{th} coordinate. The solution, again requires iteration.

When rigid coupling is made as above, the formulation does not permit to take the coordinate where the non-linear element is attached as the coupling node; because, in rigid coupling the receptance matrix of the coupled system does not include the receptances related to the coupling node, whereas the amplitude of the displacement of the non-linear coordinate is required in the analysis. Yet, flexible coupling can easily overcome this difficulty.

2.4 Structural Modification of a Non-linear Structure by Using Modal Model

The basic methodology presented in this study can also be implemented in structural modification problems. Consider a MDOF linear system for which the receptance matrix $[\alpha]$ at frequency ω is known. When this system is modified without increasing the total degrees of freedom of the system, the receptance matrix $[\gamma]$ of the modified structure can be written as [21]

$$[\gamma] = [I] + [\alpha][D]]^{-1} [\alpha] \quad (23)$$

where

$$[D] = [\Delta K] - \omega^2 [\Delta M] + i [\Delta H] \quad (24)$$

Here, $[\Delta K]$, $[\Delta M]$ and $[\Delta H]$ represent the stiffness, mass and damping matrices of the modifying structure, respectively. If the modification is local, the above equations can be written in terms of partitioned matrices [21], which reduces the computation time considerably.

Now if we apply the same modification method to a non-linear system, then $[\alpha]$ in Eq. (23) will be the pseudo receptance matrix of the non-linear system which can be obtained by modal synthesis by using identified response dependent modal parameters discussed above. Thus the response dependent pseudo receptance of the modified system will be given by

$$[\gamma(\omega, X_i)] = [I] + [\alpha(\omega, X_i)][D]]^{-1} [\alpha(\omega, X_i)] \quad (25)$$

which can be used to find X_i . Again, an iterative solution is required. For large systems, the formulation given in [21] can be employed to reduce the computational effort.

3. CASE STUDIES

The application and the validation of the methods proposed are demonstrated by using simple discrete systems for the sake of simplicity. In each case, simulated FRFs generated at different response levels are used as pseudo experimental data. In practice, sine sweep vibration test is to be used. Modal parameters obtained through the identification of pseudo experimental FRFs are expressed as a function of response amplitude. The modal model of the non-linear system constructed is then employed in response computations. Identification of modal parameters is performed by using MODENT®. The responses obtained from modal model are compared with the frequency response of the system calculated by harmonic balance approach.

3.1 Case Study 1

The system used in [9] is considered in this case study. As shown in Figure 3, it is a 2-DOF system with cubic stiffness.

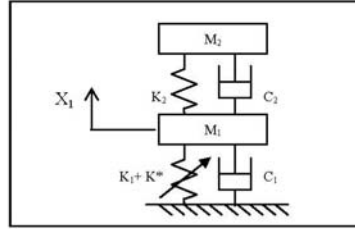


Figure 3. The system considered in Case Study 1

The properties of the system are as follows:

$$M_1 = 20 \text{ kg}, M_2 = 2 \text{ kg}, \quad K_1 = 8 \times 10^6 \text{ N/m}, K_2 = 8 \times 10^5 \text{ N/m},$$

$$K^* = 10^{10} \cdot X_1^2 \text{ [N/m]}, \quad C_1 = 2.15 \times 10^2 \text{ Ns/m}, C_2 = 21.5 \text{ Ns/m}$$

By using the pseudo experimental FRF curves obtained in the frequency range of 60-160 Hz, for several $|X_1|$ values ranging between 2.4 mm and 8.6 mm, $|X_1|$ dependent modal parameters are obtained as given in Figures 4 to 6.

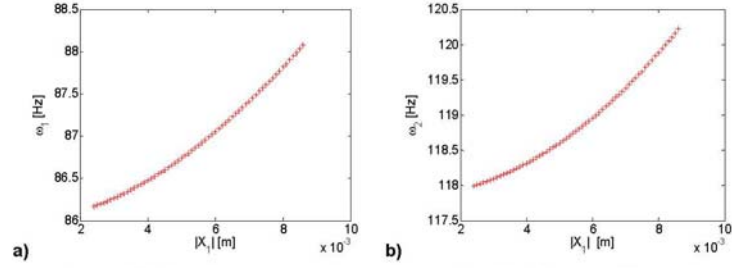


Figure 4. Natural frequency variations with respect to $|X_1|$. (a) mode 1 (b) mode 2

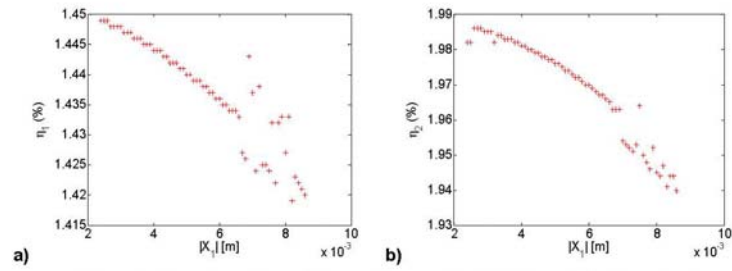


Figure 5. Damping ratio variations with respect to $|X_1|$. (a) mode 1 (b) mode 2

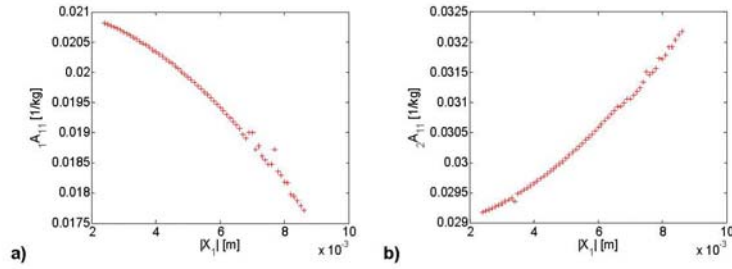


Figure 6. Modal constant variations with respect to $|X_1|$. (a) mode 1 (b) mode 2

As can be seen from the figures, modal parameters of the non-linear system follow a trend and therefore they can be expressed in terms of proper mathematical functions that fit to the corresponding data points. The scattered values observed in the graphs of damping ratio and modal constants are believed to be due to the identification algorithm used in MODENT®. In practical applications even more scattered points are expected due to measurement errors. In order to see the effect of measurement errors, case studies with polluted simulated FRF values were also carried out. Since analytical expressions are fit to modal data points, it was observed that having scattered data does not affect the results significantly.

Frequency response of the system at forcing levels of 2000N and 4000N are calculated by using the modal model and presented in Figures 7 - 9 in decibel scale. The force is applied at the first mass to which the non-linear element is connected. The excellent match of the responses obtained from the modal model with those calculated by harmonic balance method demonstrates the validity of the modal model and the approach suggested. Note that both approaches are valid if the basic assumption (harmonic excitation results in harmonic response at the same frequency) holds true. Figures 8 and 9 show solutions for both increasing and decreasing frequency sweep. Very slight differences are observed between the results of this study and the HBM only around jump, and it is believed that they are due to using different numerical computational algorithms in both approaches.

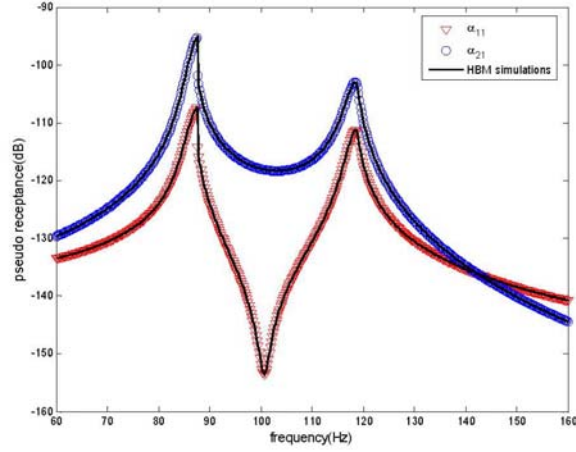


Figure 7. Pseudo FRFs of the system at $F_1 = 2000\text{N}$

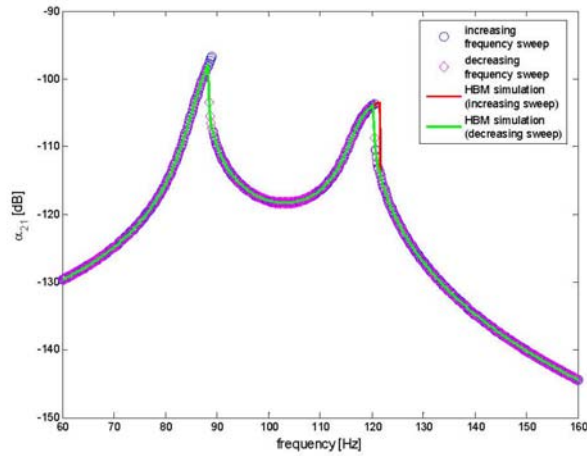


Figure 8. Pseudo receptance, α_{21} of the system at $F_1 = 4000\text{N}$

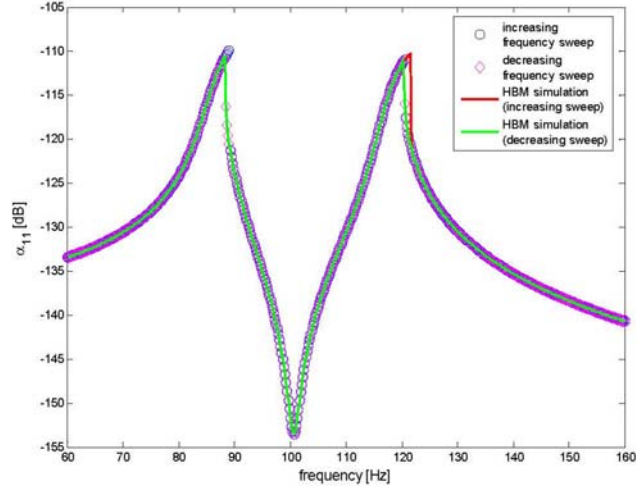


Figure 9. Pseudo receptance, α_{11} of the system at $F_1 = 4000\text{N}$

3.2 Case Study 2

In this case study, the 2-DOF system considered in the first case study is coupled with an undamped linear subsystem, and the coupled system is analyzed by using the approach proposed. System matrices of the linear subsystem are as follows:

$$M_L = \begin{bmatrix} 1 & 0 \\ 0 & 1 \end{bmatrix} \text{kg}, K_L = \begin{bmatrix} 10^5 & -10^5 \\ -10^5 & 1.1 \times 10^5 \end{bmatrix} \text{N/m}$$

The coupled system is obtained by rigidly connecting the first mass of the linear system to the second mass, M_2 , of the non-linear system shown in Figure 3.

Pseudo receptance matrix of the non-linear system is calculated by using the modal model obtained in the first case study, and the pseudo receptance matrix of the coupled 3-DOF non-linear system is calculated by using the receptance coupling approach proposed. The frequency response of the coupled system at a forcing level of 3000N applied at the "non-linear coordinate" is shown in Figure 10 in decibel scale. Again a very good agreement is obtained between the results of this study and HBM solutions, except around jump frequency at the third mode, most probably due to the reason explained in Case Study 1.

3.3 Case Study 3

In this case study, again the system in the first case study is used as the original system, and the following mass and stiffness modifications are made:

$$\Delta M = \begin{bmatrix} 1 & 0 \\ 0 & 1 \end{bmatrix} \text{kg}, \Delta K = \begin{bmatrix} 5 \times 10^5 & -5 \times 10^5 \\ -5 \times 10^5 & 5.5 \times 10^5 \end{bmatrix} \text{N/m}$$

Frequency response of the modified system at forcing level of 2000N is calculated from the modal model of the original non-linear system and the modifying mass and stiffness matrices. The result is shown in Figure 11

in decibel scale. Force is applied at the second mass. In this figure, solutions for both increasing and decreasing frequency sweep are shown. It is again possible to observe the jump around the first resonance of the system, where the results deviate from those of HBM.

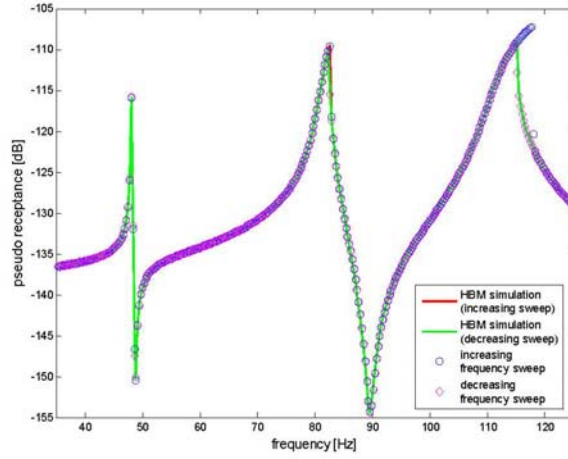


Figure 10. Pseudo receptance, α_{11} of the coupled system when there is a force of $F = 3000\text{N}$ at the "non-linear coordinate"

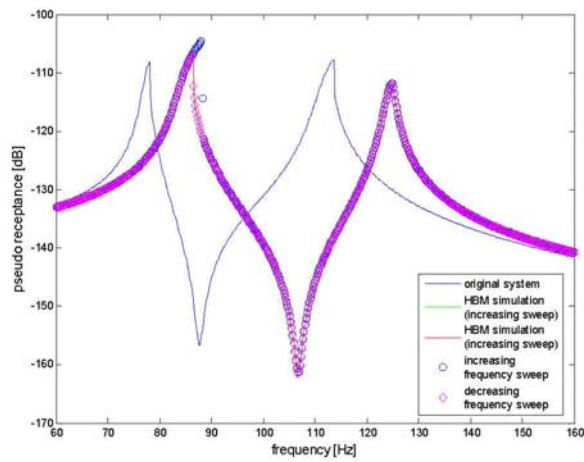


Figure 11. Pseudo receptance α_{11} of the modified system when there is a force of $F = 2000\text{N}$ at the "non-linear coordinate"

4. CONCLUSIONS

A method is proposed for modal identification and modal analysis of non-linear systems. The modal model of the system is obtained by identifying modal parameters from the linear FRF drawn for constant displacement amplitude of the "non-linear coordinate" (the coordinate where non-linear element is connected). Repeating the identification for different response amplitudes, identified modal parameters can be expressed as functions of the response amplitude of the "non-linear coordinate". It is demonstrated with case studies that the modal model can successfully be employed in the response prediction of the system at any forcing level. The uses of the same modal model in dynamic coupling of the identified non-linear system with a linear system, and in the dynamic modification analysis of the non-linear system are also formulated and validated by case studies.

As the modal parameters are represented as functions of the response itself, an iterative solution is required in each analysis. Fixed point iteration is used as the numerical solution, and a weighting coefficient is employed in order to provide convergence at frequencies near resonance.

The agreement observed between the frequency responses obtained by using the method proposed in this study with those of the harmonic balance method demonstrates the validity of the modal model and the methods suggested, provided that the basic assumption "harmonic excitation results in harmonic response at the same frequency" holds true, as both approaches base on this assumption. However, a slight mismatch is observed between the solutions of this study and those of HBM only around frequencies where jump occurs. It is believed that this is due to using different numerical solution algorithms in both approaches. The current work involves in employing better solution algorithms in both approaches.

The methods suggested are applicable to non-linear systems where nonlinearity is between a single coordinate and the ground. Furthermore the describing function for the nonlinearity should be frequency independent. Extension of the study to generalize the method for systems where nonlinearity is at an arbitrary location is the subject of the current work.

5. REFERENCES

- [1] Mertens, M., Van der Auweraer, H., Vanherck, P., Snoeys, R., "Detection of Nonlinear Dynamic Behaviour of Mechanical Structures", 4th International Modal Analysis Conference, Los Angeles, California, USA, 712-719, 1986.
- [2] He, J., Ewins, D. J., "A Simple Method of Interpretation for the Modal Analysis of Non-linear Systems," 5th International Modal Analysis Conference, London, England, 626-634, 1987.
- [3] Bohlen, S., Gaul, L., "Vibrations of Structures Coupled by Nonlinear Transfer Behaviour of Joints; A Combined Computational and Experimental Approach", 5th International Modal Analysis Conference, London, England, 86-91, 1987.
- [4] Lin, R. M., Ewins, D. J., "On the Location of Structural Nonlinearity from Modal Testing - A Feasibility Study", 8th International Modal Analysis Conference, 497-515, 1990.
- [5] Vakakis, A. F., Ewins, D. J., "Effects of Weak Nonlinearities on Modal Analysis", 10th International Modal Analysis Conference, San Diego, California, USA, 73-78, 1992.
- [6] Song, H. W., Wang, W. L., "Non-Linear System Identification Using Frequency Domain Measurement Data", 16th International Modal Analysis Conference, Santa Barbara, California, USA, 746-752, 1998.
- [7] Özer, B., Özgüven, H. N., "A New Method for Localization and Identification of Nonlinearities in Structures", 6th Biennial Conference on Engineering Systems Design and Analysis, Istanbul, Turkey, 2002.
- [8] Goge, D., Sinapius, M., Fullekrug, U., Link, M., "Detection and Description of Non-Linear Phenomena in Experimental Modal Analysis via Linearity Plots", International Journal of Non-Linear Mechanics, Volume 40, Issue 1, Non-linear Fluid Mechanics, 27-48, 2005.
- [9] Özgüven, H. N., İmregün, M., "Complex Modes Arising from Linear Identification of Nonlinear Systems", The International Journal of Analytical and Experimental Modal Analysis, Volume 8, Issue 2, 151-164, 1993.

- [10]** Özgüven, H. N., İmregün, M., Kuran, B., "Complex Modes Arising From Linear Identification of Non-Linear Systems", 9th International Modal Analysis Conference, Florence, Italy, 644-650, 1991.
- [11]** Setio, S., Setio, H. D., Jézéquel, L., "Modal Analysis of Nonlinear Multi-degree-of-freedom Structures", International Journal of Analytical and Experimental Modal Analysis, Volume 7, Issue 2, 75-93, 1992.
- [12]** Jézéquel, L., Setio, H., Setio, S., "Nonlinear Modal Synthesis in Frequency Domain", 8th International Modal Analysis Conference IMAC, Orlando, 334-340, USA, 1990.
- [13]** Chong, Y. H., İmregün, M., "Modal Parameter Extraction Methods for Non-Linear Systems", 16th International Modal Analysis Conference, Santa Barbara, California, USA, 728-735, 1998.
- [14]** Chong, Y. H., İmregün, M., "Variable Modal Parameter Identification for Nonlinear MDOF Systems – Parts I & II", Journal of Shock and Vibration, Volume 8, Issue 4, 217-227, 2000.
- [15]** Chong, Y. H., İmregün, M., "Coupling of Non-Linear Substructures Using Variable Modal Parameters", Mechanical Systems and Signal Processing, Volume 14, Issue 5, 731-746, 2000.
- [16]** Perinpanayagam, S., Robb, D., Ewins, D. J., Barragan, J. M., "Non-linearities in an Aero-engine Structure: From Test to Design", 2004 International Conference on Modal Analysis Noise and Vibration Engineering, Leuven, Belgium, 3167–3182, 2004.
- [17]** Budak, E., Özgüven, H. N., "A Method for Harmonic Response of Structures with Symmetrical Non-linearities", 15th International Seminar on Modal Analysis, Leuven, Belgium, 901–915, 1990.
- [18]** Budak, E., Özgüven, H. N., "Iterative Receptance Method for Determining Harmonic Response of Structures with Symmetrical Non-Linearities", Mechanical Systems and Signal Processing, 75–87, 1993.
- [19]** Tanrikulu, Ö., Kuran, B., Özgüven, H. N. and Imregun, M., "Forced Harmonic Response Analysis of Non-linear Structures", AIAA Journal, Volume 31, 1313 - 1320, 1993.
- [20]** Gelb, A., and Vander Velde, W. E., "Multiple-Input Describing Functions and Nonlinear System Design", McGraw Hill, 1968.
- [21]** Özgüven, H. N., "Structural Modifications Using Frequency Response Functions", Mechanical Systems and Signal Processing, Volume 4, Issue 1, 53-63, 1987.